This is to certify that the
dissertation entitled

WHEN ANDROGEN RECEPTORS GO AWRY: MUSCLE SPECIFIC EXPRESSION TRIGGERS SPINAL BULBAR MUSCULAR ATROPHY (SBMA)

presented by

Jamie Ann Johansen

has been accepted towards fulfillment
of the requirements for the

Ph.D degree in Neuroscience

Cynthia J Jordan
Major Professor's Signature

11/25/2008
Date

WHEN ANDROGEN RECEPTORS GO AWRY: MUSCLE SPECIFIC EXPRESSION TRIGGERS SPINAL BULBAR MUSCULAR ATROPHY (SBMA)

By

Jamie Ann Johansen

A DISSERTATION

Submitted to
Michigan State University
in partial fulfillment of the requirements
for the degree of

DOCTOR OF PHILOSOPHY

Neuroscience

2008

ABSTRACT

WHEN ANDROGEN RECEPTORS GO AWRY: MUSCLE SPECIFIC EXPRESSION TRIGGERS SPINAL BULBAR MUSCULAR ATROPHY (SBMA)

By

Jamie Ann Johansen

Spinal Bulbar Muscular Atrophy (SBMA) is a motor neuron disease, typically viewed as neurogenic in origin, meaning triggered by problems that begin in motoneurons. SBMA is caused by a mutation in the androgen receptor (AR) gene involving an expansion of CAG repeats coding for glutamines in the protein. We created a transgenic (tg) mouse line in which a rat AR cDNA with a wildtype (wt) number of glutamine residues (22) is expressed exclusively in skeletal muscle fibers at very high levels. Most notably, only untreated transgenic *male* mice and not female mice develop a severe neuromuscular phenotype resembling SBMA, paralleling the prominent sex bias of SBMA in humans. This phenotype is characterized by an androgen-dependent loss in motor function, loss of muscle fibers and motor axons, and changes in muscle gene expression consistent with denervation. In contrast, tg females appear

healthy until treated with testosterone (T) as adults, again demonstrating the androgen-dependence of the disease phenotype in our mouse model. As little as 3 days of T treatment induces a marked loss of motor function in tg females, and by 10 days, tg females look like diseased males, including having kyphosis and motor dysfunction. Furthermore, flutamide, an AR antagonist, successfully prevents the rapid demise of T treated tg females and may be a potential therapeutic for treating SBMA. Finally, I show that male mice having functional ARs *only* in muscle fibers and not elsewhere also exhibit an androgen-dependent motor disease phenotype. These results indicate that severe neuromuscular dysfunction mimicking SBMA can be induced by over-expression of the wt AR exclusively in muscle fibers. Results from both tg males and females suggest that ligand activation of wt ARs in muscle fibers is sufficient to trigger motor neuron disease, suggesting that SBMA and possibly other motor neuron diseases may in fact be myogenic and that muscles offer a new and accessible target for therapeutics.

Acknowledgements

Thank you to Dr. Cindy Jordan, my graduate advisor, who has always been supportive and compassionate as she guided me down the path I travel. I am honored to be the first of many graduate students, and I hope to have similar rewarding experiences with my graduate students, and to learn from her example. Thank you to Dr. Marc Breedlove, Dr. Tony Nunez and Dr. Steve Schneider, who comprised the rest of my committee and provided valuable input and guidance along the way. Thank you to Dr. Lynwood Clemens, who got me hooked on neuroscience as an undergraduate, and encouraged me to pursue it. Thank you to my collaborators, Dr. Andrew Lieberman and Dr. Ashley Monks who have helped me with this undertaking.

I am very thankful for those in my lab who helped me with a variety of things. I am extremely grateful to Chas Jensen, Cindy Knaff, Sarah Lansing, Heather Malinowski, Ernestine Mitchell, Diane Redenius, Nicole Timm, Sandy Troxell, and Shenna Washington, for all the technical assistance over my years here. I could not have done it without you. I also need to thank Dr. John Morris, and Dr. Dave Swender, who shared their art of "beer-thirty", which made long days in the lab enjoyable when I first started.

I am thankful of my family, my parents for the years of encouragement and support, for always believing in me and making me the person I am today. My sisters, who both have always been there for me. I am extremely thankful to all

my friends, in particular Jennifer Cummings, who has always been there every step of the way.

This work was supported by a predoctoral NRSA award (NS54517) and NIH Grant support: NS0450195 (CLJ), NS051257 (DAM), NS055746 (APL).

Table of Contents

LIST OF TABLES

LIST OF FIGURES

Images in this thesis/dissertation are presented in color.

ABBREVIATIONS

AChR – acetylcholine receptor alpha

ALS – amyotrophic lateral sclerosis

AR – androgen receptor

BC – bulbocavernosus muscle

CMV – cytomegalovirus

DLN – dorsolateral nucleus

EDL – extensor digitorum longus skeletal muscle

HSA – human skeletal actin

HSA-AR – transgenic mice overexpressing androgen receptors in skeletal muscles exclusively

HD – Huntington's Disease

LA – levator ani skeletal muscle

RDLN – retrodorsolateral nucleus

PolyQ – polyglutamine expansion

SBMA – spinal bulbar muscular atrophy

SCA – spinocerebellar ataxia

SMA – spinal muscular atrophy

SNB – spinal nucleus of the bulbocavernosus

Tg – transgenic HSA-AR mice

Tfm – testicular feminization mutation

Tfm/tg (Tfm/HSA-AR)– transgenic mice overexpression androgen receptors in skeletal muscles, and also devoid of endogenous androgen receptors elsewhere in the body

Wt – wildtype

INTRODUCTION

I begin with an introduction to the spinal nucleus of the bulbocavernosus (SNB) a sexually dimorphic set of motoneurons and a series of questions leading to the generation of transgenic mice. The goal of my research at the start was to address questions relating to sexual differentiation and the masculinization of the SNB system. However, we inadvertently created a mouse with a neurodegenerative phenotype resembling Spinal Bulbar Muscular Atrophy (SBMA). I provide an introduction for this disease, and characterize the mouse model that is the focus of my dissertation.

Spinal Nucleus of the Bulbocavernosus

The spinal nucleus of the bulbocavernosus (SNB) is a sexually dimorphic set of motoneurons that innervate the bulbocavernosus (BC) and levator ani (LA) skeletal muscles in rodents (Breedlove and Arnold, 1980). The BC/LA muscles attach exclusively to the base of the penis and are necessary for male copulatory behavior (Sachs, 1982). These skeletal muscles are also highly responsive to androgens. For example, castration in adulthood causes these muscles to atrophy, and dendrites and neuromuscular junctions to shrink (Breedlove and Arnold, 1981; Balice-Gordon et al., 1990; Goldstein et al., 1990), while testosterone replacement can reverse this and maintain the system (Balice-Gordon et al., 1990; Goldstein et al., 1990). The BC/LA are unique skeletal

muscles, as they posses a striking androgen responsiveness that other skeletal muscles do not. For example, the extensor digitorum longus (EDL) is a hindlimb skeletal muscle that neither increases in size or atrophies with adult androgen manipulations (Monks et al., 2004).

Although, the SNB system is sexually dimorphic in adulthood, it is sexually monomorphic during fetal development. The muscles are present in both sexes and are approximately the same size (Cihak et al., 1970), the number of motoneurons in the SNB region are approximately equal (Nordeen et al., 1985), and the neuromuscular junction between motoneurons and the target muscle are functional (Rand and Breedlove, 1987). Just before birth the muscles continue to grow in males while shrinking in females (Cihak et al., 1970), and the number of motoneurons in the SNB region declines only slightly in males, but quite precipitously in females (Nordeen et al., 1985). Perinatal androgen treatment of females prevents the loss of muscle targets and motoneurons, while perinatal androgen deprivation of males causes the system to die (Breedlove and Arnold, 1983c, 1983a). Additionally, XY animals with a defect in the gene for the androgen receptor (*tfm*), possess a very feminine SNB system (Breedlove and Arnold, 1981). Therefore, androgens developmentally ensure the survival of motoneurons and target muscles in males, while too little androgen in females cause the SNB system to die (Breedlove and Arnold, 1983b).

Where does androgen act to masculinize the system? It has been shown that androgens do not act on brain afferents to the SNB motoneurons to keep them alive, because even when the connections from the brain to the spinal cord

were severed in newborn female rats, androgen treatment still spared the SNB system (Fishman and Breedlove, 1985). Evidence also suggests that motoneurons do not respond directly to androgen (Freeman et al., 1996). Utilizing female rats who are mosaic for functional androgen receptors (AR), it was shown that even motoneurons lacking a functional AR can still be saved by perinatal androgen treatment (Freeman et al., 1996). Therefore, SNB motoneurons without the capacity to respond directly to androgens could still be spared by the hormone. Thus, neither brain afferents nor the SNB motoneurons themselves are the primary site of androgen action for sparing the system.

By a process of elimination, these data suggest that the target muscles (BC and LA) are the tissues that directly respond to androgens during development, and that this sparing of the target muscles indirectly causes the innervating SNB motoneurons to survive. Blocking androgens locally with flutamide reduces the number of SNB motoneurons that survive, providing further evidence that the BC/LA muscles are the site of action (Fishman and Breedlove, 1992). However there are multiple cell types in muscle, there are muscle fibers, fibroblasts, Schwann cells, and satellite cells. In rats, the LA which is highly responsive to androgens, also contains more myonuclei positive for AR than the androgen insensitive EDL (Monks et al., 2004). In Chapter 1, I will further examine androgen responsiveness in mice. Do BC/LA muscles in adult male mice have a similar enrichment of ARs, as in rats? If so, what cells in these muscles express AR?

To further examine the role of different AR-expressing cell types in conferring androgen responsiveness to the BC/LA, we created a transgenic mouse line in which an AR transgene is expressed in muscle fibers, and not the other cell types in muscle. The mice contain a rat AR construct driven by the HSA (human skeletal actin) promoter, which selectively drives transgene expression in muscle fibers, at high levels. Unexpectedly, very few transgenic males survive beyond birth, and even more surprising, the male mice that did survive developed a disease phenotype characterized by muscle weakness, atrophy, and early death. We believe we have inadvertently created a transgenic mouse model of Spinal Bulbar Muscular Atrophy (SBMA), or Kennedy's disease.

Spinal Bulbar Muscular Atrophy

Clinical and Pathological Features

SBMA is an adult onset, slowly progressive lower motoneuron disease characterized by proximal spinal and bulbar muscular weakness and atrophy. Symptoms of SBMA are finger tremor, muscle cramps following exercise, progressing to shoulder and pelvic girdle weakness. Signs of androgen insensitivity are also present, such as gynecomastia, testicular atrophy, and reduced fertility (Kennedy et al., 1968; Arbizu et al., 1983; Nagashima et al., 1988; Sobue et al., 1989; Dejager et al., 2002).

A loss of lower motoneurons through all spinal segments, and a loss in brainstem motor nuclei is present (Nagashima et al., 1988; Sobue et al., 1989). There is also a loss of large myelinated axons in the ventral roots of the spinal

cord (Kennedy et al., 1968; Sobue et al., 1989), while dorsal roots are mostly spared (Sobue et al., 1989). Clarke's columns and Onufrowicz nucleus are also well preserved (Kennedy et al., 1968; Nagashima et al., 1988; Sobue et al., 1989).

Striking pathology is observed in skeletal muscles. Atrophic fibers are scattered in groups, or among normal or hypertrophic fibers; muscle fiber nuclei can be centralized or pyknotic and clumped together (Kennedy et al., 1968). There are also occasional split fibers (Harding et al., 1982; Sobue et al., 1989). Additionally, there is a switch to a more oxidative metabolism in muscle fibers, with Type 1 (slow) and Type 2a (fast fatigue resistant) fibers predominating, revealed by ATPase staining (Harding et al., 1982; Sobue et al., 1989). Also evident is a disorganized myofibrillar network, accompanied by a decrease in oxidative enzyme activity in the core of the muscle fiber. These are referred to as "ring" fibers (Harding et al., 1982; Sobue et al., 1989), and can be revealed by NADH staining and to a lesser degree by hematoxylin and eosin (H&E) staining.

Most clinical evaluations conclude that muscle pathology exhibited by SBMA patients represent neurogenic atrophy, a result from motoneuron death, and that muscle pathology (myopathy) is secondary (Zoghbi and Orr, 2000). However, some suggest that SBMA may have a myogenic component (Harding et al., 1982; Yu et al., 2006b). Pathology in SBMA patient biopsies showed changes that are indicative of muscle disease, including hypertrophied fibers, disorganized myofribillar network, loss of oxidative enzyme activity and ring fibers (Harding et al., 1982). It is highly debatable whether the myopathic changes

seen are primary or secondary to motoneuron loss, however our mouse model highlights the myogenic contribution given that we have only manipulated gene expression in skeletal muscles. Our model suggests that SBMA may indeed be a muscle disease and that motoneuronal dysfunction and death originates from the muscle.

Molecular basis of SBMA

SBMA is a recessive X-linked inherited disease, caused by a mutation in the AR gene. The mutation involves an expansion in the number of CAG repeats in the first exon of the AR, that code for glutamines in the protein. The higher the number of CAG repeats, the earlier the age of onset and more severe the disease (La Spada et al., 1991; Zoghbi and Orr, 2000). Polyglutamine (polyQ) repeats are responsible for other neurodegenerative diseases, such as Huntington's diseases (HD), and spinocerebellar ataxias (SCA) types 1,2,3,6,7,17. The mutated AR in SBMA is thought to take on a "gain of function" and become cytotoxic. Lack of a functional AR does not lead to SBMA; for example, both human and rodents who have a severely dysfunctional AR because of a mutation in the AR gene, do not exhibit SBMA (Yarbrough et al., 1990; Chung et al., 1998; Hellwinkel et al., 1999; Thiele et al., 1999). However, it is clear that the AR loses some of its normal function in SBMA because affected males exhibit signs of partial androgen insensitivity (Dejager et al., 2002).

Nuclear aggregates are considered a hallmark of polyQ diseases, including SBMA (Orr and Zoghbi, 2007). Mutated ARs are found within nuclear

aggregates in motor neurons and skeletal muscles. Nuclear aggregates tend to co-localize with ubiquitin which tags proteins for degradation, and molecular chaperones such as heat shock proteins (HSP) which promote proper protein folding and enhance degradation of AR. Transcriptional regulators such as CREB binding protein (CBP) also co-localize with nuclear aggregates (Zoghbi and Orr, 2000; Adachi et al., 2003). Over-expression of molecular chaperones, such as HSP70 has been shown to decrease aggregation, and improve motor functions in polyQ models, including SBMA (Cummings et al., 2001; Adachi et al., 2003). Molecular chaperones may play a protective role by enhancing degradation of the mutant protein, and/or by sequestering the mutant protein (Bailey et al., 2002; Adachi et al., 2003). Additionally, nuclear aggregates contain the N-terminal fragment, not the C-terminus of the AR in SBMA patients and transgenic animal models (Li et al., 1998; Chevalier-Larsen et al., 2004). However, there is controversy surrounding whether nuclear aggregates are toxic or not. In some models of polyQ diseases the mutant protein can cause toxicity without the development of aggregates (Saudou et al., 1998; Arrasate et al., 2004).

Mouse Models of SBMA Disease

Several mouse models have been developed that utilize full length human AR containing polyglutamine repeats (97-120 polyQ) driven by a promoter that directs gene expression in a wide variety of cells (Katsuno et al., 2002; McManamny et al., 2002; Chevalier-Larsen et al., 2004; Sopher et al., 2004).

These mice show an SBMA phenotype of muscle weakness, atrophy, leading to decreased coordination and activity. A significant finding of these models is that the phenotype appears androgen dependent. Males are more severely affected than females, but castrating males ameliorates symptoms, and testosterone treatment in females elicits the disease phenotype (Katsuno et al., 2002; McManamny et al., 2002; Chevalier-Larsen et al., 2004). These models also mimic the pathology seen in SBMA patients. In some models, there is a depletion of motoneuron and muscle fiber populations, and nuclear aggregates are present in neuronal and non-neuronal cell types, such as skeletal muscle fibers (Katsuno et al., 2002). Additionally, muscle pathology includes atrophic fibers, angular fibers, and hypertrophied fibers, as seen in humans. Muscle fibers exhibit internal nuclei, and a increase in oxidative metabolism (McManamny et al., 2002; Katsuno et al., 2003a; Sopher et al., 2004). Because the mutant SBMA allele in these transgenic mice is broadly expressed across different tissues and cell types using the cytomegalovirus (CMV) promoter (McManamny et al., 2002; Katsuno et al., 2003a; Sopher et al., 2004), prion protein promoter (Abel et al., 2001; Chevalier-Larsen et al., 2004) or human AR promoter (Adachi et al., 2001), they do not address the question of where the mutant allele acts to cause the disorder.

Therapeutics and treatment of SBMA

SBMA is commonly misdiagnosed at amyotrophic lateral sclerosis (ALS), myasthenia gravis, chronic inflammatory neuropathy or metabolic myopathy

(Chen and Fischbeck, 2006). Approximately 1 in 25 patients diagnosed with ALS actually have SBMA after genetic testing (Chen and Fischbeck, 2006). However there is no effective treatment available for patients with SBMA. Among the avenues being explored as potential therapeutics there are histone deacetylase (HDAC) inhibitors, and anti-androgens. Although molecular chaperones have been shown helpful in animal models, no clinical trials have been pursued yet.

Acetylation and deacetylation of histones plays an important role at the level of transcription. In general, increased levels of histone actetlyation increase transcriptional activity by relaxing chromatin and helping to unwind DNA, while histone deacetylation can decrease transcription levels and repress gene expression by making DNA less accessible (de Ruijter et al., 2003; Rouaux et al., 2004). A reduction in histone acetylase activity is associated with polyQ diseases, suggesting that HDAC inhibition would help to improve acetylase activity (Chen and Fischbeck, 2006). Indeed, HDAC inhibitors have been successful in alleviating symptoms in mouse models of ALS, SBMA and other polyQ diseases (Steffan et al., 2001; Ferrante et al., 2003; Minamiyama et al., 2004; Ying et al., 2006; Rouaux et al., 2007). HDAC inhibitors currently are in clinical trials for another inherited motor neuron disease Spinal Muscular Atrophy (SMA), and are may be useful in SBMA as well (Chen and Fischbeck, 2006).

Anti-androgens are also a likely therapeutic now that ligand dependence has been recently demonstrated. Castration of tg animals with SBMA results in a reversal of the disease (Katsuno et al., 2002). Flutamide, an androgen antagonist, has surprisingly not been successful, while leuprorelin, a

gonadotrophin-releasing hormone (GnRH) analogue which reduces testosterone release from the testes has been effective (Katsuno et al., 2003b). Leuprorelin is now in clinical trials (Banno et al., 2006).

Overview

While most mouse models of SBMA utilize CAG repeats to induce the disease phenotype, the basis of the disease in humans, we find that CAG repeats are *not* essential to the disorder. In Chapter 2, an overall characterization of transgenic males at a behavioral, cellular and molecular level demonstrates how our mouse model develops a similar disease phenotype as the mouse models described above. However, our mice express a *wildtype* AR containing a *normal* number of glutamine repeats only in skeletal muscle, recapitulating the same loss of motor function, muscle pathology and neurodegeneration. Additionally, we find that the disease phenotype can be elicited by manipulating AR expression only in skeletal *muscle fibers*, suggesting that SBMA is actually a myogenic, not a neurogenic disorder. Further, I demonstrate the profound androgen dependence of the SBMA phenotype in our female model of SBMA in Chapter 3. I describe data on transgenic female mice that when treated with testosterone, rapidly develop a neuromuscular disease phenotype similar to transgenic males. Remarkably, this can be fully reversed with the subsequent removal of testosterone. In Chapter 4, I ask whether the anti-androgen, flutamide, is successful in ameliorating disease symptoms in our

SBMA model. Not only does flutamide positively affect our female mice with SBMA, but it also enhances survival of transgenic males treated prenatally.

CHAPTER 1

Johansen, J. A., Breedlove, S. M., Jordan, C. L. (2007) "Androgen Receptor Expression in the Levator Ani Muscle of Male Mice." Journal of Neuroendocrinology **19**(10): 823-826.

CHAPTER 1: ANDROGEN RECEPTOR EXPRESSION IN THE LEVATOR ANI MUSCLE OF MALE MICE

Abstract

The spinal nucleus of the bulbocavernosus (SNB) is a sexually dimorphic group of motoneurons that innervates the bulbocavernosus (BC) and levator ani (LA), skeletal muscles that attach to the base of penis. In many species, including mice, rats and hamsters, the LA and BC have been found to be highly responsive to androgen and in rats, these muscles mediate several effects of androgen on the SNB system. However, characterizing the SNB system in mice is important because of the availability of genetic models in this species. In this study we examined AR expression in skeletal muscles of C57/BlJ6 adult male mice using immunoblotting and immunocytochemistry (ICC), comparing the LA to the androgen-unresponsive extensor digitorum longus (EDL). We find similar differences in AR expression for these muscles in the mouse as previously reported for rats. In mice, the LA contains more AR protein than does the EDL. At the cellular level, the LA contains a higher percentage of AR positive myonuclei and fibroblasts than does the EDL. Finally, AR expression is enriched at the neuromuscular junction of mouse LA fibers. The increased expression of AR in the LA compared to the EDL, in both muscle fibers and fibroblasts

indicates that each cell type may critically mediate androgen action on the SNB system in mice.

Introduction

The spinal nucleus of the bulbocavernosus (SNB) is a sexually dimorphic group of motoneurons innervating the bulbocavernosus (BC) and levator ani (LA) muscles (Breedlove and Arnold, 1981; Forger et al., 1997; Monks et al., 1999). These skeletal muscles are highly responsive to androgens. For example, castration in adulthood causes these muscles to atrophy and their neuromuscular junctions to shrink, unlike limb muscles (Breedlove and Arnold, 1981; Balice-Gordon et al., 1990). Studies in rats also indicate that androgen acts directly on these muscles to regulate their size, and also the length of dendrites in the innervating SNB motoneurons (Kurz et al., 1986; Zuloaga et al., 2006).

The BC/LA muscles in rats are also enriched for androgen receptor (AR) compared to limb muscles (Antonio et al., 1999; Monks et al., 2006b). At the cellular level, a high percentage (74%) of nuclei within LA fibers stain for AR as opposed to a low percentage (3%) in the extensor digitorum longus (EDL) limb muscle (Monks et al., 2004). We have begun to use transgenic mouse models to identify the cellular targets within muscle that mediate androgen action on the SNB system. However, important preliminary work is needed to characterize AR expression in the SNB system of wildtype mice. Does the BC/LA in C57/BlJ6 adult male mice have a similar enrichment of ARs, as in rats? If so, what cells in these muscles express AR?

Methods

All animal procedures were approved and performed in compliance with the Michigan State University Institutional Animal Care and Use Committee, in accordance with the standards in the NIH Guide for the Care and Use of Laboratory animals.

Immunoblotting. The BC/LA and EDL muscles were harvested from three 90 day old C57/BlJ6 male mice (Jackson Laboratory) deeply anesthetized with isoflurane, and exsanguinated. Muscles were frozen on dry ice, homogenized in RIPA buffer, 20ug of total protein from the supernatant was loaded onto 8% tris-glycine gel, run at 125V for two hours, transferred to a nitrocellulose membrane at 45V for 2 hours, and probed for AR (N-20, Santa Cruz, 1:500), followed by anti-rabbit-HRP (Santa Cruz, 1:1000) and detected by Luminol (Santa Cruz).

Immunocytochemistry. Six adult 90 day old male C57/BlJ6 mice (Charles River) were anesthetized with isoflurane, and their LA and EDL muscles were harvested, frozen with liquid nitrogen in OCT-filled cryomolds and stored at -80° C until sectioning. Muscles were cross-sectioned at 10um using a cryostat, thaw mounted onto gel-subbed slides, and stored at -80° C until stained. Adjacent muscle sections were distributed across 6 series of slides. Sections were quadruple stained for the following cellular markers: AR, basal lamina (B2), acetylcholine receptors, and DNA as previously described (Monks et al., 2004). Briefly, sections were stained first for AR using a rabbit polyclonal antibody (PG21 from Upstate, 1:500) and visualized using a peroxidase Elite ABC kit (Vector) and nickel-enhanced diaminobenzidine. Following AR staining, sections

were stained for basal lamina (rat monoclonal anti-B2 laminin, Chemicon, 1:10,000) and acetylcholine receptors (AlexaFluor-488 alpha-bungarotoxin, Molecular Probes,1:100). B2 laminin was visualized using a biotinylated anti-rat secondary antiserum (Vector, 1:200), followed by Cy3-strepavidin (Jackson ImmunoResearch 1:1800). Sections were stained for 5 minutes in DAPI (1ug/ml, Sigma), dehydrated and coverslipped with DPX (Sigma). Slides were stored long term at -20° C. Controls sections were subjected to the same staining conditions except the AR antiserum was omitted.

Results

Using combined transmitted and fluorescent light, nuclei were classified as myonuclei (inside the basal lamina) or fibroblasts (outside the basal lamina), and further classified as synaptic or nonsynaptic (Figure 1, Figure 2). Nonsynaptic myonuculei were further classified into two types. Type 1 nonsynaptic myonuclei were located within the same cross section of fiber with a visible neuromuscular junction, and Type 2 were located in cross sections that did not have a visible neuromuscular junction (Figure 1, Figure 2). Statistical analysis was done using Statview (version 5.0.1). Separate 2-way ANOVAs were done to assess AR expression in myonuclei and fibroblasts, with muscle (LA vs. EDL) as between groups factor, and region (synaptic vs. nonsynaptic) as a repeated factor. Fisher's PLSD post-hoc comparisons were used. No mean differences were detected between Type 1 and Type 2 nonsynaptic myonuclei and so were collapsed in the analyses.

Immunoblotting revealed a distinct band at the expected molecular weight of ~112 kDa for each LA and EDL sample (Figure 3). Qualitative assessment of the blot suggests that the BC/LA in mice contains more AR than the EDL (Figure 3), comparable to the difference reported in rats (Monks et al., 2006b). Given that ARs appear similarly enriched in the BC/LA of mice compared to rats, we next examined the cellular distribution of AR in the LA and EDL in C57/BlJ6 adult male mice.

We found that the percent of AR positive myonuclei (nuclei within muscle fibers) is significantly greater in the androgen-responsive LA compared to the androgen-unresponsive EDL (Figure 4A, $F(1,10)=53.57$, $p<.0001$). There was also a main effect of region (synaptic vs nonsynaptic) on AR+ myonuclei ($F(1,10)=16.78$, $p<.003$), and a marginal interaction ($F(1,20)=4.27$, $p<.0656$). These results indicated that the percent of AR positive myonuclei in LA muscle fibers is significantly increased at the neuromuscular junction, compared to outside the junction of LA fibers (Figure 4B, $p<.02$), but a similar synaptic enrichment of AR positive myonuclei was not detected in the EDL (Figure 4B, $p=.1345$). In contrast to the pattern seen in rats, AR positive fibroblasts were also significantly higher in the LA compared to the EDL (Figure 4A, $F(1,10)=6.62$, $p<.03$). There were no apparent differences in AR expression between fibroblasts in synaptic versus nonsynaptic regions of muscle, which was also the case in rats (Monks et al., 2004), (Figure 4C, $F(1,10)=3.25$, $p=.0799$) nor a significant interaction ($F(1,10)=3.25$, $p=.1018$).

Discussion

These results are consistent with the idea that AR in muscle fibers may critically mediate androgen action on the SNB system. We find that total AR protein expression is higher in the androgen-responsive LA compared to the androgen-unresponsive EDL in adult male mice, similar to what has been reported in rats (Monks et al., 2004). Likewise, we find that the LA contains a much higher proportion of AR positive myonuclei than the EDL, accounting for some of the differences in overall AR content. Because AR expression within muscle fibers correlates with the degree of androgen responsiveness, androgens may act via LA muscle fibers to influence the muscle directly and SNB motoneurons indirectly. However, unlike rats, AR expression in mouse fibroblasts also correlates with androgen responsiveness. Thus, androgens may act through one or both cell types within muscle to influence the BC/LA muscles and SNB motoneurons. Future studies that manipulate AR gene expression in select populations of cells will help to identify the direct cellular targets in muscle that mediate androgen action on the SNB system.

CHAPTER 2: OVEREXPRESSION OF WILD-TYPE ANDROGEN RECEPTOR IN MUSCLE RECAPITULATES POLYGLUTAMINE DISEASE

Abstract

We created transgenic mice that over-express wildtype androgen receptor (AR) exclusively in their skeletal muscle fibers. Unexpectedly, these mice displayed androgen-dependent muscle weakness and early death. Transgenic (tg) males show profound losses in muscle strength and a shortened stride length. Tg males also show changes in muscle morphology, including fewer fibers, regions of atrophy, fibers with internal nuclei and a general shift towards an oxidative metabolism. Tg males also show changes in gene expression indicative of denervation, and exhibited a loss of motor axons. These features reproduce those seen in models of spinal bulbar muscular atrophy (SBMA), also known as Kennedy disease, a polyglutamine expansion disorder caused by a CAG repeat expansion in the AR gene. These findings demonstrate that toxicity in skeletal muscles is sufficient to cause SBMA symptoms and suggest that overexpression of wildtype AR can exert toxicity comparable to the polyglutamine-expanded protein. Furthermore, therapeutic approaches targeting skeletal muscle may provide an effective treatment for SBMA.

Introduction

Spinal bulbar muscular atrophy (SBMA) is an X-linked, slowly progressive disease characterized by adult onset muscle weakness, atrophy, and motoneuron loss. Signs of androgen insensitivity, such as gynecomastia, testicular atrophy, and reduced fertility, are also present (Kennedy et al., 1968; Arbizu et al., 1983; Nagashima et al., 1988; Sobue et al., 1989; Dejager et al., 2002). Because the muscle pathology seen in SBMA resembles "neurogenic" responses to denervation, the disease is widely assumed to be triggered by pathology that begins in motoneurons.

In humans, SBMA is caused by an expansion of a trinucleotide CAG repeat, which encodes a polyglutamine (polyQ) tract in the amino terminus of the androgen receptor (AR). On average, the higher the number of CAG repeats, the earlier the disease onset (La Spada et al., 1991). An expansion in the polyQ repeats in other proteins has also been linked to neurodegenerative diseases, such as Huntington's diseases (HD), and the spinocerebellar ataxias (SCA) types 1,2,3,6,7,17. For SBMA and other polyQ diseases, repeats greater than 40 appear to confer a toxic gain of function (Zoghbi and Orr, 2000). Intranuclear inclusions, or aggregates, are a distinguishing pathological feature, however whether these aggregates play a causative role in the development of symptoms remains controversial (Orr and Zoghbi, 2007).

We created a transgenic (tg) mouse line in which a rat AR cDNA encoding a wildtype (wt) number of glutamine residues (22) is driven by the

human skeletal α-actin (HSA) promoter, resulting in over-expression of AR protein in skeletal muscle fibers. Our studies of AR in skeletal muscle (Monks et al., 2004; Monks et al., 2006a) led us to generate these tg mice so we were quite surprised when we discovered a striking phenotypic resemblance between these mice and mouse models of SBMA. Given that the current doctrine asserts that SBMA is caused by an expanded polyQ AR acting in motoneurons, this similarity was very surprising since our AR transgene encodes for only 22 glutamines and is expressed exclusively in skeletal muscle fibers and not in motoneurons. In this chapter I describe the behavioral, cellular and molecular features in our model which suggest that SBMA may, in fact, begin in muscle fibers, and that high expression levels of the wildtype AR protein is sufficient to cause SBMA.

Methods

Generation of Tg Mice

AR cDNA was subcloned from pCMV-AR (kind gift of Dr. Elizabeth Wilson (UNC) into pBS and the KpnI site of the multiple cloning sequence of the resulting subclone was converted into a NotI site using oligonucleotide linkers. LacZ was subcloned from pCMV-BGAL (Invitrogen). Both cDNAs were ligated into the NotI site of pBSX-HSA (kind gift of Dr. Jeff Chamberlain, UWash, HSA was originally cloned in Dr. Larry Kedes lab (Muscat and Kedes (1987) Mol Cell Biol 7:4089-99). Tg animals were produced by pronuclear injection of C4 X C57/BL6J zygotes. Tg animals were identified using PCR amplification of

transgene specific regions. Founding tg animals were mated to C57/BL6J mice and their progeny analyzed. Seven founding lines of HSA-AR mice showed varying levels of AR transgene expression. Three lines of tg mice displayed a severe neuromuscular disease phenotype, and four lines showed no phenotype. We focused on two lines (141 and 78) that each show significant over-expression, but are either symptomatic or asymptomatic for the behavioral disease phenotype.

PCR Identification of Tg mice

Polymerase chain reaction (PCR) was used to determine the genotype of individual mice. Ear punches were taken from the tg mice, lysed in 50ul lysis buffer containing Proteinase K by incubating overnight at 55 degrees. Samples were then diluted with 200ul sterile water and then placed at 95 degrees for 1 hr to inactivate Proteinase K. PCR was carried out on 10ul of each sample using forward agtagccaacagggaagggt and reverse cagattctggaacgctcctc primers to detect the HSA-AR transgene, and positive animals were determined.

Motor function tests

Hang Test - Mice were tested for muscle strength using the hanging wire test. Mice were placed on a wire grid and turned upside down 40cm above a counter and the to fall up to 120 seconds was measured (Sopher et al., 2004). These and all procedures with mice were reviewed and approved by the Michigan State University Institutional Animal Care and Use Committee.

Paw Print analysis - To measure gait properties, the mouse's front feet were painted with non-toxic acrylic red paint and the hindpaws painted with blue. The mice were placed at one end of a piece of paper and guided to walk along it (Taylor et al., 2001). Stride length was measured from front and hindlimbs.

Tissue Harvesting and Processing

Animals were deeply anesthetized with isoflurane. EDL muscles were collected for histology, weighed, placed in OCT filled cryomolds, and frozen in liquid nitrogen. Muscles were cryostat (Leica) sectioned at 10um. Quadriceps were harvested and frozen on dry ice for Western Blot analysis. Spleen was harvested and frozen on dry ice for Southern Blot analysis. Spinal columns were harvested and placed in buffered formalin for at least 30 days before ventral roots were harvested, and spinal cords sectioned on a sliding microtome at 30 um.

Western Blots

AR immunoblotting was carried out to confirm specific overexpression of AR in muscle. Quadricep muscle, spinal cord, testis, and heart tissues were harvested from animals under deep isoflurane anesthesia, and frozen on dry ice. Tissues were homogenized, and centrifuged at 12,000g for 5 minutes. 20ug of total protein from supernatant was loaded onto 8% tris-glycine SDS-PAGE gel and run at 125V for two hours. Proteins were transferred to a nitrocellulose membrane and probed for AR (N-20, Santa

Cruz, 1:500), followed by anti-rabbit-HRP (Santa Cruz, 1:1000) and detected by Luminol (Santa Cruz).

Southern Blots

Three positive adult animals from lines 14, 141 and 78 were used for southern blot analysis to determine copy number of the transgene. Tissue from kidneys or spleen was homogenized, digested overnight with Proteinase K and DNA was extracted and resuspended in water. Samples were digested with the restriction enzymes KPNI and BamHI, which cut out a 3kb fragment of the HSA-AR plasmid. The DNA was separated by electrophoresis using a 1% agarose gel, stained with ethidium bromide, and photographed using the Biorad Gel documentation system. Gels were then depurinated in .2M HCL for 10 minutes, denatured in a solution of 1.5M NaOH and 0.5M NaCl for 40minutes, and then neutralized in a solution of 1.5M NaCl, 0.5M Tris-Cl pH 7.2, and 0.001M EDTA. The gels were then blotted overnight onto Hybond N+ Nylon Membrane using 20xSSC and exposed to UV light to cross link the DNA to the membrane. Primers, foward ctggttgtcactacggagct and reverse ctgggggttatctggagcc, which amplify a 700 bp fragment of the HSA-AR plasmid were used to make 32P dCTP labeled probe. The membranes were hybridized to the probe for 72 hours at 65 degrees, blots were washed, and exposed to film. The 3Kb bands of interest were quantified using a phosphoimager (STORM from Amersham).

Morphometrical Analysis

Quantification of muscle number and size - One cross section in the EDL from the belly of the muscle was stained with H&E and analyzed to determine fiber number and size. Pictures were taken with a 20X objective and printed out. Every fiber in the section was counted. Fiber size was measured using the Stereo Investigator program (MicroBrightfield). The section was outlined at low power, and then muscle fibers were sampled with a 40X objective using the "fractionator" probe every 300um throughout the cross section. All fibers that intersected with the sampling box were measured.

Quantification of axon number and size – Lumbar 4 (L4) and 5 (L5) ventral roots were harvested from formalin fixed spinal cords, embedded in plastic, sectioned at 1um, and stained with Toluidine Blue. Images were taken from one cross section with a 40X objective and printed for each animal. Every myelinated axon was counted in the section. To measure the cross sectional area of axons, the L5 cross-sections were then analyzed using the Stereo Investigator program (MicroBrightfield). Sections were first outlined at a low power, and then axons were sampled with a 63X objective using the "fractionator" probe every 100um with a random rotation throughout the section. All axons within the sampling box were measured.

Quantification of motoneuron number and size – Formalin fixed lumbar spinal cords were cross sectioned at thirty microns on a freezing sliding microtome and Nissl stained. Motoneuron number and soma size

were measured in three lower lumbar motor pools, the spinal nucleus of the bulbocavernosus (SNB), the dorsolateral nucleus (DLN) and the retrodorsolateral nucleus (RDLN) using BioQuant Life Science Software. Each region was identified at low magnification and then counted and their nuclei and somas traced with a 60X objective. From caudal to rostral, twenty sections were measured starting at the first section in which the SNB could be identified. Counts were corrected for missing sections, by using the average of the sections before and after the missing section.

Androgen Receptor (AR) staining

To further address specificity of the AR transgene, we crossed line 78 (L78) tg male mice to testicular feminization mice (tfm) which lack functional androgen receptors, offering a null background for AR in which to assess AR transgene expression. Adult male mice of three different genotypes (wt, *tfm* or *tfm*/HSA-AR) were perfused with saline followed by 4% phosphate buffered paraformaldehyde. *Tfm* and *tfm*/HSA-AR mice received s.c. injections in the nape of the neck of 500 ug of testosterone propionate dissolved in 0.05 ml sesame oil 1.5 – 2 hours prior to sacrifice to enhance detection of nuclear AR in spinal motoneurons. Because such *tfm* male mice have extremely low levels of plasma T (Jordan, unpublished observation), any cellular AR present might not be detected in such mice without treatment with exogenous T which induces extant AR to concentrate in the nucleus, allowing its detection. Spinal cords were harvested, postfixed for one hour in the same fixative and then stored

overnight at 4 degrees C in 20% phosphate buffered sucrose. Thirty micron cross sections cut using a freezing sliding microtome were collected in phosphate buffered saline and then stained for AR following a previously published protocol (Zuloaga et al, 2006). Sections from all three genotypes were stained in a single run using all the same reagents to avoid introducing differences that might simply represent artifact. AR stained sections were lightly counterstained with the Nissl stain Neutral Red before coverslipping to reveal AR negative motoneurons. The AR antiserum was PG-21 (a gift from Gail Prins), a rabbit polyclonal directed against the first 21 amino acids of the AR. Images are motoneurons in the DLN at a comparable rostrocaudal level of the spinal cord for all three genotypes.

Statistical Analysis

Within founding lines, tg males were compared to their wt brothers or aged-matched wt males using independent groups T-tests with level of significance set at $p=0.05$ two-tailed, and N = number of animals in each group.

Results

The HSA-AR transgene is overexpressed exclusively in muscle fibers and not motoneurons.

Reporter mice carrying an HSA-LacZ (encoding β-galactosidase, Figure 5A) construct showed uniform and specific expression in skeletal muscle fibers only, and lacked any expression in fat or neural tissues, confirming that the HSA

promoter drives gene expression selectively in skeletal muscle fibers (Figure 5B,C), consistent with other reports (Brennan and Hardeman, 1993). HSA-LacZ pups stained darkly for β-galactosidase in skeletal muscles, but staining was absent in the brain and in wildtype (wt) pups (Figure 5B). Closer examination of 30 day old HSA-LacZ mice showed that skeletal muscles stained darkly for β-galactosidase in extensor digitorum longus (EDL) cross sections, while staining was absent in motoneurons (Figure 5C), further confirming the high specificity of the HSA promoter.

Mice carrying the HSA-AR construct, containing a normal number of glutamines (Figure 6A) were generated, which resulted in over-expression of AR protein in skeletal muscle fibers (Figure 6B). Additionally, we crossed our HSA-AR mice with mice that have the testicular feminization mutation (*tfm*) of the *AR* gene. *Tfm* males express little to no AR protein (Charest et al., 1991), offering a null background for AR in which to assess AR transgene expression. As expected, Western blots of tissues from such *tfm*/HSA-AR male progeny revealed AR in skeletal muscle, and essentially none in spinal cord, testes, or heart (Figure 6C).

tfm/HSA-AR mice also demonstrated that lumbar motoneurons do not contain AR protein when examined with immunocytochemistry. *tfm*/HSA-AR mice resemble *tfm* mice, which lack functional ARs , and were devoid of positive AR immunoreactivity (Figure 7). This was in contrast to wt male mice, which show prominent AR staining in lumbar motoneurons (Figure 7). Therefore, AR

transgene expression is highly specific for skeletal muscle fibers, and is not expressed in motoneurons.

Seven founding lines of HSA-AR mice showed varying levels of AR transgene expression. Three lines of tg mice displayed a severe neuromuscular disease phenotype, and four lines showed no phenotype. We focused on two lines (141 and 78) that each show significant over-expression (Figure 6F), but are either symptomatic or asymptomatic for the behavioral disease phenotype. No differences were detected in testosterone levels between tg and wt mice from either line 141 (L141) or line 78 (L78) [mean $\pm$ SEM in nmol/L: L141 wt =19.1 $\pm$ 6.6 (N=12), tg = 14.8 $\pm$ 7.02 (N=4), $p > 0.7$, L78 wt =10.8 $\pm$ 4.8 (N=13), tg = 11.38 $\pm$ 3.9 (N=19), $p > 0.9$]. Southern blot analysis shows that male L141 tg mice, presenting a severe disease phenotype, have a higher gene copy number than L78 tg males which showed normal motor function (Figure 6D). L141 mice also show higher levels of muscle AR mRNA and protein compared to L78 (Figure 6E, F). Therefore, disease severity correlates with a higher copy number of the AR transgene, and higher expression of AR mRNA and protein.

Transgenic males with the highest AR expression in skeletal muscles develop motor deficits.

Very few L141 tg males survive beyond birth (Table 1), but those that survive to adulthood develop a marked reduction in body weight, kyphosis, and striking deficits in muscle strength and motor coordination typical of

other tg mouse models of SBMA (Figure 8). For example, adult 141 tg males show marked deficits on the hang test (Figure 8C) indicating a profound loss of muscle strength compared to wt controls, and deficits in ambulation, including an altered gait and shortened stride as revealed by their paw print records (Figure 8D). L78 tg males show some mortality at birth (Table 1) and reduced body weight (Figure 8B) compared to wt littermates, but do not show discernable motor deficits as adults (Figure 8C,D).

Transgenic males exhibit comparable muscle pathology as in other SBMA mouse models and humans with SBMA.

We examined a hindlimb skeletal muscle, the extensor digitorum longus (EDL) for histological signs of pathology. In symptomatic L141 tg male mice, hematoxylin and eosin (H&E) stained cross-sections showed marked abnormalities, including small atrophic fibers, internal nuclei, and fiber splitting (Figure 9A), similar to reports of muscle biopsies of human SBMA patients. Nicotinamide adenine dinucleotide (NADH) stained EDLs revealed increased oxidative metabolism and an altered myofibrillar organization (Figure 9A), also commonly observed in SBMA affected muscles. L141 tg males have approximately half the number of EDL muscle fibers compared to wt controls (Figure 9B), but there is no difference in average fiber size [mean $\pm$ SEM in um^2: wt =1478.2 $\pm$ 91.2 (N=11), tg = 1303.2 $\pm$ 92.5 (n=4), $p > 0.31$]. Despite the presence of atrophic fibers in muscle from tg males, there is no difference in size

distribution of muscle fibers between tg and wt males (Figure 10). Surprisingly, behaviorally asymptomatic L78 tg males also show considerable pathology in the EDL, including small atrophic fibers, internal nuclei and alterations in NADH staining (Figure 9A). L78 tg males also show a significant loss in EDL fiber numbers, but this loss was not as great as seen in L141 male tg mice (Figure 9B). There was no change in average muscle fiber size compared to wt littermates [mean $\pm$ SEM in um^2: wt =1566.6 $\pm$ 79.7 (N=13), tg = 1379.8 $\pm$ 55.6 (n=12), $p > 0.07$], however the size distribution was altered in L78 tg males (Figure 10). The obvious muscle pathology in 78 males, despite no apparent behavioral phenotype, suggests that a certain amount of fiber pathology and loss can be tolerated before motor deficits appear.

Only symptomatic L141 tg male mice show axonopathy.

We also found that the number of motor axons in the fifth lumbar ventral root is reduced only in the severely affected L141 tg males (Figure 9C), suggesting neurodegeneration in these mice. However, we found no difference in average cross-sectional area of axons [mean $\pm$ SEM in um^2: wt =45.5 $\pm$ 4.43, tg = 45.2 $\pm$ 8.51], nor in the size distribution of these axons (Figure 11). Counts of the number of motor axons in L4 also indicate a significant deficit in tg L141 males compared to their wt controls [mean $\pm$ SEM: wt = 698 + 31.92 (N = 5) vs tg = 537 $\pm$ 34.82 (N = 4), $p < 0.04$]. Notably, axon number was not reduced in asymptomatic L78 tg males, despite significant losses in muscle fiber number (Figure 9C).

Surprisingly, we found no evidence of motoneuron loss or atrophy. In all three motor groups, the spinal nucleus of the bulbocavernosus (SNB), the dorsolateral nucleus (DLN) and the retrodorsolateral nucleus (RDLN), there were no significant losses in either motoneuronal number or soma size in L141 tg male mice compared to wt controls (Figure 12). These data suggest that HSA-AR mice exhibit axonopathy which may precede motoneuron cell death. Because only L141 tg males show axon loss but tg males from both 141 and 78 lines show considerable muscle pathology, these data also suggest that axon loss is secondary to muscle pathology.

Changes in muscle gene expression are consistent with denervation in L141 tg male mice.

We examined three genes that are commonly upregulated when muscles are denervated: acetylcholine receptor alpha subunit (AChR), myogenin and myogenic differentiation (MyoD) (Duclert et al., 1991; Eftimie et al., 1991; Weis, 1994; Kostrominova et al., 2000; Sanes and Lichtman, 2001; Mejat et al., 2005). Recent evidence also suggests that AChR and myogenin are upregulated in muscles from mouse models of SBMA (Yu et al., 2006b). We also examined vascular endothelial growth factor (VEGF) expression in skeletal muscles, which decreases after denervation (Wagatsuma and Osawa, 2006) and is also implicated in several motoneuron disease including SBMA (Lambrechts et al., 2003; Azzouz et al., 2004; Sopher et al., 2004; Wang et al., 2007). We found that AChR, myogenin and MyoD were upregulated in skeletal muscles of L141 tg

male mice compared to wt controls, whereas $VEGF_{164/188}$ mRNA was significantly downregulated in skeletal muscles of L141 tg males compared to wt brothers (Figure 13). These results are consistent with changes seen in other mouse models of SBMA and denervation (Eftimie et al., 1991; Sopher et al., 2004; Yu et al., 2006b). Importantly, no changes were observed in behaviorally asymptomatic L78 tg males. These results are also consistent with neurogenic atrophy (Eftimie et al., 1991; Wagatsuma and Osawa, 2006) and suggest that HSA-AR and other polyQ AR mouse models share a common molecular etiology, even though our model is unique in expressing a wt AR exclusively in skeletal muscles.

Discussion

Most clinical evaluations in SBMA patients conclude that muscle pathology represents neurogenic atrophy, resulting from motoneuron death, and that muscle pathology (myopathy) is secondary to neuropathy (Zoghbi and Orr, 2000). Our mice display behavioral, neuronal and muscular pathologies that are typically viewed as "neurogenic" in origin but result from a genetic manipulation that originates in muscle fibers. Tg male mice show a prominent kyphosis, profound motor deficits, muscle pathology, changes in muscle gene expression consistent with denervation, and a loss of motor axons. These findings implicate muscle AR in SBMA and suggest that overexpression of wildtype AR can recapitulate the pathological consequences of polyQ expansion of AR. These findings also question

whether other disorders regarded as "motoneuron" diseases may actually be muscle diseases that eventually cause motoneuronal pathology. Since we find substantial myopathy, including fiber atrophy and loss, without significant losses in motoneurons, these results suggest that motoneuronal death is a *response* to, rather than a *cause* of, pathological changes in muscles and is likely to be a rather late event in the disease process.

Interestingly, our gene expression results are also consistent with neurogenic atrophy (Eftimie et al., 1991; Wagatsuma and Osawa, 2006). We see similar changes in gene expression as other SBMA mouse models (Sopher et al., 2004; Yu et al., 2006b), which are typically viewed as neurogenic in origin. This outcome suggests that our muscle-specific model and other polyQ AR mouse models share a common molecular etiology. However, our mouse model perturbs AR expression only in muscle fibers, suggesting that SBMA may in fact be a myogenic disease, originating in the muscles and causing secondary loss of motoneurons. Further, our model indicates that such indices of neurogenic atrophy can result from processes that originate in muscle.

Amyotrophic lateral sclerosis (ALS) is another disease characterized by loss of motoneurons and muscle fiber atrophy that has been traditionally considered due to primary loss of motoneurons, which causes the "neurogenic" pathology in muscle. However, some evidence indicates that ALS pathology may not originate in motoneurons. The SOD mutant allele that induces ALS-like symptoms in mice has no effect when expressed solely in neurons (Pramatarova

et al., 2001; Lino et al., 2002), and in mice that are mosaic for the SOD allele, motoneurons carrying the disease gene survive (Clement et al., 2003). However, a third group has reported that neuron specific expression of SOD at extremely high levels, accomplished by making mice homozygotic for the mutation, show an ALS like phenotype (Jaarsma et al., 2008). Therefore, at extremely high levels it is possible to induce the disease phenotype by expressing the disease gene solely in neurons. However, this same approach has not been used to examine SOD in muscle.

To date, no study has specifically expressed the SOD mutation in skeletal muscles to address whether SOD in muscles is sufficient to induce disease. The SOD mutation has been knocked down in muscle using several techniques. First, a lentivirus to produce siRNA suppressed SOD levels by 60% (Miller et al., 2006). Second, using Cre recombinase under the control of the muscle creatine kinase promoter, the SOD mutation was excised from skeletal muscles. However only a 25% reduction in mRNA and protein was seen (Miller et al., 2006). Both techniques failed to ameliorate disease onset, symptoms and progression (Miller et al., 2006). Although the authors conclude that muscle does not have a role in ALS, it is possible that mutant levels of SOD were not reduced enough to have an effect. Until the SOD mutation has been expressed exclusively in skeletal muscles, this conclusion is premature.

Furthermore, expression of insulin-like growth factor (IGF-1) exclusively in skeletal muscles delayed disease onset and progression, and enhanced motoneuron survival in the SOD(G93A) model of ALS (Dobrowolny et al., 2005).

While IGF-1 could not enter the blood stream, it is possible that it has local effects on both the muscle and nerve terminals. However, because the origin of IGF-1 in this study is exclusively from muscles, this result strongly suggests that muscle may have a primary role in ALS. Expression of glial cell line derived neurotrophic factor (GDNF) exclusively in muscle also delayed disease onset, progression and enhanced survival in the same SOD mouse model of ALS. In contrast, specific expression of GDNF in astrocytes offered no protective effects (Li et al., 2007). These studies highlight the importance of trophic support for motoneurons from muscle.

Symptomatic L141 male mice exhibit significant losses in L4 and L5 ventral root axons but not at the level of motoneuronal cell bodies. Similar "dying back" axonopathies are observed in many, indeed most, models of motoneuron disease, including models of ALS, spinal muscular atrophy (SMA) (Frey et al., 2000; Cifuentes-Diaz et al., 2002; Fischer et al., 2004; Pun et al., 2006) and notably, SBMA (Sobue et al., 1989; Chevalier-Larsen et al., 2004; Katsuno et al., 2006b; Yu et al., 2006a). For example, the SOD1 (G93A), progressive motoneuropathy (pmn) and motoneuron degeneration mouse (Mnd) mouse models all show a loss of synaptic connections before symptoms appear (Frey et al., 2000). Furthermore, in the SOD1(G93A) mouse model, degeneration is first seen at the neuromuscular junction, followed by axonal loss and eventually motoneuron loss (Fischer et al., 2004). Additionally, in one model of SMA, a loss of L4 and L5 axons is seen prior to motoneuron loss, and motor axons are more severely affected than motoneuronal somata by the smn (survival motor neuron)

mutation (Cifuentes-Diaz et al., 2002). Thus, axonopathy usually precedes motoneuronal cell (body) death, suggesting that motoneurons in our L141 male mice might eventually die as part of this process, if the mice were to survive long enough.

Nuclear aggregates are a hallmark pathological feature in many neurodegenerative diseases, including polyQ diseases. However, In tg mouse models of Huntington's and SBMA nuclear aggregates do not necessarily confer toxicity (Ferrante et al., 2003; Minamiyama et al., 2004). Nuclear aggregates were not detected in our model, furthering the idea that the aggregates are not the cause of muscle pathology, motoneuron loss or behavioral deficits.

Our tg mice show that abnormally high levels of wt AR proteins in muscles have the same toxic potential as AR proteins with an expanded polyQ expressed at lower levels. Similarly, over-expression of wt Ataxin-1 in *Drosophila* and mouse models of spinocerebellar ataxia Type 1 causes neurodegeneration (Fernandez-Funez et al., 2000; Tsuda et al., 2005). Similar examples also exist for other neurodegenerative diseases. For example, elevated levels of wt α-synuclein via gene amplification can cause Parkinson's disease similar to the mutant form of the protein (Singleton et al., 2003), and wt expression of human SOD can also cause mild ALS like symptoms (Jaarsma et al., 2000). One question raised by our data is whether over-expression of *any* protein in muscle fibers is toxic. This seems unlikely since we do not find either perinatal lethality or motor deficits in our reporter male mice that express βgal, driven by the *same* HSA promoter, in their muscle fibers. Furthermore, it is clear that expression

levels also influence the degree of toxicity of mutant proteins. For example, a stronger promoter confers a higher toxicity to expanded polyQ allele than a weaker promoter (Abel et al., 2001; Duennwald et al., 2006). These findings suggest that protein expression levels and polyQ length can both contribute to protein toxicity.

While most tg mouse models of SBMA utilize an expanded polyQ repeat to induce the disease phenotype, mimicking the etiology of the disease in humans, our tg mouse model indicates expanded polyQ repeats are *not* required to cause the disorder. Our mouse model develops a similar phenotype with over-expression of the *wildtype* AR containing a *normal* number of glutamine repeats, showing the same loss of motor function and muscle pathology as other mouse models. Moreover, we find that the disease phenotype can be elicited by manipulating AR expression only in skeletal *muscle fibers*. Our model may provide insight into the critical mechanisms underlying polyQ diseases and perhaps other presumed neurogenic motoneuron diseases such as ALS.

CHAPTER 3: RECOVERY OF FUNCTION IN A MYOGENIC MOUSE MODEL OF SPINAL BULBAR MUSCULAR ATROPHY

Abstract

Spinal bulbar muscular atrophy (SBMA) is a neurodegenerative disease caused by a CAG repeat expansion in the androgen receptor (AR) gene, typically viewed as a disease that begins in motoneurons. However, transgenic (tg) male mice expressing a wildtype rat AR cDNA exclusively in skeletal muscle fibers display core features of SBMA, including obvious kyphosis and loss of motor function, challenging this assumption. Tg females have normal motor function until treated with testosterone (T). We now show that despite profound motor dysfunction, such T-treated tg females exhibit no loss of muscle fibers or motor axons. Moreover, muscles from such tg females show denervation-like changes in gene expression, suggesting that changes in synaptic transmission may critically mediate the loss of motor function characteristic of SBMA. Tg females rapidly recover function after T treatment ends. Results from our model suggest that androgens act on ARs in muscle to trigger SBMA, possibly through synaptic dysfunction, but can be fully reversed.

Introduction

Spinal bulbar muscular atrophy (SBMA) is an adult onset, slowly progressive lower motoneuron disease characterized by proximal spinal and bulbar muscular weakness and atrophy. The known cause of SBMA is an expansion of a CAG repeat in the androgen receptor (AR) gene, resulting in an expanded polyglutamine repeat in the AR protein (La Spada et al., 1991). Signs of androgen insensitivity are also present, such as gynecomastia, testicular atrophy, and reduced fertility (Kennedy et al., 1968; Arbizu et al., 1983; Nagashima et al., 1988; Sobue et al., 1989; Dejager et al., 2002). Most clinical evaluations conclude that muscle pathology exhibited by SBMA patients represents neurogenic atrophy, resulting from motoneuron death, and that muscle pathology (myopathy) is secondary (Zoghbi and Orr, 2000).

However, a primary role of muscle in SBMA has been implicated by our transgenic (tg) mouse model in which the wildtype (wt) AR is over-expressed exclusively in muscle fibers (Monks et al., 2007). These mice have a rat AR cDNA driven by the HSA (human skeletal α-actin) promoter, which selectively drives transgene expression in muscle fibers (Monks et al., 2007). We created these mice to test hypotheses unrelated to neuromuscular disease, but unexpectedly found that tg mice exhibit a male biased, androgen-dependent disease phenotype like that of SBMA (Monks et al., 2007). Specifically, gonadally intact tg males show a loss of motor function that tg females do not. However, once tg females are treated with androgens they rapidly develop a disease comparable to that of tg males. Disease symptoms in late-stage tg

males are accompanied by deficits in the number of muscle fibers and motor axons, consistent with cell loss causing the motor dysfunction. However, castration can restore motor function in severely diseased tg males, casting doubt on the relationship between cell loss and motor dysfunction. Finally, muscles of symptomatic tg males show changes in gene expression that have been implicated in SBMA (Sopher et al., 2004; Yu et al., 2006b), and are suggestive of denervation (Klocke et al., 1994; Kostrominova et al., 2005), including increases in mRNA for AChRα, myogenin and myoD and a decrease in VEGF mRNA.

The current study addresses several remaining questions. Does comparable cell loss accompany the loss of function in T-treated tg females? Can severely compromised tg females recover motor function after the end of androgen treatment, comparable to the effect of castration in severely diseased tg males? Finally, will androgen induce the same changes in muscle gene expression in tg females as in diseased tg males, and will such changes reverse once androgen treatment ends? We now show that the precipitous loss of motor function induced by androgens in tg females is completely reversed within a week of halting treatment. We further show that impairment of motor function is independent of cell loss but is accompanied by androgen-dependent changes in muscle gene expression that also revert to normal once androgen treatment ends.

Methods

Generation and identification of transgenic mice. Transgenic (tg) mice were generated and genotyped as previously described (Monks et al., 2007). Two lines were selected for in-depth characterization: a severely affected line (L141) that expresses high levels of AR and a less severely affected line that expresses lower levels of the transgene (L78) (Monks et al., 2007). Tg animals from these two founding lines were mated to C57/BL6J mice and their progeny were analyzed. Animals were group housed, with water and food provided *ad libitum*. All animal procedures were approved and performed in compliance with the Michigan State University Institutional Animal Care and Use Committee, in accordance with the standards in the NIH Guide for the Care and Use of Laboratory animals.

Androgen dependence in tg females. Tg and wildtype (wt) age-matched females (70-126 days) from L141 and L78 were ovariectomized under deep anesthesia using isoflurane, and given either a testosterone (T)-containing or blank Silastic capsule (1.57 mm i.d. and 3.18 mm o.d., effective release length of 6 mm) s.c. just caudal to the scapula. Incisions were closed by suturing the muscle wall and with 9mm staples. The T capsule resulted in low physiological levels of T (11.29 nmol/L $\pm$ 1.28 nmol/L, n=33) comparable to endogenous wt male mice levels (16.19 nmol/L $\pm$ 3.7 nmol/L, n=31). Behavior was measured 2-4 hours before surgery (Day 0) and on Days 3, 5, 7, 9 after surgery. Most animals from L141 were sacrificed on day 9, but a few had to be sacrificed on Day 7, due to severe disease progression. Only females surviving to 9 days

were included in statistical analyses. Some females from L78 were sacrificed after 9 days, but because L78 tg females did not express a disease phenotype at that time, we extended the treatment period for some females to 8 weeks to determine whether a longer exposure to T would induce disease. T levels after 8 weeks (9.5 $\pm$ 1.2 nmol/L, n=7) were comparable to females treated for only 10 days (see above). Behavioral data on L141 tg females has been previously reported (Monks et al., 2007), and these same females were included in our analysis of cellular measures that we report here.

Recovery of function after T treatment. To assess whether the effects of T on motor function are reversible, a separate group of females from the symptomatic L141 line were ovariectomized and given either a T or a blank capsule as described above. On day 9, these females were re-anesthetized and capsules were *removed.* All behavior tests were measured on days 0 (before T treatment), 1, 3, 5, 7, 9 (during T treatment), and on days 10, 12, and 15 (1, 3 and 6 days after T removed) except for rotarod performance, cage activity, and stride length which were measured only on Days 0, 9 and 15. Animals were sacrificed after behavioral testing on day 15, and tissues harvested.

Behavioral methods. Motor function was evaluated using the hang test, stride length, and rotarod task as previously described (Monks et al., 2007). Grip strength was also assessed using a grip strength meter (Columbus Instruments) to measure forelimb grip strength, and combined hindlimb and forelimb grip strength as in other mouse models of SBMA (Chevalier-Larsen et al., 2004; Yu et al., 2006b). The grip strength meter was positioned horizontally, and mice were

held by the tail and lowered toward the apparatus. Mice were allowed to grasp the metal grid with their forelimbs only, or all limbs and then were pulled off. The force applied to the bar at the moment the grasp was released was recorded as the peak tension (g). The test was repeated 6 consecutive times within the same session, and the highest and lowest value from the 6 trials was dropped. The remaining four values were averaged together and recorded as the grip strength for that animal. For cage activity, four quadrants were drawn on a piece of paper and placed underneath a clear mouse cage. Each mouse was placed into the clear cage and the number of quadrants visited and the numbers of rears were recorded during 30 seconds.

Tissue harvesting and processing. Animals were deeply anesthetized with isoflurane. Extensor digitorum longus (EDL) muscles were placed in OCT filled cryomolds, frozen in liquid nitrogen, and stored at -80° C until sectioned on a cryostat (Leica) at 10um. Anterior tibialis muscles were also harvested and either frozen with liquid nitrogen in OCT filled cryomolds, or in microcentrifuge tubes on dry ice, for mRNA analysis. Spinal columns were placed in buffered formalin for at least 30 days before lumbar four and five (L4 and L5) ventral roots were harvested. L4 and L5 roots were embedded in Epon resin (Araldite 502: Poly/Bed 812: DDSA) and semi thin 1um cross sections collected and stained with toluidine blue.

Morphometric Analysis. Muscles and ventral roots were quantified as previously described (Monks et al., 2007). Briefly, 10um EDL cross sections were stained with hematoxylin and eosin (H&E), and every fiber

was counted in a single cross section from the belly of the muscle. Muscle fiber size was measured using the Stereo Investigator program (MicroBrightfield) to obtain unbiased samples. All motor axons were counted from single cross sections of L4 and 5 ventral roots. Cross sectional area of motor axons was also estimated from the same sections using the Stereo Investigator program (MicroBrightfield).

Gene expression analysis. Total RNA isolated from anterior tibialis muscles with Trizol (Invitrogen) served as a template for cDNA synthesis using the High Capacity cDNA Archive Kit from Applied Biosystems. Gene-specific primers and probes labeled with a fluorescent reporter dye and quencher were used (Applied Biosystems) for *acetylcholine receptor* α-*subunit* (AChR), *myogenin* and *myogenic differentiation factor 1* (MyoD). TaqMan assays were performed using 5 ng aliquots of cDNA. Replicate tubes were analyzed for the expression of 18S ribosomal RNA (rRNA) using a VIC-labeled probe. Threshold cycle (Ct) values were determined by an ABI Prism 7900HT Sequence Detection System, and relative expression levels were calculated using the standard curve method of analysis. Values are expressed relative to the control group.

Vascular endothelial growth factor isoform 164 and 188 (VEGF) mRNA was measured as previously described (Monks et al., 2007). Briefly, total RNA was isolated from limb muscles using Trizol and analyzed using gel electrophoresis and spectrophotometry. Samples were DNase I treated prior to reverse transcription using a dT_20 VN primer (Sigma, Oakville,ON) with SuperScript II. Resultant cDNA was diluted 1:8 for future use. Each cDNA

reaction had a control reaction without reverse transcriptase (no RT control). qPCR reactions were then assembled using SYBR Green Jumpstart Taq ReadyMix (Sigma, Oakville, ON) and VEGF primers (atcttcaagccgtcctgtgt and aatgctttctccgctctgaa) or GAPDH primers (caaggctgtaggcaaagtc and gaccacctggtcctctgtgt). Samples were incubated at 95C for 10 min prior to thermal cycling (40 cycles of: 95C for 30 s, 57C for 30 s, and 72C for 30 s) using the Mx4000 System (Stratagene, La Jolla, CA). Melting curves were determined for all PCR products. The ROX-normalized fluorescence measurements analyzed using the LinRegPCR program to correct for efficiency of each reaction. The expression of VEGF was normalized to the level of GAPDH within each sample.

Statistics. Data were analyzed using Statview 5.0.1. To assess the effects of testosterone administration on body weights and behavioral measures, 3-Way ANOVAs were performed using treatment (two levels) and genotype (2 levels) as between-subject measures, and time as a within-subject, repeated measure. To assess the effects of testosterone on cellular measures such as muscle fiber number, axon number, fiber size, axon size, and relative gene expression, 2-way ANOVAs were performed with treatment and genotype as between-subjects factors. To assess recovery of motor functions after T removal, 2-way ANOVAs were performed with treatment (2 levels) as a between-subjects factor and time as a within–subjects factor. Significant 2-way interactions were found on all behavioral tests; therefore unpaired t-tests were performed at individual time points to determine when the two treatment groups

differed. Unpaired t-tests were performed to compare gene expression levels between the two groups. For all analyses, $p \leq .05$ were considered significant.

Results

Motor function rapidly recovers after the end of testosterone treatment.

L141 tg females treated with testosterone (T) capsules rapidly develop a neuromuscular disease phenotype consisting of a marked loss of motor strength (Monks et al., 2007). To determine whether the androgen-induced phenotype is reversible, we treated a cohort of L141 tg females with T for 9 days and then *removed* the capsules. The statistical analyses revealed significant main effects of treatment and time on all measures, and significant interactions (Table 2). Although performance and body weight is equivalent between the two tg groups at day 0 (just before treatment begins), T induces a rapid decline in both body weight and motor performance during the 9 day treatment period (Figure 14). T-treated tg females lose 30% of their body weight during this time, and develop large deficits in motor performance. However, once the T capsules are removed, tg females regain motor function within 3 days (Figure 14B-D). Body weight lags behind recovery of motor function but is fully restored a week after T treatment ends (Figure 14A). T-treated tg females also show marked deficits in rotarod performance, stride length and cage activity by day 9 but recovered fully on these measures by 6 days after the end of T treatment (Figure 14E- I). These data suggest that changes in muscle strength occur independent of changes in body weight. A similar dissociation is observed during disease progression, when

losses in muscle strength based on forelimb grip strength and the hang test precede losses in body weight (see Figure 14A-D).

L78 tg females do not lose motor functions when given testosterone.

In contrast to L141 tg females (Figure 15A-D), T treatment of tg females from the L78 line, in which tg males are asymptomatic, does *not* cause weight loss (Figure 15E), or muscle weakness after 9 days (Figure 15F – H). In fact, tg females gained weight and improved performance on the hang test during this period, leading to significant effects of time on these measures (Table 3). There were no main effects of genotype, or hormone treatment on other behavioral measures (Table 3). No motor deficits were seen in L78 tg females even after 8 weeks of T treatment (data not shown).

L141 tg female mice show a decline in food intake, after motor deficits are evident.

L141 tg female mice show a decline in food intake, starting after 4 days of T-treatment, which continues until the end of the 9 day treatment period (Figure 16A, ps<.05). Notably the reduction in food intake occurs after motor deficits appear. Significant main effects of genotype ($F(1,17)=7.3$, $p=.01$), treatment ($F(1,17)=13.6$, $p=.001$), and time ($F(8,136)=14.6$, $p=.0001$) were found. There were no significant effects of genotype or treatment on water intake (

Figure 16B), although it did vary over time ($F(7,133)=4.4$, $p=.0002$). Food efficiency was also calculated (body weight/food intake), and remained unchanged (Figure 16C). No significant main effects on genotype, or treatment were found, however there was a main effect of time ($F(8,112)=6.6$, $p=.0001$). Post-hoc analyses were performed on days 2-9 to eliminate the effects of surgery on food intake. Blood glucose levels were measured with a glucose meter in L141 T-treated tg females, and appeared to be lower than either blank treated tg females, and blank or T-treated wt females at the time of sacrifice [wt/blank = 393 mg/dl (n=2), wt/Tcap = 240 mg/dl (n=1), tg/blank = 341 mg/dl (n=2), tg/Tcap = 115 mg/dl (n=2)]. Together these data suggest that a loss of motor function contributes to the reduction in food intake, and that glucose metabolism is as expected for a fasting animal.

No loss of muscle fibers or ventral axons despite profound losses of motor function in L141 tg female mice.

Because L141 T-treated tg females show severely compromised motor function, we asked whether cellular losses accompanied the loss of motor function in this line. Unexpectedly, T did not affect the number of EDL muscle fibers (Figure 17A), nor their size (Figure 17B) despite its devastating effect on motor function in L141 T-treated tg females. Similarly, neither the number nor size of motor axons in L4 and L5 were significantly affected by T in L141 tg females (Figure 17E). There were no significant main effects of either genotype or hormone treatment on any of these measures (Table 4). Cellular measures

were not examined in L78 mice, given that no losses in muscle fibers or axons were seen in symptomatic L141 tg females. These results indicate that neither motoneuron nor muscle fiber losses are required for deficits in motor function, suggesting cell dysfunction rather than loss underlies the motor deficits triggered by T in tg females.

Both symptomatic L141 and asymptomatic L78 tg females show histopathology in skeletal muscles.

EDL muscles were analyzed for pathological markers of neuromuscular disease. H&E staining reveals that L141 tg females treated with T show both small angular and rounded fibers suggestive of neurogenic atrophy and occasional fibers with centralized nuclei (Figure 18A). However, the frequency of fibers containing centralized nuclei is low in both T- and control-treated L141 tg muscles and not significantly different (0.39% $\pm$ 0.18 vs. 0.51% $\pm$ 0.13, respectively), suggesting that this pathological marker is unrelated to expression of the disease phenotype. While pathology in muscles of symptomatic L141 tg females is qualitatively similar to that seen in L141 tg males (Monks et al., 2007), it was considerably less marked. For example, NADH staining suggests only mild increases in oxidative metabolism in T-treated L141 females (Figure 18B). Surprisingly, muscles from L78 tg females that remain asymptomatic after 8 weeks of T treatment also showed pathology consisting of occasional centralized nuclei and altered myofilament organization (Figure 18C, D). Some muscle

fibers exhibit a central core of dark NADH staining, suggesting an area rich in mitochondria and largely devoid of myofilaments, (Figure 18D). This is in contrast to the relatively uniform distribution of mitochondria and myofilaments normally seen in skeletal muscle fibers, and in contrast to central core myopathies, ring fibers, and target fibers (Mills, 2007). However, given that this "donut" pattern of staining is most prominent in muscles of T-treated L78 tg mice that exhibit *normal* motor function, such pathology is apparently unrelated to muscle strength.

Changes in muscle gene expression indicative of denervation in L141 but not L78 tg females.

We next examined the expression of three genes that are upregulated in L141 symptomatic tg males (Monks et al., 2007), *myogenin*, *acetylcholine receptor α-subunit (AChR)*, and *myogenic differentiation factor 1* (*myoD*), using reverse transcriptase quantitative-PCR (qPCR). There were significant main effects on AChR and myogenin gene expression (Table 5). Muscles of symptomatic T-treated L141 tg females show a significant upregulation of AChR (Figure 19A, $p<.0025$) and myogenin (Figure 19B, $p<.0033$) after 9 days of T treatment. There was a similar upregulation of myoD expression, although this response fell short of significance (Figure 19C, $p=.09$), comparable to that seen in a knock-in (KI) polyglutamine mouse model of SBMA (Yu et al., 2006b). Muscle gene expression in tg females without T were comparable to wt control females, showing no effect on these genes in wt muscle. Importantly, no such

changes were observed in behaviorally asymptomatic L78 tg females treated with T for 9 days (Figure 19E-G, Table 5). Because expression of these genes is similarly increased in denervated muscles (Klocke et al., 1994; Kostrominova et al., 2005), these data suggest denervation of muscles may underlie the loss of motor function in T-treated L141 tg females.

We also examined gene expression of *vascular endothelial growth factor* (VEGF), which is downregulated in muscles of symptomatic L141 tg males (Monks et al., 2007). VEGF mRNA was expressed at lower levels in T-treated tg L141 females (Figure 19D), although this decrease did not reach statistical significance compared to blank-treated tg females ($p=.07$). In asymptomatic L78 females, T did not affect VEGF expression levels (Figure 19H).

Expression of most genes recovers after testosterone treatment ends.

qPCR revealed that the genes upregulated in T-treated tg females were restored to normal levels 6 days after the end of T treatment. AChR, myogenin and myoD mRNA were the same in muscles of blank-treated tg females as in muscles of tg females that had formerly received T (Figure 19I-K). Surprisingly, there was a significant reduction in the level of VEGF mRNA in females that had previously received T (Figure 19L, $p<.0096$), suggesting that L141 tg females may indeed suffer a loss of VEGF during T-treatment and that the loss persists after the recovery of function.

Discussion

Normally L141 tg females overexpressing wildtype AR in muscle fibers are asymptomatic, yet rapidly lose motor function when provided with male-typical levels of T. We have found T exposure is fatal after 9 or 10 days in tg females, and death in these animals may result from motor dysfunction that is too severe to permit eating or drinking. However, L78 tg females, which express the AR transgene at a lower level (Monks et al., 2007), do not develop a disease phenotype after T treatment. Furthermore, after 9 days of T treatment which brings L141 females close to death, full recovery from behavioral symptoms can be achieved after just 3 days of T cessation. This rapid recovery seems inconsistent with any possible recovery in the number of motoneurons, motoneuronal axons or muscle fibers and indeed we find no significant losses in either muscle fibers or motor axons after 9 days of T-treatment. These findings call into question whether cell loss plays any role in the behavioral deficits seen in our T-treated tg mice.

qPCR indicates that transcripts of *myogenin*, and *acetylcholine receptor* α-*subunit*, which are elevated following denervation (Klocke et al., 1994; Kostrominova et al., 2005), are also increased in L141 tg females given T, comparable to levels seen in a KI model of SBMA (Yu et al., 2006b). The upregulation of these genes by T *only* in symptomatic L141 tg females, and not in asymptomatic L78 tg nor wt mice indicates that this response to T may underlie the loss of motor function. Because expression of AChR and myogenin are similarly increased by denervation, muscle denervation may occur early in the

disease process. Skeletal muscles affected by Huntington disease, another polyglutamine expansion disorder, do not show a similar response (Strand et al., 2005), suggesting this increased gene expression is specific to motoneuron diseases such as SBMA, and spinal muscular atrophy (Sedehizade et al., 1997).

Although VEGF levels were not significantly different in our L141 females treated with T for nine days, it was significantly different in L141 females 6 days after T capsules were removed. This suggests that either VEGF was indeed lower at nine days and we failed to detect it, or that VEGF mRNA levels are slower to change than mRNAs for AChR, myogenin and myoD. However, given that the downregulation in VEGF mRNA persisted after motor function recovered, the decline in VEGF may not contribute to the loss of motor function in T-treated tg female mice. Therefore, deficits in VEGF may be a response rather than a cause of disease. Alternatively, other trophic factors could be compensating for a loss of VEGF.

The upregulation of AChR and myogenin could also be due to regenerative processes in the muscle. MyoD family members (including myogenin), and AChR are typically upregulated in muscle satellite cells during development and regeneration (Duclert et al., 1991; Shi and Garry, 2006). It is not yet clear whether the increases in gene expression reflect regeneration of damaged muscle fibers, denervation or both. Future studies directly examining neuromuscular synapses may help answer this question. Importantly, upregulation of AChR and myogenin, and downregulation of VEGF, is also seen in other mouse models of SBMA (Sopher et al., 2004; Yu et al., 2006b),

suggesting that the androgen-dependent loss of motor function exhibited by these various models may involve the same pathogenic events originating in muscle.

Cellular dysfunction appears to underlie the deficits in motor function, both in our model and others (Katsuno et al., 2002; Chevalier-Larsen et al., 2004; Monks et al., 2007). T-treated tg females do not appear to lose either muscle fibers or motor axons despite significant losses in motor function. Because recovery of function is possible, this too suggests that dysfunction rather than cellular loss underlies the loss of function. In AR-122Q mice described by Chevalier-Larsen et al. (2004), substantial motor deficits are present in males but no motoneuron losses or muscle pathology were observed, indicating that dysfunction is responsible for the loss of motor function (Chevalier-Larsen et al., 2004). It is also notable that the AR-97Q mice described by Katsuno et al. (2002) develop signs of neurogenic muscle atrophy, without motoneuron loss. These findings also support the idea that the neurological phenotype associated with SBMA may result from neuronal dysfunction rather than neuronal loss. Importantly, data from our model suggest this neuronal dysfunction can be triggered by signals that originate in the muscle.

Fiber type grouping was not evident in NADH stained EDLs in our T-treated tg female mice, suggesting that fibers have not been re-innervated by collateral sprouts. However, because the pattern of gene expression suggests denervation, it may be that synaptic dysfunction rather than loss is involved. If dysfunctional motor terminals still occupy the junction, this might preclude

sprouts from re-innervating such junctions. It is also possible that early perturbations in axonal transport without motoneuronal loss could contribute to losses in motor function and produce the denervation-like profile in the muscles, as suggested by data in our model (Kemp and Jordan, personal communication) and other models of SBMA (Chevalier-Larsen et al., 2004; Katsuno et al., 2006a).

Histology in H&E stained muscles shows a pathological feature of centralized nuclei in some fibers, however, we find that such fibers with internal nuclei are no more frequent in T-treated L141 mice with poor motor function than in control-treated tg females that have normal motor function. This suggests that the centralized nuclei in our model are unrelated to the loss of motor function. Also unrelated to a loss of motor function in our model is the alteration in the myofibrillar network in NADH stained EDL, as we see more of this type of pathology in asymptomatic L78 tg females. Thus, such basic histological markers used regularly to diagnose disease are likely an epiphenomenon rather than a cause of disease.

Our model is highly androgen-dependent, and we can quickly "turn on" or "turn off" the disease in our tg females. When T is removed from females, they quickly recover motor functions and body weight within days, adding to a growing body of literature that the symptoms of SBMA can be reversed. For example, tg mice broadly expressing a 97 polyQ AR also exhibit profound androgen-dependence (Katsuno et al., 2002). T treatment of tg females induces disease, while castration of males ameliorates symptoms (Katsuno et al., 2002). In a

different tg model that expresses a 112 polyQ AR, males are more severely affected than females, and castration ameliorates symptoms in tg males (Chevalier-Larsen et al., 2004). Androgen-dependence has also been demonstrated in a human case. T will worsen symptoms of patients with SBMA, while cessation of T treatment restores motor function to pretreatment levels (Kinirons and Rouleau, 2006).

While our mice do not express the expanded polyQ allele of the AR, they recapitulate many key features of SBMA, as seen in both humans and in other mouse models of this disease, and suggest that there is a common etiological pathway involved. One likely candidate is changes in muscle which trigger synaptic dysfunction, inducing a denervation-like atrophy. Our tg mice offer an unique opportunity to study early disease mechanisms that precede motor dysfunction, allowing insight into the mechanisms which trigger disease. Cellular and molecular changes seen in late-stage SBMA patients may reflect the result, rather than the cause, of motor dysfunction. Additionally, these mice lend themselves to testing therapeutics, as the phenotype develops quickly and is fully reversible. Our studies demonstrate that muscle is an important site of disease pathogenesis in SBMA, and raises the possibility that interfering with androgen action in muscles will ameliorate motor dysfunction in this disease.

CHAPTER 4: FLUTAMIDE IS PROTECTIVE IN A MYOGENIC MOUSE MODEL OF SPINAL BULBAR MUSCULAR ATROPHY

Abstract

Spinal Bulbar Muscular Atrophy (SBMA) is caused by a CAG repeat expansion in the androgen receptor (AR) gene. The toxicity of mutant AR is only realized when activated by ligand, suggesting that interference with AR activity might be therapeutic. Expressing a wildtype (wt) AR transgene exclusively in skeletal muscle fibers causes an androgen-dependent SBMA phenotype in mice, but few transgenic (tg) males survive birth. We now report that the androgen antagonist flutamide rescues males from perinatal death. Tg females are asymptomatic unless treated with testosterone (T), which rapidly induces disease. Flutamide also ameliorates disease progression in such T-treated tg female mice. Introducing the AR transgene into otherwise AR-deficient (tfm) mice induces an androgen-dependent loss of motor function, demonstrating that AR acting in muscle fibers alone can induce SBMA symptoms. Flutamide may be an effective therapeutic for SBMA and may act through muscles to ameliorate symptoms.

Introduction

Spinal Bulbar Muscular Atrophy (SBMA) is an X-linked, slowly progressing disease characterized by adult onset muscle weakness and atrophy, and motoneuron loss. Signs of androgen insensitivity, such as gynecomastia, testicular atrophy, and reduced fertility, are also present (Kennedy et al., 1968; Arbizu et al., 1983; Nagashima et al., 1988; Sobue et al., 1989; Dejager et al., 2002). In humans, the cause of SBMA is an expansion of a trinucleotide CAG repeat, which encodes a polyglutamine (polyQ) tract in the amino terminus of the androgen receptor (AR). An expansion in the polyQ tract in other, unrelated proteins has been linked to eight other neurodegenerative diseases, including Huntington's disease (HD), and the spinocerebellar ataxias (SCA) types 1,2,3,6,7,17. For most polyQ diseases, the protein is thought to confer a toxic gain of function although a loss of normal function may also play a role in some of these diseases (Orr and Zoghbi, 2007). However, rats, mice and humans that are completely androgen-insensitive because of the testicular feminization mutation (*tfm*) in the AR gene, exhibit no neurodegeneration (Ono et al., 1974; Wilson and Davies, 2007), suggesting a toxic gain of AR function rather than loss of function underlying SBMA pathology.

Unlike the affected proteins in other polyQ diseases, the function of normal AR protein is relatively well understood, including critical functions in sexual differentiation and male reproduction (Morris et al., 2004; Wilson and

Davies, 2007). Moreover, there are numerous pharmacological tools available to modify AR function. Given recent data suggesting that SBMA is an androgen-dependent disease (Katsuno et al., 2002; Chevalier-Larsen et al., 2004), flutamide is a natural choice for therapy, since it is a potent AR antagonist, successfully treating prostate cancer (Antonarakis et al., 2007). However, in animal and cell models, anti-androgens such as flutamide have had mixed results, having no effect or worsening symptoms (Takeyama et al., 2002; Katsuno et al., 2003b). Because flutamide causes AR to translocate to the nucleus but blocks its activation, these results raise questions about whether activation per se or nuclear accumulation of AR is required for pathogenesis (Katsuno et al., 2002; Takeyama et al., 2002; Katsuno et al., 2003b).

Our transgenic (tg) mouse model that expresses wt AR at relatively high levels only in striated muscle fibers shows the same androgen-dependent loss of motor function (Monks et al., 2007) as seen in those mouse models of SBMA expressing the expanded polyQ AR allele (Katsuno et al., 2002; McManamny et al., 2002; Chevalier-Larsen et al., 2004; Sopher et al., 2004; Yu et al., 2006c). The androgen-dependent manner of the disease is striking in our model. Many tg male mice die on the day of birth, possibly because of the surge of testosterone at this time (Ward and Weisz, 1980; Weisz and Ward, 1980; Motelica-Heino et al., 1988), but those that survive the perinatal period exhibit an androgen-dependent loss of motor function. Castration of these diseased males in *adulthood* largely restores motor function. Moreover, we find that testosterone

(T) treatment of otherwise *asymptomatic* adult tg females rapidly induces SBMA symptoms (Monks et al., 2007).

Given the controversy regarding the efficacy of AR antagonists, we tested flutamide in our model. We now report that flutamide is indeed effective in rescuing tg males from perinatal death, and that such "rescued" males express the expected disease phenotype as adults. The muscles from these males show changes in gene expression consistent with denervation comparable to that reported previously for tg males not rescued by prenatal flutamide (Monks et al., 2007). We also found flutamide largely protects tg females from the disease-inducing effects of T exposure in adulthood. Finally, we introduced the tg into AR-deficient (*Tfm*) male mice, which therefore have functional ARs only in muscle fibers (Monks et al., 2007). These males display the SBMA phenotype, demonstrating that AR activation in muscle fibers alone is sufficient to account for these symptoms of SBMA. These data provide striking evidence that AR acting exclusively in *muscle fibers* can lead to an SBMA disease phenotype, which can be fully ameliorated by blocking activation of AR.

Methods

Generation and identification of transgenic mice. Transgenic (tg) mice were generated and genotyped as previously described (Monks et al., 2007). Animals were group housed, with water and food provided *ad libitum*. All animal procedures were approved and performed in compliance with the Michigan State

University Institutional Animal Care and Use Committee, in accordance with the standards in the NIH Guide for the Care and Use of Laboratory animals.

Prenatal flutamide rescue of tg males. Timed pregnant dams from tg line 141 (L141) were injected with 5 mg flutamide/ 0.1 ml propylene glycol s.c. on gestational (G) days 15 – 20 (the day females were mated was designated as day 0). Ano-genital distance (AGD) of resulting pups was measured at weaning to confirm that the dose of flutamide was effective. Motor function was assessed in resulting tg and wt males at 5 weeks of age, and weekly until sacrificed (64-197 days), using the hang test and stride length as described below.

Generation of tg/tfm males. A tg L141 male produced in the colony (without prenatal flutamide treatment) had sperm harvested for *in vitro* fertilization (University of Michigan Transgenic Animal Model Core, Ann Arbor, MI). *Tfm* female carriers were superovulated and eggs harvested. After fertilization, embryos were transferred into pseudopregnant recipient B6D2F1/J mice. Four founding females were produced carrying both the transgene and the *tfm* allele. Founding females were bred with C57Bl/J6 males, and were treated with flutamide as described above during gestation except treatment began one day earlier (G14 – 20). Male offspring were of four different genotypes: wt, *tfm*, tg or of particular interest to us, mice that had both the *tfm* allele of the endogenous *AR* gene and the transgene expressing wt AR in skeletal muscles (tg/tfm). Male tfms exhibit low levels of circulating testosterone (T) in adulthood (Zuloaga et al., 2008a), so were treated with T at 124 days of age to determine whether such mice would express an SBMA phenotype when the *only* ARs available for

activation are in muscle fibers. Two tfm males and three tg/tfm males were implanted with one T-filled Silastic capsule (1.57 mm i.d., 3.18 mm o.d., effective release length of 6 mm) under isoflurane anesthesia, which results in low physiological levels of T (Zuloaga et al., 2008b). Body weights, grip strength, rotarod, hang test, open field cage activity and stride length were collected immediately prior to surgery (day 0), and on days 1, 3, 5, 7, 9 post T implantation. On day 9, T capsules were removed and recovery of motor function was monitored on days 10, 12 and 15.

Flutamide rescue of testosterone treated tg females. Twelve adult (97-136 day old) tg L141 female mice were pre-treated with either flutamide (n=6, 5mg/day in 0.1ml propylene glycol) or vehicle (n=6) delivered via s.c. injection one day prior to ovariectomy. Females were ovariectomized under isoflurane anesthesia, and each were given a testosterone (T) filled Silastic capsule (described above). Flutamide (5mg/day in 0.1ml propylene glycol) or 0.1 ml vehicle (propylene glycol) treatment was continued on the day of surgery and daily thereafter. Behavioral measurements were taken on the day of surgery (Day 0, before surgery), and on days 3, 5, 7, and 9 after surgery, except grip strength, which was measured daily. A second cohort of tg females were also treated as above, except were sacrificed on Day 7. Vehicle (n=1) and flutamide (n=2) treated tg females, 10-14 months of age, were used to generate spinal cords for AR immunohistochemistry.

Behavioral methods. Hang test, gait analysis, and rotarod were measured as previously described (Monks et al., 2007). Grip-strength was

assessed using a grip strength meter (Columbus Instruments) to measure forelimb grip strength, and combined hind limb and forelimb grip strength. The grip strength meter was positioned horizontally, and mice were held by the tail and lowered toward the apparatus. Mice were allowed to grasp the metal grid with their forelimbs only, or all limbs and then were pulled off. The force applied to the bar at the moment the grasp is released was recorded as peak tension (g). The test was repeated 6 consecutive times within the same session, and the highest and lowest value from the 6 trials was dropped. The remaining four values were averaged together and were recorded as the grip strength for that animal (Chevalier-Larsen et al., 2004). Cage activity was assessed by measuring the number of horizontal and vertical movements in a novel environment (16"x 16" Plexiglas chamber) during 5 minutes, using the Versamax activity monitor (AccuScan Instruments, Columbus, OH). The chamber was cleaned with 70% ethanol between each test. Data were analyzed using the Versamax software.

Tissue harvesting and processing. Animals were deeply anesthetized with isoflurane. Extensor digitorum longus (EDL) muscles were collected, weighed, placed in OCT filled cryomolds, and frozen in liquid nitrogen. Muscles were cryostat (Leica) sectioned at 10um, and stored at -80°C. In males, anterior tibialis (TA) muscles were also frozen in OCT filled cryomolds in liquid nitrogen and later used for RNA analysis. In females, TA muscles were harvested and frozen on dry ice in microcentrifuge tubes for RNA analysis. Spinal columns were placed in buffered formalin for at least 30 days before harvesting the fifth

lumbar (L5) ventral root. L5 ventral roots were embedded in Epon resin (Araldite 502: Poly/Bed 812: DDSA) and sectioned at 1um.

The second cohort of tg females were deeply anesthetized with isoflurane, perfused with saline followed by 4% paraformaldehyde, and spinal cords were harvested. Spinal cords were post-fixed for one hour, and transferred to 20% phosphate buffered sucrose. Spinal cords were sectioned at 30 um using a freezing sliding microtome.

Morphometrical analysis. Muscles and ventral roots were quantified as previously described (Monks et al., 2007). Briefly, every fiber was counted in one cross section taken from the belly of the EDL muscle that was stained with hematoxylin and eosin (H&E). Fiber size was measured from this same cross section using the Stereo Investigator program (MicroBrightfield) to ensure unbiased sampling. Alternate sections of EDL were stained with NADH. Motor axons were counted in a single cross section of L5 ventral root and their size measured on the Stereo Investigator program (MicroBrightfield) as previously described (Monks et al., 2007).

Androgen receptor immunostaining. Spinal cord and EDL muscle sections were blocked for nonspecific staining in 10% normal goat serum and then incubated with 1.07 µg/ml of PG-21 antiserum (1:1,000 for spinal cords, 1:500 for muscles, kindly provide by Gail Prins) for 48 hrs at 4° C. ARs were visualized using a peroxidase Elite ABC kit (half strength, Vector Laboratories), and a biotinylated goat anti-rabbit secondary (1:400 for spinal cords, 1:3200 for

muscles) and nickel-enhanced 0.025% diaminobenzidine in 0.05 M tris (pH 7.2) as the chromogen and 0.006% vol/vol hydrogen peroxide as previously described (Jordan et al., 1997; Zuloaga et al., 2006). Muscles sections were double labeled with anti-rat B2 laminin (1:10,000 Chemicon) overnight at 4° C, incubated in mouse adsorbed biotinylated anti-rat secondary antibody (1:200, Vector laboratories) and visualized with Cy3-Strepavidin (1:900). Spinal cords were counterstained with neutral red to visualize cell bodies.

Gene expression analysis. Total RNA isolated from anterior tibialis muscles with Trizol (Invitrogen) served as a template for cDNA synthesis using the High Capacity cDNA Archive Kit from Applied Biosystems. Gene-specific primers and probes labeled with a fluorescent reporter dye and quencher were used (Applied Biosystems) for *acetylcholine receptor* α-*subunit* (AChR), *myogenin* and *myogenic differentiation factor 1* (MyoD). TaqMan assays were performed using 5 ng aliquots of cDNA. Replicate tubes were analyzed for the expression of 18s ribosomal RNA (rRNA) using a VIC-labeled probe. Threshold cycle (Ct) values were determined by an ABI Prism 7900HT Sequence Detection System, and relative expression levels were calculated using the standard curve method of analysis. Values are expressed relative to the control group. *Vascular endothelial growth factor* isoform 164 and 188 (VEGF) mRNA was measured as previously described (Monks et al., 2007). Briefly, total RNA was isolated from limb muscles using Trizol and analyzed using gel electrophoresis and spectrophotometry. Samples were DNase I treated prior to reverse transcription using a dT_20 VN primer (Sigma, Oakville,ON) with SuperScript II. Resultant

cDNA was diluted 1:8 for future use. Each cDNA reaction had a control reaction without reverse transcriptase (no RT control). qPCR reactions were then assembled using SYBR Green Jumpstart Taq ReadyMix (Sigma, Oakville, ON) and VEGF primers (atcttcaagccgtcctgtgt and aatgctttctccgctctgaa) or GAPDH primers (caaggctgtaggcaaagtc and gaccacctggtcctctgtgt). Samples were incubated at 95C for 10 min prior to thermal cycling (40 cycles of: 95C for 30 s, 57C for 30 s, and 72C for 30 s) using the Mx4000 System (Stratagene, La Jolla, CA). Melting curves were determined for all PCR products. The ROX-normalized fluorescence measurements analyzed using the LinRegPCR program to correct for efficiency of each reaction. The expression of VEGF was normalized to the level of GAPDH within each sample.

Statistics. Statistics were analyzed using Statview 5.0.1. For males in experiment 1, a chi square test compared the proportion of tg males alive at weaning when prenatally treated with flutamide versus undisturbed litters. Unpaired t-tests compared flutamide rescued tg males to their wt brothers on behavioral, cellular, and molecular measures. In experiment 2, to assess the effects of flutamide in preventing androgen induced losses in motor function in L141 tg females, 2-way ANOVAs were performed with treatment (2 levels) as an independent, between-subject factor and time as a within subject, repeated measure. Unpaired t-tests comparing the treatment groups were also done at individual time points for post-hoc tests when there were significant effects of time and/or significant treatment and time interactions. In experiment 3, a 2-way ANOVA assessed the effect of T treatment on motor function in tfm versus tg/tfm

males, with genotype as a between subject independent measure, and time as a within subject, repeated measure. For all analyses results were considered significant if $p \leq .05$.

Results

Prenatal flutamide rescues tg males from perinatal death, but does not prevent expression of motor deficits in adulthood.

We treated pregnant dams during late gestation with the anti-androgen flutamide to test whether exposure to prenatal androgens cause the perinatal lethality seen in 141 tg males. Flutamide-exposed tg and wt males exhibited the expected shortened ano-genital distance at weaning, comparable to females (data not shown), confirming that this dose was effective in blocking activation of ARs necessary for prenatal masculinization of the external genitalia. This dose has also been used to successfully feminize male rats (Gladue and Clemens, 1978; Breedlove and Arnold, 1983d; Casto et al., 2003). A chi square test revealed that flutamide treatment clearly rescued some male tg mice (Table 6), significantly increasing the number surviving to weaning when compared to survival of tg male when no prenatal flutamide was given ($p<.0001$, Cramer's V =.271). However, there were still fewer surviving tg males than would be expected by chance alone ($p<.0001$, Cramer's V = .205) among the prenatal flutamide-treated litters. Prenatal flutamide did not alter plasma testosterone

levels in adulthood [flutamide exposed males= 21.0 ± 5.7 nmol/L (n=16) versus unexposed males = 15.9± 5.1 nmol/L (n=15), p = 0.52].

In adulthood, the prenatal flutamide rescued tg males showed a reduced body weight (Figure 20A, p<.0004) compared to their wt brothers (which were also exposed to flutamide prenatally). Flutamide rescued tg males developed comparable motor weakness as reported for L141 tg males unexposed to flutamide (Monks et al., 2007). Flutamide rescued tg males were unable to hang on a wire grid (Figure 20B, p<.001), and showed a shortened stride (Figure 20C, p<.007), similar to the few untreated L141 tg males that survive to adulthood (Monks et al., 2007). We also observed comparable deficits in motor function at all ages examined (as early as 5 weeks).

Additionally, prenatally flutamide rescued tg males show a significant loss of EDL muscle fibers (Figure 21A, p<.008) compared to their wt brothers, but no change in average fiber cross sectional area (Figure 21B, p=.13). Rescued tg males did not show any significant loss in the number of L5 axons at the time of sacrifice (Figure 21C, p=.4798), but did show a reduction in motor axon size (Figure 21D, p=.0199). Suggesting that axons may atrophy before their eventual loss, or perhaps reflecting a reduction in the size of motor units, given the fewer number of muscle fibers available for innervation.

When muscle sections were stained with NADH, fibers in EDL muscles of tg males stained more darkly and showed a more uniform pattern of staining than the checkerboard pattern typical of wt EDL muscle (Figure 22), suggesting a generalized shift toward oxidative metabolism in tg muscles. While the mean

size of muscle fibers was not different in tg and wt males, there were occasional small atrophic fibers observed in cross sections of EDL from tg males (Figure 21).

Quantitative rt-pcr revealed an upregulation in mRNA expression of *acetylcholine receptor alpha* (Figure 23A, p=.0002), *myogenin* (Figure 23B, p=.0002) and *myogenic differentiation factor 1* (Figure 23C, p=.0186) in tg muscles compared to wt muscle, similar to differences reported for untreated tg males (Monks et al., 2007). However, mRNA for *vascular endothelial growth factor* (VEGF) was normal compared to controls (Figure 23D, p=.5), in contrast to the differences reported in untreated tg males (Monks et al., 2007). Importantly, because tg males in this study were compared to their wt male littermates who were also exposed to flutamide prenatally, the differences between tg and wt male mice cannot be attributed to flutamide treatment.

Flutamide ameliorates loss in motor function in tg females given testosterone.

Tg females given testosterone (T) rapidly lose body weight and motor function, dying by days 9 or 10 (Monks et al., 2007). Flutamide on its own does not induce disease in our tg female mice (data not shown), but successfully prevents much of the rapid disease progression induced by T (Figure 24). There was a significant main effect of flutamide on body weight (p=.0007), as these females maintained their body weight completely, unlike females given T plus the vehicle control. Unpaired t-tests revealed that flutamide treated tg females

weighed significantly more on days 4-9 of treatment than vehicle treated tg females (ps<.05, Figure 24A). Flutamide also rescued the motor function of tg females treated with T (Figure 24B – F). Although such flutamide-exposed tg females showed mild losses in motor function over time, they were still significantly improved compared to T-treated females given vehicle, which showed dramatic losses in body weight and motor function over the nine day treatment period. Circulating levels of T were no different between T-treated tg females exposed to flutamide or vehicle (Tcap+vehicle =26.7 + 2.8 nmol/L, Tcap+flutamide =28.6 + 4.1 nmol/L, p=.7), arguing that flutamide improves motor performance not by reducing levels of T but by blocking AR function in the relevant tissues controlling motor function.

Thus, there were significant main effects of flutamide on combined limb grip strength (p=.0009), forelimb grip strength (p=.031) hang test (p=.001), rotarod (p=.011), and stride length (p=.01), in addition to a significant main effect of time and significant interactions of time and treatment on all behavioral measures (Table 7). Grip strength for both forelimbs and all limbs was significantly improved on days 4-9 compared to controls (ps<.05, Figure 24B, C). On the hang test, an improvement was seen as early as day 3 and continued until the end of treatment on day 9 (ps<.05, Figure 24D). Flutamide also significantly improved performance on the rotarod starting at day 5 (ps<.05, Figure 24E), and largely prevented the effects of T on stride length on days 5-9 compared to vehicle controls (ps<.05, Figure 24F). Figure 25 demonstrates that

AR is localized to the nucleus with T + flutamide treatment, as expected, in both muscle and spinal cord sections.

Tfm male mice expressing wt AR only in skeletal muscle fibers develop an androgen-dependent loss of motor function.

L141 tg males crossed onto a tfm background (tg/tfm males) lack functional AR throughout the body, including the brain and spinal cord, with the one exception being skeletal muscle fibers where AR is present due to expression of the transgene (Monks et al., 2007). Because tfm male mice have very low levels of T (Zuloaga et al., 2008a), tfm and tg/tfm males were treated with T in adulthood to raise their T titers to that of normal adult males.

While tg/tfm male mice have a lower body weight than tfm males before T treatment (Figure 26A), they exhibit normal motor function (on day 0) until treated with T (Figure 26B,- E). Remarkably, tg/tfm males develop a profound neuromuscular phenotype when treated with T, while tfm males without the AR transgene do not. There was a main effect of time, and significant interactions on body weight, forelimb and combined limb grip strength, and open field activity (Table 8). T treatment induces significant weight loss only in tg/tfm males and not in tfm males (Figure 26A), starting on days 5-10 (ps <.05). Motor function also rapidly declined with T. Both forelimb and combined limbs grip strength was diminished by day 3 (Figure 26B,C, ps<.0001). Horizontal cage activity during the open field test also showed a similar decline, evident as soon as day 1

(Figure 26D, p<.0006). Vertical movements, or the number of rears, was also reduced by day 3 (Figure 26E, p<.0012). This phenotype is identical to that described for L141 tg males on a C57B/J6 background, as previously reported (Monks et al., 2007). Furthermore, when T treatment ceased, tg/tfm males regained motor function and body weight (Figure 26). One day after T treatment ended on day 10, the number of rears returned to pretreatment levels (Figure 26E, p=.2). By 3 days after T treatment ended, day 12, body weight (p=.4) and forelimb grip strength (p=.4) returned to baseline levels, being no longer significantly different from day 0. By 7 days after T treatment ended, combined limbs grip strength (p=.6), and horizontal cage activity returned to pretreatment levels (p=.18).

Discussion

We found flutamide was indeed effective in our mice, rescuing tg males from perinatal death, and ameliorating the behavioral disorders caused by androgen treatment in adult tg females. The perinatal effect of flutamide on tg males likely ameliorates the surge in T levels at parturition in male rodents (Ward and Weisz, 1980; Weisz and Ward, 1980; Motelica-Heino et al., 1988). However, prenatal exposure to flutamide does not stop disease progression, since flutamide-rescued tg males as adults exhibit deficits in motor function, have fewer muscle fibers and smaller ventral root axons than normal, and die prematurely. Such flutamide rescued tg males also have normal levels of circulating testosterone in adulthood, which appears sufficient to drive disease. Since

motoneuron axon size tends to correlate with the number of muscle fibers each innervates, or motor unit size (Bernstein and Lichtman, 1999), the decreased number of muscle fibers in tg males may mean that motor units are also smaller.

Flutamide rescued tg males did not show axon loss, unlike untreated tg males (Monks et al., 2007). It is possible that unexposed tg males are more severely affected and that if flutamide rescued males were to survive longer they too would show axon loss. In this regard, flutamide rescued tg males closely resemble the model described by Katsuno et al. (2002), where AR-97Q mice express a full length human AR allele under the control of the CMV promoter and exhibit androgen-dependent deficits in motor behavior, signs of muscle atrophy, and reduced axonal size but no loss of motoneurons (Katsuno et al., 2002). Our mice overexpress AR exclusively in muscle fibers; yet exhibit a remarkably similar androgen-dependent phenotype. Our findings suggest an axonal dysfunction resulting in denervation, but in our model, the denervation is triggered by disease events originating in muscle fibers, since this is where the AR transgene is expressed.

However, it is also possible that the reduced size of motor axons reflects a loss of trophic support from muscles that is not causally related to the size of their motor units. While VEGF levels are unaffected in flutamide-rescued tg males, it is possible that other muscle-derived factors are reduced in muscles of affected tg males which may underlie the decrease in axonal size. Glial derived neurotrophic factor (GDNF) and neurotrophin-4 (NT-4) mRNAs in the AR113Q mouse model of SBMA were found to be expressed at lower levels in tg muscles

compared to wildtype muscles (Yu et al., 2006b), and could also be similarly downregulated in our tg model, but this remains to be tested. Axon size is also correlated with neurofilaments, and axons lacking the ability to transport neurofilaments tend to be smaller. In 112Q-AR mice described by Chevalier-Larson (2004), a reduction in unphosphorylated neurofilament heavy chain (NF-H) has been implicated, which could also lead to axonal transport deficits. Schwann cells not only myelinate axons but also maintain their long-term functional integrity, and maintain axon caliber (Bernstein and Lichtman, 1999). Damage to surrounding Schwann cells could also potentially affect axon size and function.

There are several mechanisms by which muscle dysfunction might lead to the retraction of motor nerve terminals and consequently denervation of muscle fibers. Given the large body of evidence indicating that muscle-derived trophic factors critically support motoneurons (Chevrel and Sendtner, 2006) a lack of trophic support from the muscle (either because of cellular dysfunction or cellular loss) could induce axonal atrophy and retraction and eventually motoneuronal death. In that case, motoneuron death would be a late event in the disease process; long after motor function begins to deteriorate. This is consistent with conclusions drawn from several other mouse models of SBMA (Chevalier-Larsen et al., 2004; Yu et al., 2006b). Other molecules could also be involved, such as cytoskeletal elements like neural cell adhesion molecule (N-CAM), agrin, rapsyn, utrophin, and dystrobrevin which help maintain neuromuscular junctions (Sanes and Lichtman, 1999, , 2001).

Flutamide rescued tg males also show an upregulation in gene expression of AChR, myoD, and myogenin, comparable to untreated tg males (Monks et al., 2007). Given that the same genes are upregulated in denervated wt muscle (Klocke et al., 1994; Kostrominova et al., 2005), our results suggest that T may trigger functional denervation of muscles in diseased mice, and that such denervation may contribute to the loss of motor function. VEGF gene expression was not significantly downregulated in flutamide rescued males, unlike tg males not exposed to flutamide (Monks et al., 2007). While it is not clear why VEGF mRNA levels were not similarly reduced in the flutamide rescued tg males, the fact that VEGF levels are normal despite significant motor impairments suggests that deficits in VEGF may be a response rather than a cause of motor dysfunction in this disease.

Evidence based on our tg mice suggests that AR acting only in skeletal muscle fibers is sufficient to trigger SBMA. However, it was possible that the disease phenotype might require activation of *both* the tg AR allele in muscle fibers and the endogenous AR allele in motoneurons. The present results from tg/tfm males argue against this possibility. When the tg mice is put onto a tfm background, which essentially knocks out functional AR due to expression of the endogenous gene, the tg/tfm males show the same disease phenotype as tg males on a wt background. Since these mice display symptoms only when androgen is present, any dysfunctional AR left in motoneurons is irrelevant to motor deficits. These data provide strong evidence that AR in motoneurons is *not* required for mice to develop symptoms of SBMA. Instead, AR acting

exclusively in skeletal muscle fibers is sufficient to cause disease. Because these mice recover motor function when T treatment ceases, interfering with AR exclusively in muscle fibers may be an effective treatment for this disease.

Our results suggest that other metabolic processes altered by T action in muscles mediate the decline in body weight, independent or secondary to changes in muscle strength. Body weights are lower in Tg/tfm males than tfm controls before motor deficits are induced with T. Additionally, changes in body weight lag behind motor deficits in T-treated tg females in this and a previous experiment (Monks et al., 2007). Our results suggest that T may be acting in several ways and that body weight and motor function is dissociable.

While flutamide did not completely prevent disease in adult tg females treated with T, it markedly improved motor function and prevented body weight loss. A higher dose of flutamide, or a more effective anti-androgen might have blocked T effects entirely. These results are contrary to findings in Katsuno (2003), where flutamide had no positive effect in their tg mouse model of SBMA. We used a much higher dose (5 mg/day versus 1.8 mg/day per mouse in Katsuno et al., 2003) and treated more frequently (every day versus every second day). Furthermore, in the gonadally intact males in Katsuno et al., flutamide may have caused an increase in testosterone and luteinizing hormone levels by interfering with steroid negative feedback, even though seminal vesicle and ventral prostrate weights were significantly reduced (Clos et al., 1988; Marchetti and Labrie, 1988; Ohsako et al., 2003). T levels were not reported in Katsuno et al. (2003). Additionally, injected flutamide is fully metabolized within 8

hrs (Knobil and Neill, 1998), suggesting that daily injections might be required to be effective.

Drosophila, expressing a full length AR with 52 polyglutamines in the eye, show an androgen-dependent neurodegeneration. However, antagonists such as flutamide were ineffective in preventing such neurodegeneration (Takeyama et al., 2002). In this model, antagonists prevented AR-activated transcription but disease symptoms worsened, suggesting that pathogenesis is independent of AR activation. Because flutamide promotes nuclear translocation of AR, these authors suggested that nuclear translocation of AR, rather than AR activation, is the critical step triggering pathogenesis (Takeyama et al., 2002). Results from our model however suggest that nuclear translocation is not sufficient to trigger disease and that AR activation is also somehow involved. The opposite effects of flutamide in these two models—promoting androgen-dependent neurodegeneration in one and preventing it another—indicates that AR, when bound to flutamide, behaves differently in the two systems. One possibility is that the drosophila eye contains a different complement of AR cofactors than found in mouse muscle. In this scenario, mutant AR in the eye may act on novel regulatory elements to cause neurodegeneration despite the absence of activation by ligand, reminiscent of the role of cofactors in mediating opposing actions of tamoxifen, the estrogen receptor antagonist, in breast versus endometrial tissue (Shang and Brown, 2002).

Flutamide has also been shown to induce nuclear translocation and increase nuclear inclusions in a PC12 cell model of SBMA expressing an AR

allele with 112 CAG repeats, although whether flutamide induced cell death in this model is unclear (Walcott and Merry, 2002). Moreover, given recent evidence that nuclear inclusions may actually be neuroprotective rather than neurotoxic (Arrasate et al., 2004), it is possible that flutamide exerted some degree of neuroprotection in PC12 cells.

Our model suggests that nuclear translocation of the AR is not sufficient to induce disease in a mammalian system, and that transactivation is needed, since blocking activation (but not translocation) with flutamide dramatically ameliorates behavioral symptoms. While it is possible that the flutamide treatment prevented nuclear translocation of transgenic AR, tissues sections from flutamide treated animals showed clear nuclear AR staining, and evidence from other studies in our lab argues against this possibility (Freeman et al., 1996). Because flutamide is an effective therapeutic in our SBMA model, flutamide might also be an effective treatment for SBMA in humans. It will be important to continue testing flutamide and other AR antagonists in other models of SBMA. In sum, our data suggest that motor dysfunction can be caused by disease events which originate entirely in the muscle, independent of AR action in the motoneurons. Given the recent progress in developing AR-modulators that target various tissues, it may be possible to develop treatments for SBMA that block AR action in skeletal muscle while sparing androgen action in other target tissues, particularly reproductive organs and the brain.

GENERAL DISCUSSION

Transgenic mice over-expressing androgen receptors in skeletal muscle fibers are a model of spinal bulbar muscular atrophy.

I have shown that quite surprisingly, a wildtype (wt) androgen receptor (AR) can exert toxicity in an androgen dependent manner, when over-expressed exclusively in skeletal muscles of mice. Transgenic (tg) mice remarkably show a similar phenotype to that of mouse models of spinal bulbar muscular atrophy (SBMA), which use a mutant SBMA allele of AR to induce disease. While our tg mice show disease symptoms in common with mouse models of other motoneuron diseases such as amyotrophic lateral sclerosis (ALS) and spinal muscular atrophy (SMA), our mice show a disease phenotype that is exquisitely sensitive to androgens, the defining feature of SBMA. Moreover, for our tg mice, we manipulated expression of the causative gene in SBMA, the *AR* gene, compelling us to argue that our mice are a model of SBMA.

I find that the loss of motor function precedes the loss in body weight, because motor deficits are evident after 3 days of T-treatment, while body weight deficits are evident after 4 days of T-treatment. I did not detect significant atrophy of muscles in transgenic females, despite the devastating loss of motor function, and severe decline in body weight, suggesting that a loss in muscle mass does not account for the loss in body weight. Food intake also significantly

declines in T-treated tg female mice after motor deficits are present, mirroring the loss in body weight. As a result, food efficiency values remained level. A reduction in food intake may have led to a loss in adipose tissue. Observations during dissection suggested that this might be the case in diseased mice, although I did not measure this directly. Blood glucose levels were as expected in T-treated tg females, exhibiting lower levels due to fasting. Altogether, this suggests that metabolic activity is normal in these mice. It seems likely that a severe loss in motor function results in the inability of the animals to eat, resulting in decreased food intake and lower body weight and eventual death due to lack of food. Alternatively, the mice may become so weak that the diaphragm becomes compromised and this could also lead to death.

There are several other instances in my data where body weight and motor functions are dissociated. Recovery of body weight also lags behind changes in motor function. For example, tg/tfm males treated with T also show a reduced body weight only after motor deficits are evident, but are slower to recover body weight after motor functions were restored. In flutamide treated tg females, body weight was maintained at normal levels, even though flutamide does not fully maintain motor function. These results also suggest that severe motor deficits are needed to induce a loss in body weight.

One could ask if any protein over-expressed would also cause disease, but this does not seem to be the case. We do not find either perinatal lethality or motor deficits in our reporter male mice that express βgal, driven by the *same* HSA promoter, in their muscle fibers. We had 4 established lines, and none of

them showed the perinatal lethality that we saw in our mice that over-expressed AR in skeletal muscle fibers. Furthermore, it is not AR protein expression alone that confers toxicity because the phenotype is highly dependent on androgens. Only when androgens are present do we see a disease phenotype. Therefore, it must be a downstream action of AR causing toxicity.

However, there are several other examples of a wt protein causing disease. Over-expression of wt Ataxin-1 in *Drosophila* and mouse models of spinocerebellar ataxia Type 1 causes neurodegeneration (Fernandez-Funez et al., 2000; Tsuda et al., 2005), elevated levels of wt α-synuclein via gene amplification can cause Parkinson's disease (Singleton et al., 2003), and wt expression of human SOD can also cause mild ALS like symptoms (Jaarsma et al., 2000).

While the current dogma asserts that SBMA, and other motoneuron diseases, originate in the motoneurons, my work directly contradicts this theory. Gene expression was manipulated only in skeletal muscle fibers, which makes the muscle the primary site of action in our model. Further, even when endogenous AR is absent in motoneurons, transgenic AR in muscle is capable of inducing comparable pathology in *both* the muscles and motoneurons in androgen-dependent manner as reported in other SBMA models in which mutant AR is broadly expressed. Neurodegeneration clearly must be a secondary result of some toxic function of AR in muscle. While I am not the first to show that a wt allele when over-expressed can cause comparable neurodegenerative disease, I am the first to show that the muscle is a primary site of pathogenesis in SBMA.

It is still not clear however what mechanisms are involved, or how a wt AR can have a toxic function. My work points towards the neuromuscular junction as a key player, but it is still not known which events are critical in inducing a loss of motor function in this disease, and which are simply a by-product of the disease itself. My work also suggests that nuclear localization of AR is itself not enough to cause motor deficits. Flutamide, when bound to AR translocates to the nucleus, but can ameliorate the disease-inducing effect of testosterone in our tg female mice. Further, it rescues tg males from perinatal death. Other mechanisms downstream of nuclear translocation, presumably involving AR action, must be involved in producing the motor deficits and eventual neurodegeneration.

Several questions emerge. Particularly, how does a wt AR acting in muscles result in a motor deficit? How does a wt AR take on a similar function as a mutant AR? Here I propose several mechanisms in which AR may gain a toxic function, whether it is the mutant form or the wt expressed at high levels.

Cellular dysfunction may result in a lack of trophic support.

Clearly cellular dysfunction underlies the loss of motor function in our SBMA mouse model, rather than cell death. Tg females dramatically lose body weight and motor functions, although no loss of either motoneurons or muscle fibers is detected. However, it remains unclear what events trigger a loss in cellular function. One scenario suggested by recent data in our lab is that AR has a toxic gain of function which depletes the trophic support for motoneurons,

such as VEGF, originating in the muscle. This lack of trophic support may destabilize neuromuscular junctions, leading to denervation and a loss of retrograde axonal transport. Axons then begin to retract, leading to their loss and more proximately the loss of muscle fibers. When AR actions are reversed by removing testosterone, it's possible that neuromuscular junctions begin to stabilize and cellular functions are restored. Alternatively, the downregulation we see in VEGF, and upregulation of genes indicative of denervation may simply be an epiphenomenon of overexpression of wt AR in muscle fibers that is unrelated to the androgen-dependent loss of motor function. However, these changes only occur when androgens are present in combination with the overexpression of AR, arguing against this possibility.

There is evidence in other models suggesting that a disruption in trophic support is involved in neurodegenerative disease. In an ALS mouse model, recombinant VEGF given systemically has preserved neuromuscular junctions, reduced astrogliosis, and prolonged the lifespan (Zheng et al., 2004; Zheng et al., 2007). In cell culture, VEGF was able to rescue MN-1 cells from death expressing a SBMA allele of AR (Sopher et al., 2004), although no one thus far has tested VEGF as a therapeutic in a SBMA mouse model. The beneficial effects of VEGF in ALS and a cellular model of SBMA and the fact that it is decreased in two mouse models of SBMA indicate that VEGF may indeed be an effective therapeutic for SBMA, and may do so by preserving the structure of function neuromuscular junctions.

Other muscle-derived trophic factors could also be involved, such as insulin like growth factor 1 (IGF-1), glial cell line-derived neurotrophic factor (GDNF) and brain-derived neurotrophic factor (BDNF). Depletion of any of these trophic factors may also contribute to a loss of motor function. IGF-1 has been implicated in a cellular model of SBMA (Palazzolo et al., 2007), and mouse models of spinocerebellar ataxia (SCA) type 1 and 7 (Gatchel et al., 2008). IGF-1 has also been successful in treating dystrophic symptoms in a muscular dystrophy mouse model (Schertzer et al., 2006) and a Huntington's disease (HD) model (Humbert et al., 2002). However IGF-1 has had mix results in mouse models of ALS (Kaspar et al., 2003; Dobrowolny et al., 2005; Messi et al., 2007). IGF-1 expressed exclusively in skeletal muscles delayed disease onset and disease progression, and enhanced motoneuron survival in the SOD(G93A) model of ALS (Dobrowolny et al., 2005). But its use as a therapeutic has been questioned, as other studies have not found IGF-1 helpful in delaying disease onset or progression (Messi et al., 2007). However, the fact the promoter for the IGF-1 gene contains an ARE suggests that this protein may be critically involved in SBMA, especially given the partial loss of AR function that accompanies SBMA (Wu et al., 2007)

IGF-1 also facilitates muscle regeneration and may be useful at combating the toxic effects of AR (Rabinovsky et al., 2003; Pelosi et al., 2007). IGF-1 has been shown to stimulate satellite cell differentiation and proliferation (Sacheck et al., 2004). It also helps restore expression of myogenin and nicotinic acetylcholine receptor subunits to normal levels and helps repair injured nerve

and muscle (Sacheck et al., 2004). IGF-1 may also be involved in preventing denervation induced muscle atrophy (Stitt et al., 2004). Together with data demonstrating that IGF-1 stimulation also reduces toxicity of the expanded polyglutamine AR in MN-1 cultured cells (Palazzolo et al., 2007), suggests that IGF-1 may also be useful as a therapeutic in our SBMA mouse model.

Gene transfer of BDNF, and also GDNF, helped to protect striatal neurons in a rat HD model (McBride et al., 2003; Mochizuki et al., 2008). Of particular interest, muscle derived GDNF was protective in an ALS rat model (Li et al., 2007) suggesting that it may also be effective in our model of SBMA. GDNF mRNA in a mouse model of SBMA was found to be expressed at lower levels in tg muscles compared to wildtype muscles (Yu et al., 2006b), but GDNF expression remains to be examined in our SBMA model. BDNF remains to be examined in any SBMA model.

To test if trophic factor depletion in muscles is necessary for a loss in motor function, one could create a mouse in which, for example, VEGF is depleted from skeletal muscles only, using a Cre/Lox system in mice. Whole animal VEGF knockout is embryonic lethal (Carmeliet et al., 1996), and BDNF knockouts die early in postnatal life (Snider, 1994). However, the effect of muscle specific deletion of any of these proteins on motor function has not been examined. For example, do mice that lack VEGF only in skeletal muscles show motor deficits? Alternatively, one could ask whether giving trophic factors as a therapeutic is beneficial. Does VEGF, or IGF-1 administration ameliorate disease? It is always possible that even if these putative neurotrophic factors are

not depleted in muscle, they could compensate for the loss of some other factor and thus serve as therapeutic agents for neuromuscular disease.

Proteosome degradation of both wt and mutant AR may result in similar toxic fragments.

Chains of ubiquitin are linked to proteins to mark them for degradation. This allows them to be recognized by the 26S proteosome, which degrades the ubiquitinated proteins into small peptides. This pathway can regulate gene transcription, as many transcription factors are ubiquitinated and degraded by the proteosome, but also can act as a quality control mechanism and eliminate misfolded or damaged proteins (Lecker et al., 2006). Both mutant and wt AR are targeted for degradation by the ubiquitin-proteosome pathway (Lin et al., 2002; Cardozo et al., 2003; Adachi et al., 2007).

Recent work indicates that polyglutamine (polyQ) proteins are difficult for the proteosome to degrade, resulting in polyQ fragments that may become trapped in the proteosome preventing normal degradation of other proteins, or released as smaller toxic fragments (Holmberg et al., 2004; Venkatraman et al., 2004; Bhutani et al., 2007). The wt AR we used includes 22 polyQs, and at high expression levels it is possible that the polyQ are not fully degraded by the proteosome, resulting in an excess of lower molecular weight polyQ rich protein fragments. In sum, in each case, the result may be an accumulation of polyQ tracts that are inherently toxic to cells (Figure 27).

One way to test this idea would be to generate a tg animal overexpressing AR without any polyQs in the protein. Are the 22 glutamines in our wt protein responsible for inducing the toxic function of AR? On the other hand, if the polyQ alone was overexpressed would it still induce motor deficits? Alternatively, we could administer a drug to our mice that improves proteosome function. Does improving proteosome function also improve motor function?

A recent study by Adachi et al. (2007) showed that improving proteosome function reduced AR protein levels, and ameliorated motor symptoms in a mouse model of SBMA. They overexpressed the protein, C terminus of the heat shock cognate protein 70 (Hsc70)-interacting protein (CHIP) in tg mice, which functions in several ways. First, it has the ability to interact with molecular chaperones such as Hsp70 and Hsp90 (Cardozo et al., 2003; Adachi et al., 2007). Second, it acts as an ubiquitin ligase tagging proteins for degradation (Cardozo et al., 2003; Adachi et al., 2007). AR is also a substrate of CHIP, and CHIP is found inmotoneurons, glia and muscles (Cardozo et al., 2003; Adachi et al., 2007). Presumably, overexpression of CHIP increases proteosome function, and aides in degradation. The authors generated tg animals that expressed both the mutant SBMA allele and CHIP, and found that CHIP effectively decreased AR protein levels and also ameliorated disease symptoms (Adachi et al., 2007). This suggests that enhancing proteosome functions may be a potential therapeutic avenue.

We currently do not have evidence of proteosome involvement in our model. With Western blots, I rather unexpectedly, detected more proteolytic

fragments in animals that had normal motor function. It is possible that proteins were more efficiently cleared or degraded in animals that were healthy, however, the fragments detected in Western blots were those of the N-terminal region that presumably contained the polyQ tract. Moreover, when the disease was induced by androgen, accumulation of such fragments was reduced. Thus, it is not clear at this time whether alterations in proteosomal processing plays a role in loss of motor and cell function in our model.

Molecular chaperones are bound to both wt and mutant AR, which may interfere with molecular chaperone functions.

In addition to the proteosome, molecular chaperones are also actively involved in degradation of misfolded proteins, the refolding of proteins to maintain their native conformation, and may play a protective role in neurodegeneration (Sherman and Goldberg, 2001; Wyttenbach, 2004). Heat shock proteins (Hsp) can interact with proteins and influence degradation. Hsp90 has been shown to both inhibit and promote protein degradation (Cardozo et al., 2003), while Hsp70 and Hsp40 have both been shown to enhance protein degradation, including AR proteins (Bailey et al., 2002). Frequently, Hsps are found in nuclear inclusions, or aggregates. Nuclear aggregates are considered a hallmark of polyQ diseases, including SBMA (Orr and Zoghbi, 2007). Mutated ARs are found within nuclear aggregates in motoneurons and skeletal muscles and tend to co-localize with ubiquitin in addition to Hsps. Transcriptional regulators such as CREB binding protein (CBP) also co-localize with nuclear aggregates (Zoghbi and Orr,

2000; Adachi et al., 2003). Over-expression of molecular chaperones, such as Hsp70 has been shown to decrease aggregation (Cummings et al., 2001). It is possible that molecular chaperones become bound to AR, or sequestered, perturbing their ability to bind to other client proteins. It is still unknown if molecular chaperones or the proteosome are involved in our SBMA model, but they have both been implicated in other SBMA mouse models (Adachi et al., 2003; Katsuno et al., 2005; Thomas et al., 2006; Adachi et al., 2007).

ASC-J9, a drug that disrupts the interaction between AR and its coregulators, also increases cell survival by decreasing AR-polyQ nuclear aggregation and increasing AR-polyQ degradation in cultured cells. Intraperitoneal injection of ASC-J9 into AR-polyQ transgenic SBMA mice markedly improved disease symptoms, as seen by a reduction in muscular atrophy (Yang et al., 2007). It is possible that coregulators may be involved in several ways. When bound, they may confer a new toxic function to AR, or impede other processing in the proteosome, therefore disrupting this bond may be beneficial.

Hsp70 when overexpressed, also markedly ameliorated motor function in the same SBMA mouse model. Mutant AR protein and aggregates were reduced by Hsp70 overexpression, suggesting enhanced degradation of mutant AR (Adachi et al., 2003). 17-allylamino-17-demethoxygeldanamycin (17-AAG), is a potent Hsp90 inhibitor, and also induces Hsp70 and Hsp40. It markedly ameliorated motor impairments without detectable toxicity, by reducing amounts of monomeric and aggregated mutant AR (Waza et al., 2005). Although the

mechanism of Hsp90 action is not clear, recent evidence suggests that blocking Hsp90 inhibits nuclear translocation without inducing a stress response (Thomas et al., 2006).

Hsp70 and its co-chaperone Hsp40 also increased expanded repeat AR solubility and enhanced the degradation of expanded repeat AR through the proteosome in a cell model (Bailey et al., 2002). Therefore increasing Hsp70 and 40, either through genetic or pharmacological means, may enhance proteosome degradation if excess wt AR in our mouse model as well.

Coregulators bound to mutant and wt AR may alter transcriptional activity.

Another cofactor that can interact with AR, and implicated in SBMA is CREB binding protein (CBP). CBP also acts as a histone acetyltransferase (HAT), thereby affecting chromatin folding, making DNA more accessible. HATs and histone deacetylases (HDACs) control both DNA accessibility and transcriptional regulation (Rouaux et al., 2004). A loss of CBP function has been linked to polyQ diseases such as spinocerebellar ataxia 7, SBMA, and HD, but also other neurodegenerative disease like Alzheimer's disease and ALS (Rouaux et al., 2004).

In a cell model of SBMA, cells over-expressing CBP showed enhanced survival, and the toxic effect of the expanded polyglutamine was blocked (McCampbell et al., 2000; McCampbell et al., 2001). In another SBMA cell model, CBP overexpression also rescued from polyglutamine toxicity, but additionally increased VEGF mRNA levels (Sopher et al., 2004). Therefore CBP

may also modify VEGF expression, providing two avenues where CBP may be beneficial. In HD models, CBP was also found to be depleted from its normal nuclear location and present in polyglutamine aggregates, and overexpression of CBP rescued polyglutamine-induced neuronal toxicity (Nucifora et al., 2001). This suggests that CBP may be sequestered, interfering with its role in transcription, and increasing CBP levels restores its normal functions.

Histone deacetylase (HDAC) inhibitors alleviate neurological phenotypes in fly and mouse models of polyQ disease, although the therapeutic effect is limited by the toxicity of these compounds. Sodium butyrate (SB), an HDAC inhibitor, was studied in a transgenic mouse model of SBMA. Oral administration of SB ameliorated neurological phenotypes as well as increased acetylation of nuclear histone in neural tissues (Minamiyama et al., 2004). Sodium valproate, another HDAC inhibitor was studied in a rat model of ALS (Rouaux et al., 2007). When injected in G86R ALS mice it maintained normal acetylation levels in the spinal cord, efficiently restored CBP levels in motoneurons, and significantly prevented motoneuron death. However, survival of treated animals was not significantly improved (Rouaux et al., 2007). Together these experiments suggest that increasing transcriptional activity through HDAC inhibitors have a therapeutic benefit.

In sum, several molecular targets could potentially be involved in our mouse model and provide a therapeutic benefit. Supplementing with trophic factors could increase survival and stability of neuromuscular junctions. Enhancing proteosome function may enhance proteosome degradation of excess

wt AR. Additionally, increasing transcriptional activity through HDAC inhibitors such as sodium butyrate, or increasing available molecular chaperones with genetic or pharmacological techniques may also alleviate disease.

Future directions

A close look at our model over the time course of disease would be beneficial in determining the cause and effect relationships between the loss in motor function and the underlying cellular and molecular changes. It is likely that some of the underlying changes are responses to some earlier event that actually triggers the disease. In our model, tg females offer an unique opportunity to address this question, since testosterone treatment induces a rapidly progressing and highly predictable decline in motor performance. What factors, or cellular processes, change before the onset of disease, and when such actions are blocked by androgen, is disease also prevented? For example, if muscles are functionally denervated before motor deficits appear, this suggests that of a loss of synaptic function may cause a loss of motor function. Or does synaptic loss simply follow the loss of function, and appear only after deficits are evident? Similarly, does VEGF mRNA become dysregulated before or after symptom onset?

Messenger RNAs indicative of denervation are upregulated in our tg mouse model, suggesting that muscles are indeed denervated. However, a more detailed approach is needed. Using immunoctyochemistry (to label pre and

postsynaptic parts of the motor synapse), one could determine if muscle fibers are indeed denervated. Alternatively, are neuromuscular junctions altered in other ways in tg animals that would suggest synaptic dysfunction?

Further work is also needed to confirm if the proteosome or molecular chaperones are involved in the etiology of disease our mouse model. Is the proteosome working properly in our mice with SBMA? Are molecular chaperones involved and can they be used to ameliorate disease as in other SBMA mouse models? It seems likely that the overexpression of AR would challenge both the proteosome and molecular chaperones, given that each is critically involved in the maintenance of protein levels, and the proper conformation of intracellular proteins. One way to examine this would be to see if proteins of interest from the ubiquitin proteosome pathway co-immunoprecipitate with AR, or are altered with AR overexpression. For example, if soluble Hsp70 was decreased in tg muscles, perhaps over-expressing Hsp70 would ameliorate disease, as it did in another SBMA model. Alternatively, drugs that increase Hsp activity could be beneficial.

CBP acts as a co-activator and modulates gene transcription presumably via its histone acetyltransferase activity. Is CBP, or its histone acetylation activity, depleted in our mouse model of SBMA? If so, would administering sodium butyrate ameliorate disease in our mice, as it has been shown to do in other models of SBMA?

Are other trophic factors also downregulated in our SBMA model? If so, do restoring trophic factor levels to normal also restore motor functions? One could

test this by giving exogenous VEGF, or IGF-1, to acute T treated tg female mice and look to see if motor function is recovered. If recovered, do genes sensitive to denervation also return to baseline levels?

Conclusions

While most tg mouse models of SBMA utilize an expanded polyQ repeat to mimic the etiology of the disease in humans, our tg mouse model indicates expanded polyQ repeats are *not* required to cause the disorder. Our mouse model develops a similar phenotype with over-expression of the *wildtype* AR containing a *normal* number of glutamine repeats, showing the same loss of motor function and muscle pathology as other mouse models. Additionally, we find that nuclear translocation of AR itself is not toxic. Therefore, preventing AR action per se, and not AR nuclear translocation may ameliorate disease in SBMA. Moreover, we find that the disease phenotype can be elicited by manipulating AR expression only in skeletal *muscle fibers* suggesting that a depletion of muscle-derived trophic factors may lead to motoneuron death and that motoneurons die as a *secondary* consequence of muscle pathology. This model also has implications for other so called "motoneuron diseases" such as ALS and SMA that historically are assumed to be caused by disease events that originate in the motoneurons and not elsewhere.

APPENDIX

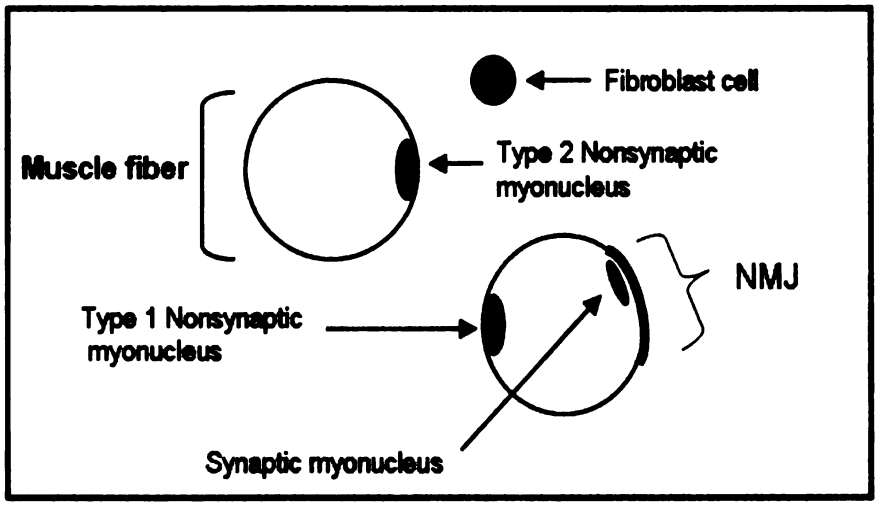

Figure 1 Schematic drawing illustrating our classification of cell types in muscle. Synaptic or endplate myonuclei are located inside the basal lamina, directly beneath the post-synaptic junction. Nonsynaptic myonuclei are divided into two sub groups. Type 1 no synaptic nuclei are present within the same cross section of fiber that has a visible neuromuscular junction, but are not directly beneath the junction. Type 2 nonsynaptic myonuclei are located within fibers containing no visible junctions. Fibroblasts lack basal lamina and reside outside the basal lamina of muscle fibers. They were judged as synaptic if visible junctions were in the field of view, and nonsynaptic if there were no visible junctions in the field of view.

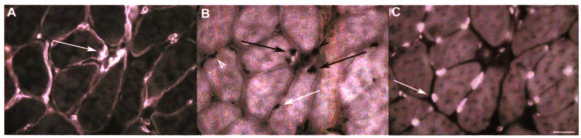

Figure 2 Cross section of levator ani stained for androgen receptor (AR), basal lamina, acetylcholine receptor and cell nuclei. (A) Basal lamina staining in the LA muscle reveals a thickening of the basal lamina at the neuromuscular junction (white arrow). (B) The same neuromuscular junction as in (A) colabelled with Alexafluor alpha bugarotoxin and AR. AR positive myonuclei are present at the neuromuscular junction, nuclei stain black (black arrows) and are classified as synaptic myonuclei. AR positive myonuclei within the same fibre, but not underneath the junction are classified as Type 1 nonsynaptic (white arrow), whereas AR positive myonuclei within fibres lacking a visible neuromuscular junction (white arrow head) are classified as Type 2 nonsynaptic. AR positive fibroblast nuclei reside outside the basal lamina (black arrow head). (C) AR negative nuclei in these various categories are evident with DAPI staining (white arrow). Scale bar = 20 um.

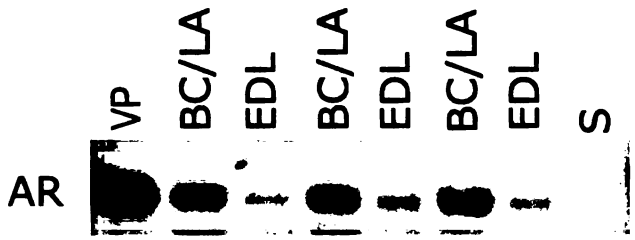

Figure 3 The androgen responsive bulbocavernosus (BC)/levator ani (LA) has more total androgen receptor (AR) (112 kDa) protein compared to the androgen unresponsive extensor digitorum longus (EDL), as revealed by western blot analysis in three different mice. VP, Ventral prostate, positive control; S, spleen, negative control.

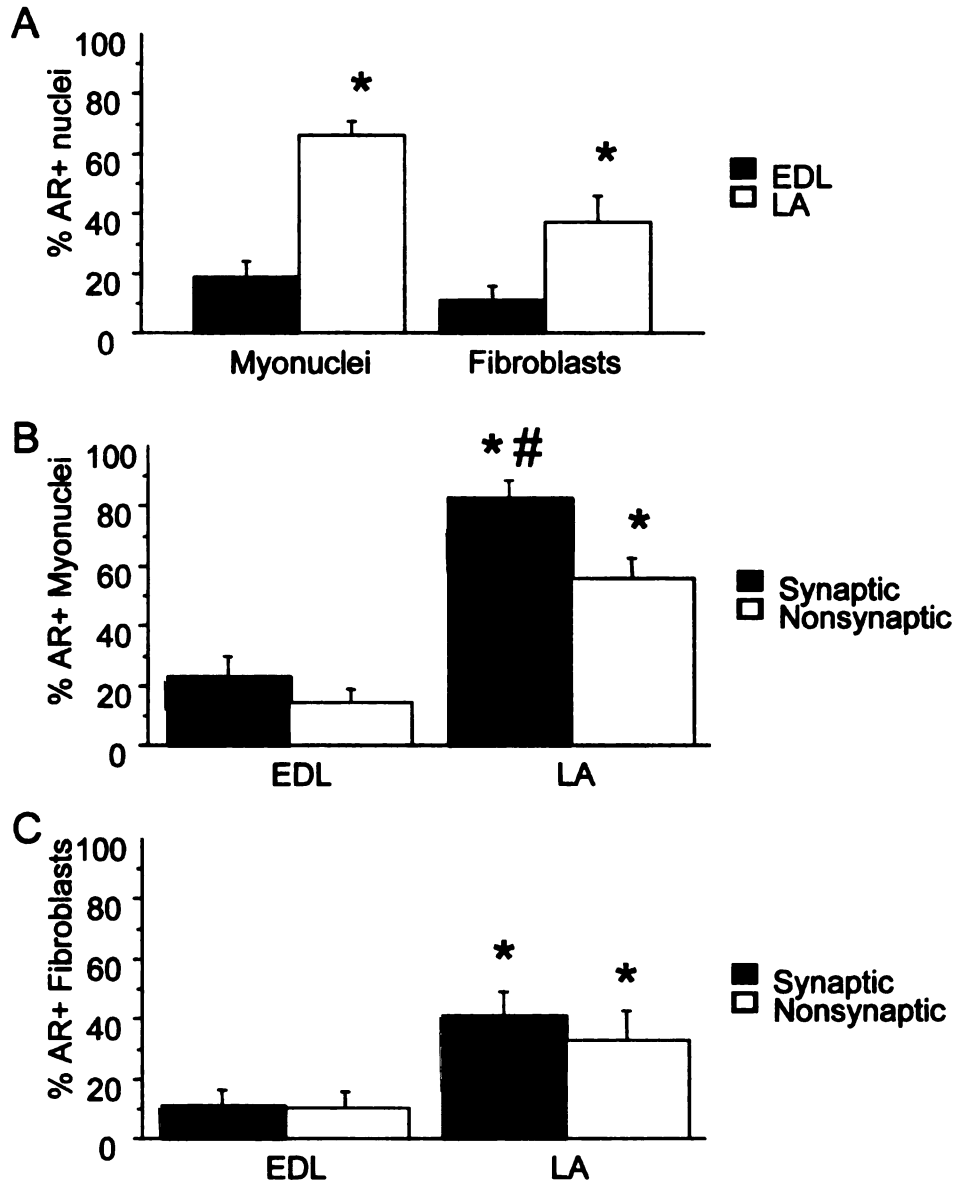

Figure 4 (A) The androgen-responsive levator ani (LA) has a greater percentage of androgen receptor (AR) positive myonuclei and fibroblasts compared to the androgen-unresponsive extensor digitorum longus (EDL). (B) The LA also shows a further enrichment of AR positive myonuclei at the neuromuscular junction compared to outside the junction, which was not seen in the EDL. (C) The percent of AR positive fibroblasts were not different between synaptic and nonsynaptic regions of muscle. *Significantly different from EDL. *Significantly different from nonsynaptic region.

L78 (n=121)

Genotype	# at birth	% of total births	# dead at birth	# alive at weaning
Tg Male	17*	14%	9	7*
wt Male	39	32%	7	32
Tg Female	35	29%	1	30
wt Female	30	25%	7	23

L141 (n=299)

Genotype	# at birth	% of total births	# dead at birth	# alive at weaning
Tg Male	46*	15%	36	3*
wt Male	75	25%	11	64
Tg Female	94	31%	16	76
wt Female	84	28%	12	72

Table 1 Male-limited Perinatal Lethality of HSA-AR Transgene. Significant perinatal attrition is observed in HSA-AR tg males but not females or in HSA-LacZ reporter mice (data not shown), suggesting that the lethality reflects an androgen-dependent function of overexpressed AR. *significantly less than expected as indicated by $\chi 2$ statistic ($p<0.05$).

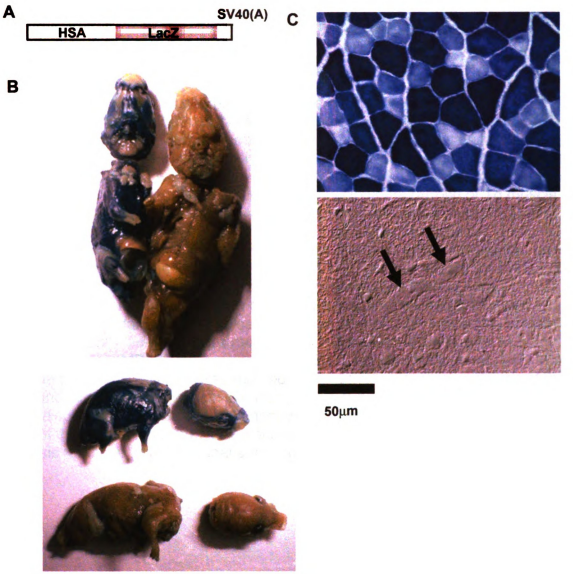

Figure 5 A) HSA-LacZ construct – the human skeletal actin (HSA) expression cassette drives expression of the LacZ sequence, which codes for β-galactosidase. B) Expression of β-galactosidase in whole neonatal tg pup is detected histochemically via X-gal, which yields a blue reaction product. A wt littermate stained identically is shown as a control. Note the uniform X-gal staining of tg skeletal muscle and the absence of ectopic staining in viscera, bone or adipose tissues. C) Photomicrograph of X-gal staining of cross sections of tg EDL muscle (Top), and tg spinal cord (Bottom) using Nomarski optics. Note the blue staining in skeletal muscle fibers and absence of blue staining in spinal cord, including motoneurons (arrows).

Figure 6 A) HSA-AR construct – the same HSA expression cassette described for HSA-LacZ mice drives expression of a rat androgen receptor (AR) cDNA. The amino acid and nucleotide sequences of the polyglutamine tract are indicated. B) AR-immunoreactivity in cross sections of extensor digitorum longus muscle prepared from wildtype (wt - left) and transgenic (Tg - right) males. Note the increase in AR-immunoreactive nuclei in muscle fibers (arrow) of Tg muscle but not in interstitial nuclei, demonstrating specific overexpression of AR in this cell type. C) Western immunoblot of various tissues from wt, testicular feminization mutant (tfm) mice, which have little to no full length AR protein, and tg mice crossed onto the tfm background (tfm/Tg). Overexpression of AR is observed in skeletal muscle samples but not other tissues from tg mice, confirming the selective expression of the AR transgene in skeletal muscles. MW=protein standards, S = wt spleen (negative control), VP = wt ventral prostate (positive control), Q= quadriceps muscle, B = bulbocavernosus/levator ani muscle sample, LMB = lumbar spinal cord, CRV = cervical spinal cord. D-F) Mice from the L141 line, which display marked motor deficits, carry more copies of the gene and express transgene mRNA and protein at higher levels than L78 mice, which display a normal behavioral phenotype. Tg males from the L14 line, which was not the focus of this study, also displayed perinatal mortality and severe kyphosis for those few males that survived to adulthood.

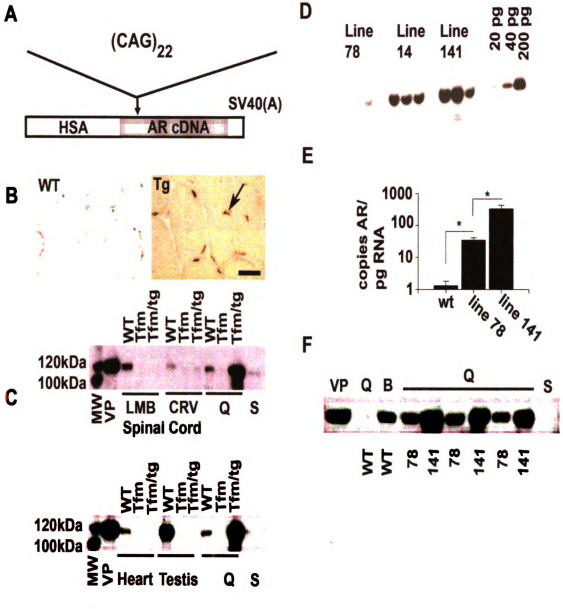
A
(CAG)22
SV40(A)
HSA
AR cDNA
B
WT
Tg
C
WT
Tfm
Tfm/tg
120kDa
100kDa
MW
VP
LMB
CRV
Q
S
Spinal Cord
Heart
Testis
D
Line 78
Line 14
Line 141
20 pg
40 pg
200 pg
E
copies AR/ pg RNA
1000
100
10
1
wt
line 78
line 141
F
VP
Q
B
S
78
141

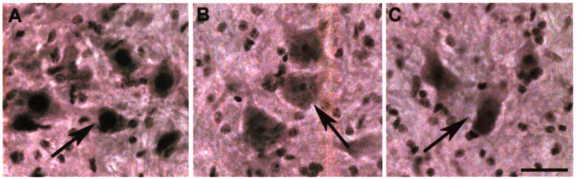

Figure 7 Although adult wt male mice (A) show robust AR immunoreactivity in nuclei of lateral motoneurons of the lumbar spinal cord, comparably located spinal motoneurons of *tfm* male mice expressing the AR transgene in their muscle fibers (B) or of *tfm*-only male mice (C) lack such nuclear AR staining, indicating that the HSA-AR transgene is *not* expressed in spinal motoneurons. Note that the nuclei of wt motoneurons are stained dark (arrow in A) as opposed to the motoneuronal nuclei of *tfm*/tg and *tfm*-only male mice that are devoid of such AR immunoreactivity (arrows in B and C, respectively). Scale bar = 30 microns.

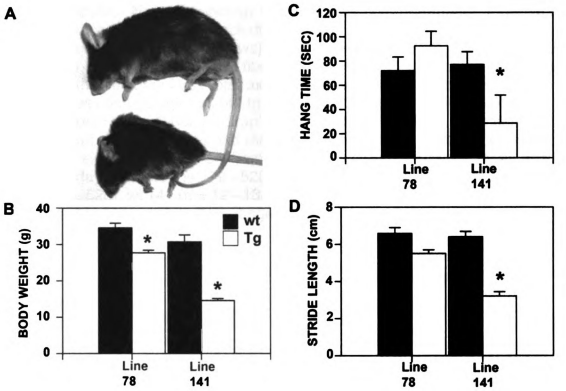

Figure 8 A) Photograph of L141 tg male and age matched wildtype (wt) brother (top). L141 tg males have reduced body weight (A, B), marked kyphosis (A) and motor deficits as revealed by the hang test (C) and paw print records (D). Despite reduced body weight, motor deficits are not observed in L78 Tg males. Graphs represent mean + SEM, open bars represent Tg males and filled bars represent wt controls. *significantly different from wt controls. wt 78 (n = 13, mean age in days: 294, range:179 - 528), 78 Tg (n = 14 - 15, mean age: 281, range: 106 - 528), wt 141 (n = 12 - 15, mean age: 131, range: 72 - 218), Tg 141 (n=6-7, mean age: 119, range: 72-179).

Figure 9 A) Photomicrographs illustrating histopathology in EDL muscle sections stained with H&E or NADH from a wt male, or L78 or L141 tg males. Muscle pathology seen in L78 and L141 tg males is typical of that seen in SBMA, including grouped atrophic fibers (arrowheads), centralized nuclei (arrows) and increased NADH staining. While the number of EDL muscle fibers (B) is reduced in tg males of both lines, the number of L5 motor axons (C) was significantly reduced relative to wt controls only in L141 tg males, which is the line with particularly poor motor function. Graphs represent mean + SEM, open bars represent tg males and filled bars represent age matched wt males. *significantly different from wt males. wt 78 (n = 10 – 13, mean age in days: 317, range:179 - 528), 78 Tg (n =13, mean age: 300, range: 106 - 528), wt 141 (n = 12 - 13, mean age: 129, range: 72 - 218), Tg 141 (n=6, mean age: 116, range: 72-179).

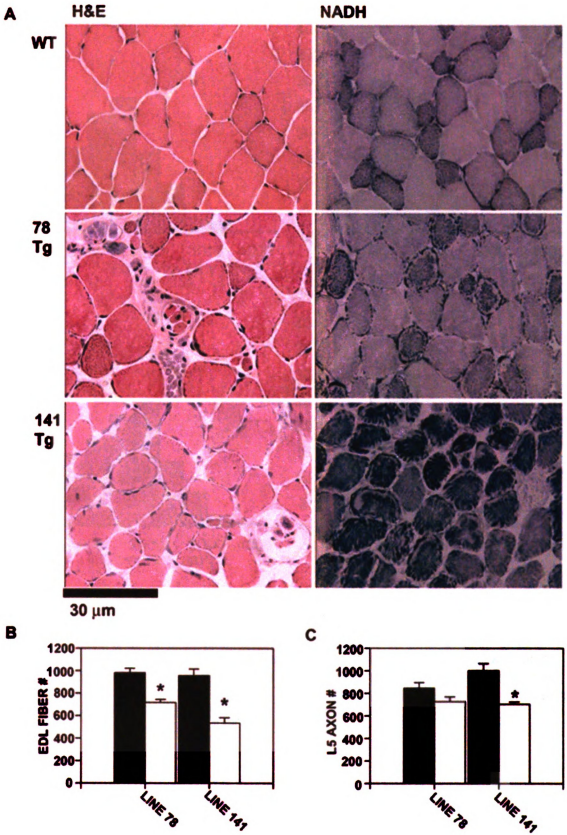
A
H&E
NADH
WT
78
Tg
141
Tg
30 μm
B
EDL FIBER #
1200
1000
800
600
400
200
0
*
*
LINE 78
LINE 141
C
L5 AXON #
1200
1000
800
600
400
200
0
*
LINE 78
LINE 141

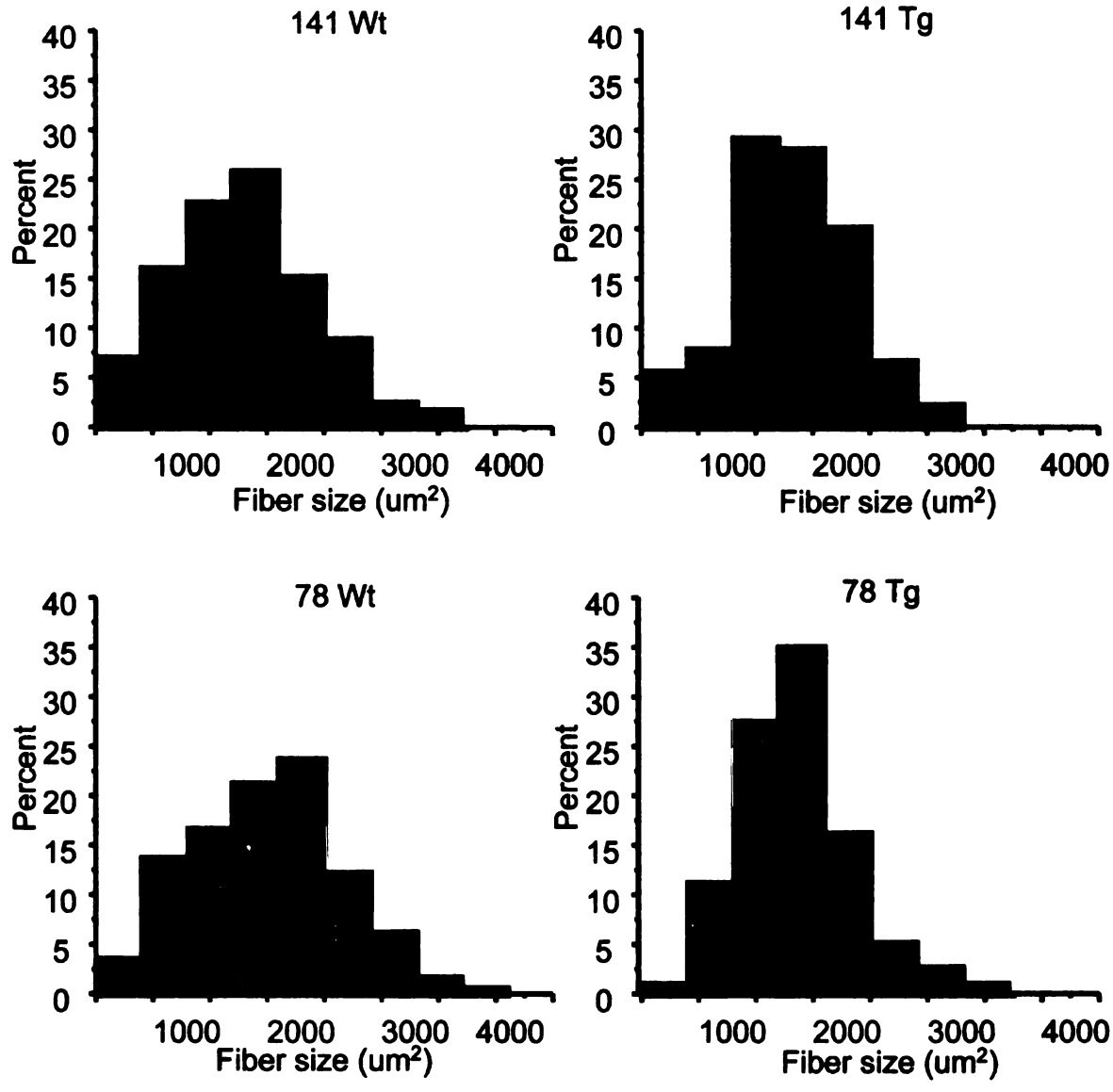

Figure 10 Frequency distribution in EDL fiber size in L141 and L78 males. No difference was seen in the frequency distribution in L141 males and their wildtype brothers ($\chi 2$=.1722, wt n=5, tg n=3), however there was a difference in the frequency distribution between L78 tg and wt males ($\chi 2$=.0006, wt n=7, tg n=7).

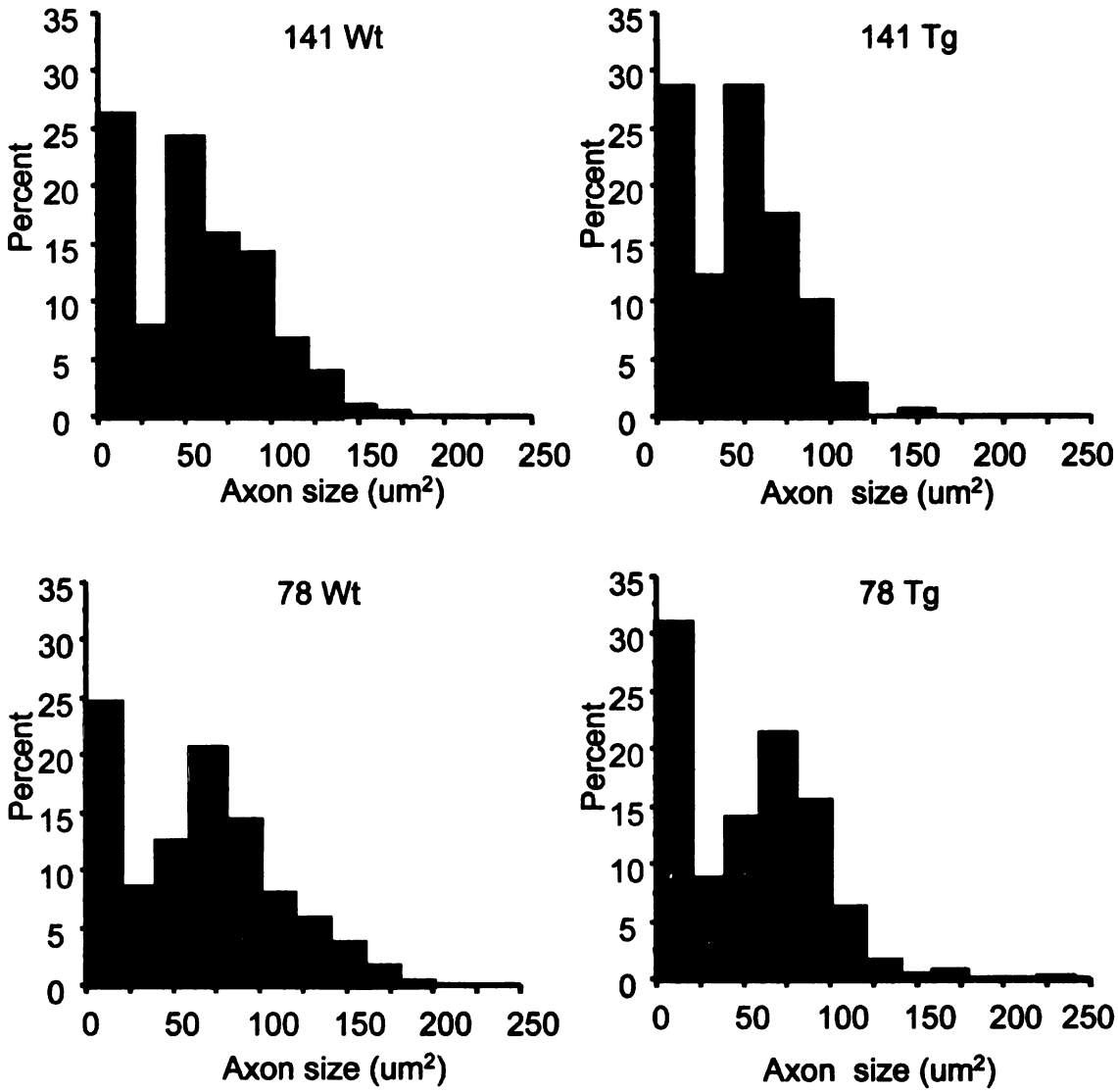

Figure 11 Frequency distribution in axon size in L141 and L78 males. There were no differences in the frequency distribution of axons in L141 tg males versus wt controls ($\chi 2$=.188, wt n=2, tg n=2), nor in L78 males compared to wt males ($\chi 2$=.46, wt n=6, tg n=6).

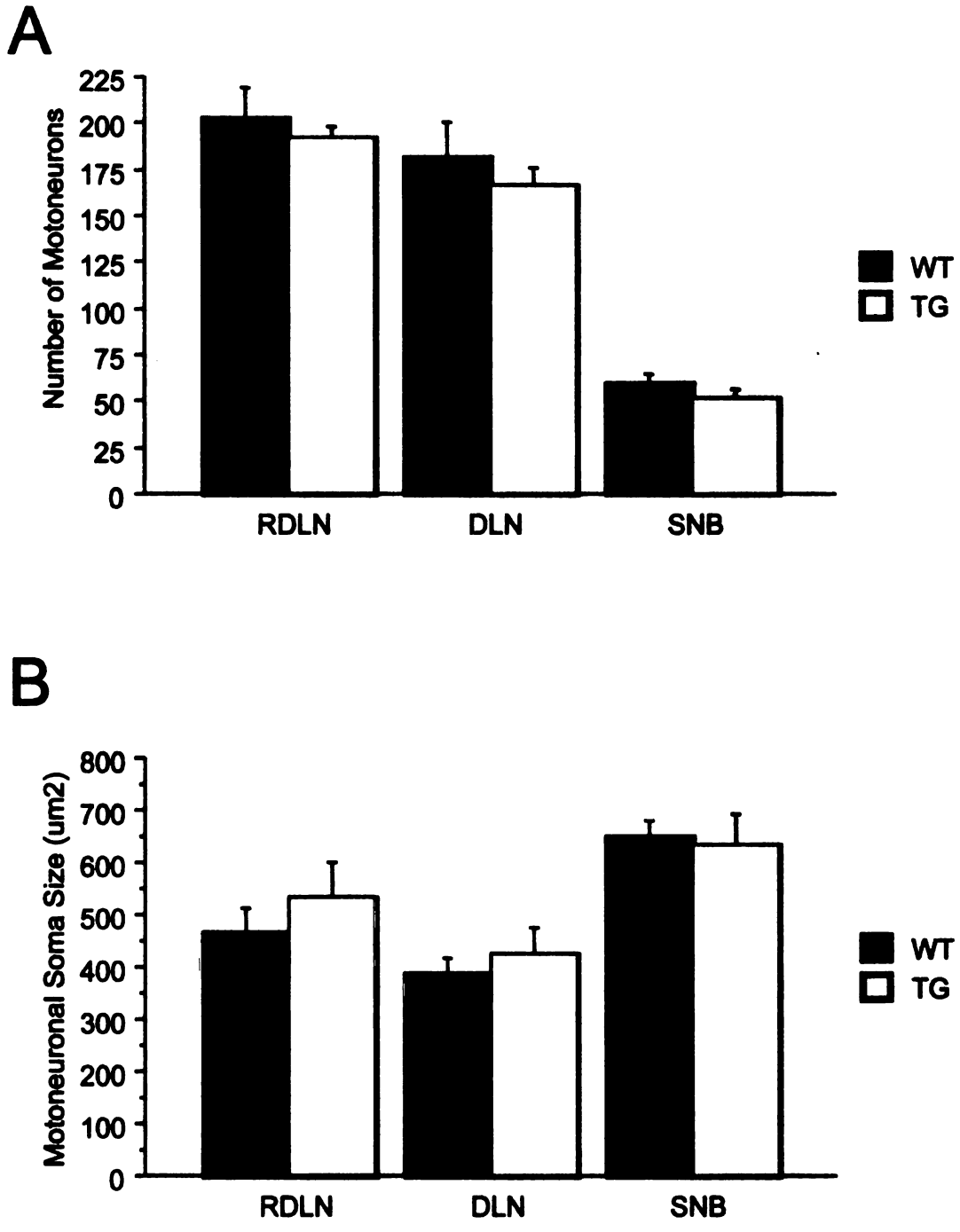

Figure 12 Motoneuron number and size is unaffected in L141 tg males despite a profound loss of motor function. A) Motoneuron numbers were measured in the spinal nucleus of the bulbocavernosus (SNB), the dorsolateral nucleus (DLN) and the retrodorsal lateral nucleus (RDLN). No loss in motoneurons were detected in tg L141 males in all three regions. B) Soma size in the SNB, DLN and RDLN was also equivalent in L141 tg and wildtype male mice. Wt n=4, tg =3

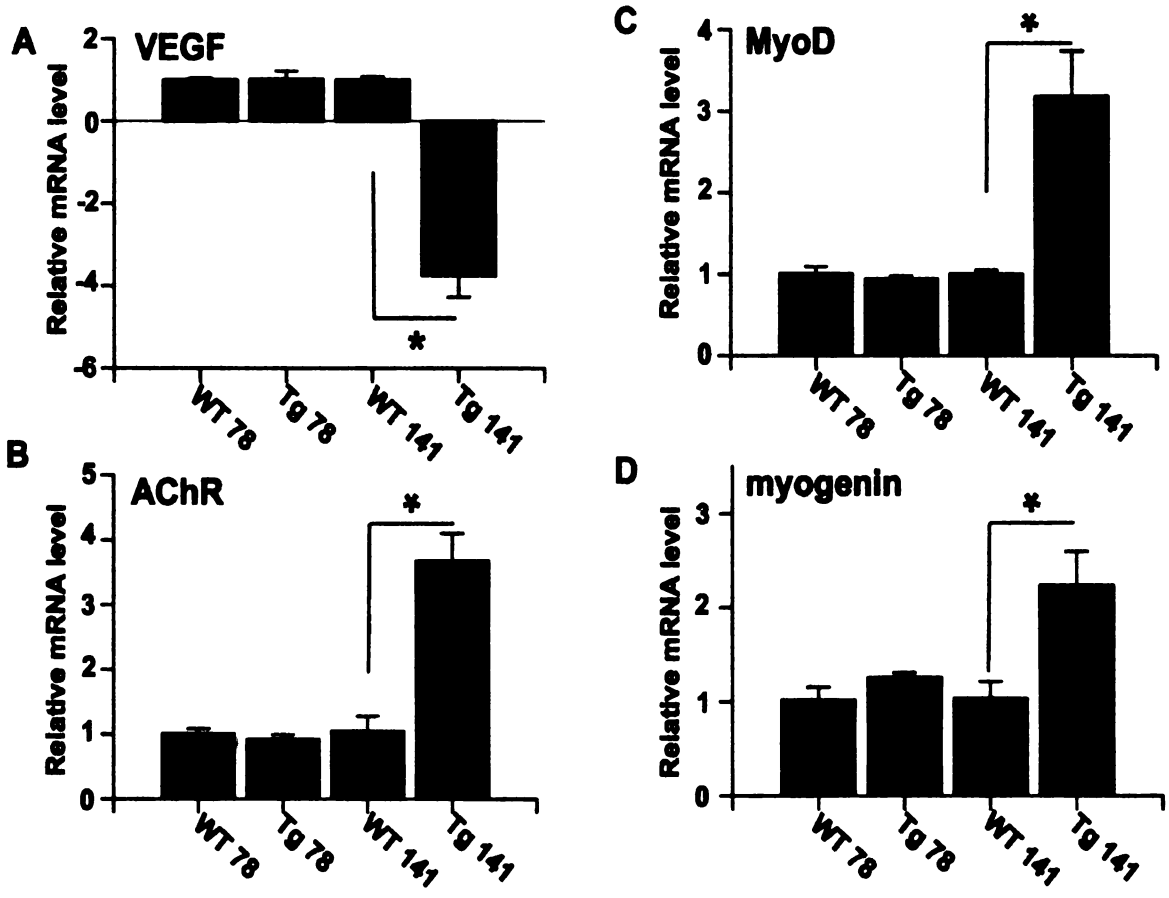

Figure 13 Quantitative RT-PCR (qPCR) estimates of mRNA abundance of vascular endothelial growth factor (VEGF) isoform 164 and 188, acetylcholine receptor alpha subunit (AChR), myogenic differentiation factor 1 (myoD), and myogenin in muscles from wt and tg males of the behavioral asymptomatic L78 line and the severely affected L141 line. Down-regulation of VEGF and up-regulation of AChR alpha, MyoD and myogenin mRNA is also observed in muscle of SBMA mouse models and/or after denervation. All estimates are differences in mRNA relative to wt brothers within the same line. Graphs represent mean + SEM, *significantly different from wt brothers. L78 mice (n=3 wt, 3 tg, mean age in days = 145, range =106-222), L141 mice (n=4 wt, 4 tg, mean age = 115, range = 72-162).

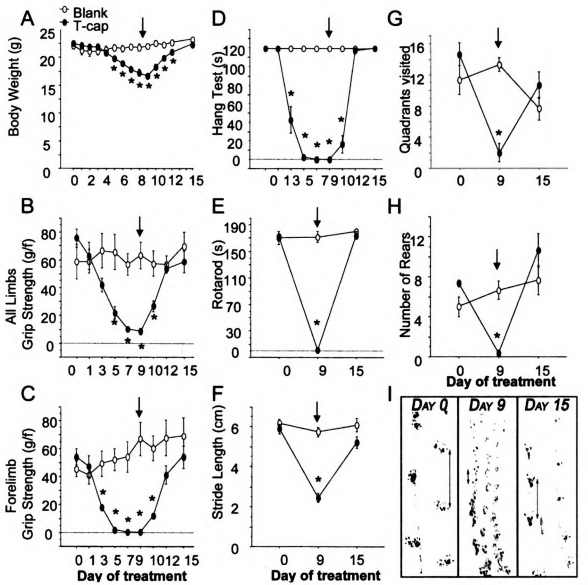

Figure 14 Transgenic (tg) females fully recover motor function after testosterone (T) treatment ends. A) L141 tg females treated with T capsules show a rapid decline in body weight compared with females given blank (B) capsules, but completely recover with the removal of testosterone on day 9 (arrow). B-I) Strikingly, tg females completely recover motor function after T capsules were removed at Day 9 (arrow). Note the uniform recovery on grip strength (B,C), hang test (D), rotarod (E), stride length (F,I) and cage activity (G,H) to pretreatment levels within 6 days after testosterone removal. *Significantly different from blank treated tg females ($p<.05$).

	Treatment	Time	Time vs Treatment Interaction
Body Weight	F(1,10)=8.46, p<.0156	F(13,130)=32.19, p<.0001	F(13,130)=36.2, p<.0001
All limbs Grip Strength	F(1,10)=5.0, p<.049	F(8,80)=12.89, p<.0001	F(8,80)=12.85, p<.0001
Forelimb Grip Strength	F(1,10)=10.46, p<.009	F(8,80)=17.0, p<.0001	F(8,80)=19.96, p<.0001
Hang Test	F(1,10)=1781.1, p<.0001	F(8,80)=91.5, p<.0001	F(8,80)=91.5, p<.0001
Rotarod	F(1,10)=158.7, p<.0001	F(2,20)=114.7, p<.0001	F(2,20)=105.9, p<.0001
Stride Length	F(1,10)=28.9, p<.0003	F(2,20)=49.5, p<.0001	F(2,20)=29.8, p<.0001
Quadrants visited	F(1,4)=7.031, p<.05	F(2,8)=5.3, p<.03	F(2,8)=12.2, p<.003
Number of Rears	F(1,4)=.450, p=.5	F(2,8)=10.4, p<.0059	F(2,8)=8.8, p<.0095

Table 2 F values, degrees of freedom and main effects of genotype and hormone treatment on recovered T-treated L141 tg females.

L78	Genotype	Treatment	Time	Genotype vs Treatment Interaction	Time vs Genotype interaction	Time vs Treatment interaction	Time vs Genotype vs Treatment interactions
Body Weight	F(1,32) = 3.4 p>.07	F(1,32) = 2.9 p>.09	F(4,128) = 17.1 p<.0001	F(1,32) = 2.9 p>.09	F(4,128) = .5 p>.7	F(4,128) = .6 p>.6	F(4,128) = .5 p>.7
Rotarod	F(1,32) = .005 p>.9	F(1,32) = .035 p>.8	F(4,128) = 1.5 p>.2	F(1,32) = .25 p>.6	F(4,128) = .125 p>.9	F(4,128) = 1.2 p>.2	F(4,128) = 1.6 p>.1
Hang test	F(1,32) = .9 p>.3	F(1,32) = .1 p>.7	F(4,128) = 5.6 p<.0003	F(1,32) = .19 p>.6	F(4,128) =.4 p>.7	F(4,128) = .07 p>.9	F(4,128) = .35 p>.8
Stride	F(1,29) = 1.6 p>.2	F(1,29) = .1 p>.7	F(4,116) = .9 p>.4	F(1,29) = .5 p>.4	F(4,116) = .9 p>.4	F(4,116) = .7 p>.5	F(4,116) = 1.3 p>.2

Table 3 F values, degrees of freedom and interactions for behavioral measures in L78 mice. Groups were wt and L78 tg females with and without testosterone.

Figure 15 Testosterone treatment for 9 days in transgenic (tg) and wildtype (wt) females from L78 and L141. A) Tg females from L141, when treated with T, show a progressive decline in body weight ($p<.0001$ compared to Day 0). B-D) L141 tg females treated with T show a rapid decline in motor performance, as shown by rotarod (B, $p<.005$), hang test (C, $p<.0028$), and stride length (D, $p<.04$). E-H) L78 tg females do not show a decline in body weight or loss in motor function when treated with T. * Significantly different from Day 0 within respective treatment group.

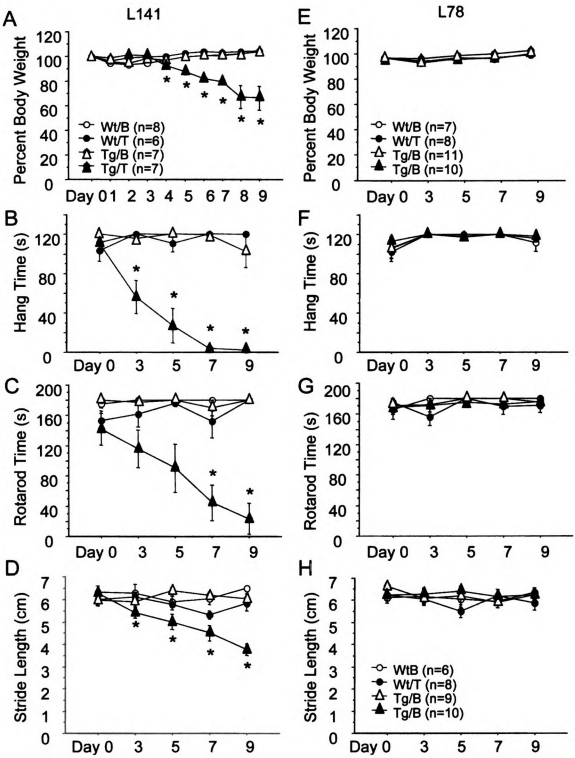
A
L141
Percent Body Weight
Wt/B (n=8)
Wt/T (n=6)
Tg/B (n=7)
Tg/T (n=7)
Day 0 1 2 3 4 5 6 7 8 9
B
Hang Time (s)
Day 0 3 5 7 9
C
Rotarod Time (s)
Day 0 3 5 7 9
D
Stride Length (cm)
Day 0 3 5 7 9
E
L78
Percent Body Weight
Wt/B (n=7)
Wt/T (n=8)
Tg/B (n=11)
Tg/B (n=10)
Day 0 3 5 7 9
F
Hang Time (s)
Day 0 3 5 7 9
G
Rotarod Time (s)
Day 0 3 5 7 9
H
Stride Length (cm)
WtB (n=6)
Wt/T (n=8)
Tg/B (n=9)
Tg/B (n=10)
Day 0 3 5 7 9

Figure 16 Daily food and water intake in 141 tg females over 9 days of T-treatment shows that food intake decreases after motor deficits appear. A) Food intake declines after 4 days of T-treatment and continues until 9 days when compared to day 2 (ps<.05), in T-treated tg L141 females. T-treated wt females also showed a significant decrease in food intake on day 7 (p<.0002), compared to day 2. Day 1 was excluded from the analyses to allow for recovery from surgery. B) Water intake does not decrease with T-treatment. C) Food efficiency (body weight/food intake) remains unchanged, suggesting that metabolic activity is normal.

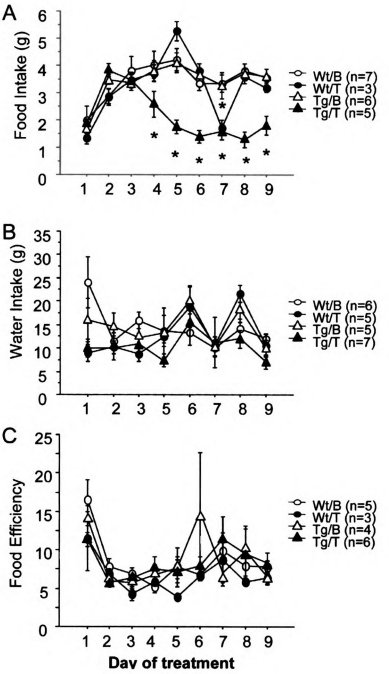
A
Food Intake (g)
Wt/B (n=7)
Wt/T (n=3)
Tg/B (n=6)
Tg/T (n=5)
B
Water Intake (g)
Wt/B (n=6)
Wt/T (n=5)
Tg/B (n=5)
Tg/T (n=7)
C
Food Efficiency
Wt/B (n=5)
Wt/T (n=3)
Tg/B (n=4)
Tg/T (n=6)
Day of treatment

Figure 17 L141 tg females treated with testosterone (T) for 9 days show no evidence of cell loss despite severe motor dysfunction. L141 tg females treated with T show no reduction in the number (A) or size (B) of EDL muscle fibers, nor in the number of axons in L4 or L5 ventral roots, suggesting that cellular dysfunction rather than cell loss may underlie motor deficits in L141 T-treated tg females.

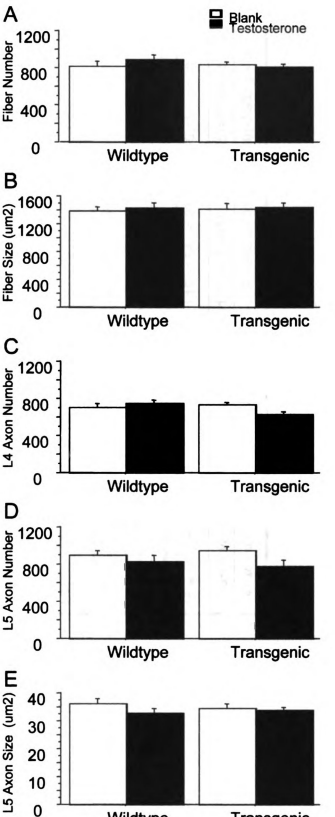
A
Blank
Testosterone
Fiber Number
1200
800
400
0
Wildtype
Transgenic
B
Fiber Size (um2)
1600
1200
800
400
0
Wildtype
Transgenic
C
L4 Axon Number
1200
800
400
0
Wildtype
Transgenic
D
L5 Axon Number
1200
800
400
0
Wildtype
Transgenic
E
L5 Axon Size (um2)
40
30
20
10
0
Wildtype
Transgenic

L141	Genotype	Treatment	Genotype vs Treatment Interaction
EDL weight (g)	F(1,24)=.161, p=.69	F(1,24)=.092, p=.76	F(1,24)=2.5, p=.13
EDL fiber number	F(1,24)=.1.5, p=.23	F(1,24)=.45, p=.50	F(1,24)=5.2, p=.03
EDL fiber size	F(1,24)=.0002, p=.99	F(1,24)=.15, p=.70	F(1,24)=.411, p=.53
L5 axon number	F(1,19)=.0003, p=.99	F(1,19)=1.54, p=.23	F(1,19)=1.9, p=.18
L5 axon size	F(1,25)=.064, p=.80	F(1,25)=1.6, p=21	F(1,25)=.65, p=.43
L4 axon number	F(1,19)=1.562, p=.23	F(1,19)=.902, p=.35	F(1,19)=3.982, p=.06

Table 4 F values, degrees of freedom and main effects of genotype and hormone treatment. Groups were wt and L141 tg females with and without testosterone.

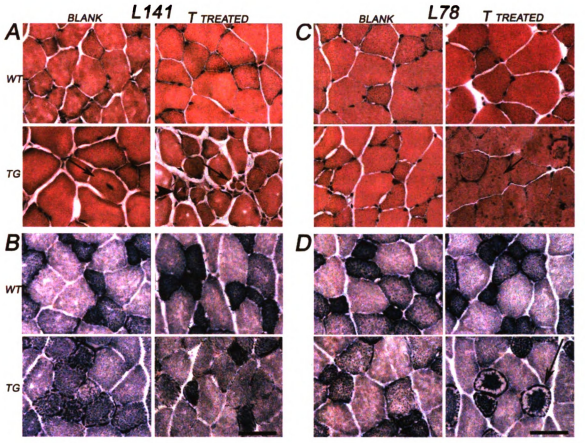

Figure 18 Extensor digitorum longus (EDL) muscle cross sections contain pathology even in mice that show no motor deficits. A) H&E stained muscles of L141 tg females treated with T (TG/T) contain small angular (arrow head), and rounded fibers (arrow). B) No marked pathology is revealed by NADH staining, however fibers appear darker in tg females treated with T. C) H&E staining of L78 females reveals little pathology. Unexpectedly, NADH staining in L78 females (D) reveals altered myofilaments, darkly staining in the center of the fiber and a peripheral area devoid of myofilaments (arrow). It appears that a certain level of pathology is tolerated before behavioral deficits become apparent. Scale bar = 50um.

Figure 19 qPCR reveals denervation-like changes in relative gene expression in muscles of diseased mice. A-C) Skeletal muscle from T-treated tg L141 females show a significant upregulation of acetylcholine receptor alpha (AChR, $p<.0025$) and myogenin ($p<.003$) compared to either wt groups or blank treated tg females, consistent with changes seen when muscles are denervated. Myogenic differentiation factor 1 (MyoD, $p=.09$) mRNA levels also increased, but not significantly. Importantly, neither T treatment nor AR transgene expression alone increase gene expression of these three genes. D) Skeletal muscles from T-treated L141 tg female mice also showed lower expression of vascular endothelial growth factor (VEGF), but it did not reach statistical significance ($p=.07$). E-H) T-treated L78 tg females do not show a similar upregulation of these genes, indicating a selective dysregulation in animals showing a loss of motor function. Values are expressed relative to control (blank) treated wt females in A-H. We also found that mRNA levels for AChR (I), myogenin (J) and myoD (K) return to baseline levels, comparable to that of blank treated tg females, by 6 days after testosterone treatment ends correlating with the recovery of motor function. However, VEGF (L) mRNA was significantly downregulated even after testosterone was removed ($p=.0096$). Values are expressed relative to blank tg females in I-L.

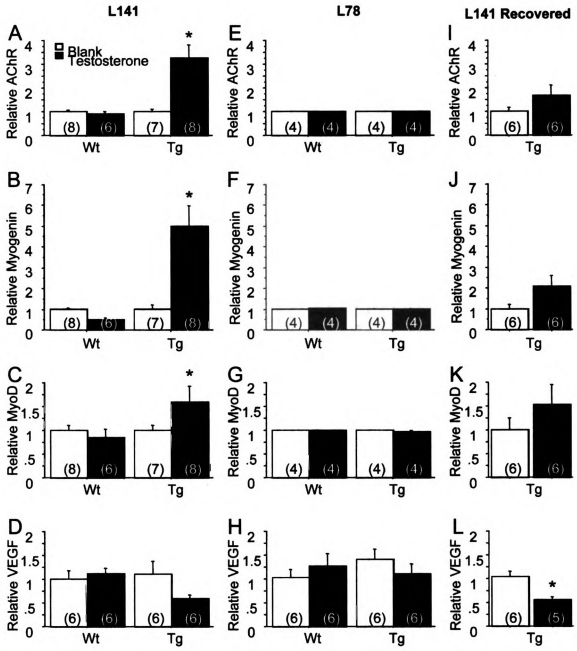
L141
L78
L141 Recovered
A
B
C
D
E
F
G
H
I
J
K
L
Blank
Testosterone
Relative AChR
Relative Myogenin
Relative MyoD
Relative VEGF
Wt
Tg
*

L141	Genotype	Treatment	Genotype vs Treatment Interaction
AChR	F(1,25)=13.4, p=.001	F(1,25)=11.6, p=.002	F(1,25)=13.4, p=.001
Myogenin	F(1,25)=14.98, p=.0007	F(1,25)=8.5, p=.006	F(1,25)=14.98, p=.0007
MyoD	F(1,25)=3.1, p=.09	F(1,25)=1.05, p=.31	F(1,25)=3.1, p=.09
VEGF	F(1,20)=2.3, p=.13	F(1,20)=3.4, p=.07	F(1,20)=1.7, p=.19

L78	Genotype	Treatment	Genotype vs Treatment Interaction
AChR	F(1,12)=.175, p=.68	F(1,12)=.016, p=.9	F(1,12)=.09, p=.76
Myogenin	F(1,12)=.151, p=.7	F(1,12)=.599, p=.45	F(1,12)=.318, p=.58
MyoD	F(1,12)=1.8, p=.2	F(1,12)=1.2, p=.28	F(1,12)=.826, p=.38
VEGF	F(1,20)=.21, p=.6	F(1,20)=0, p>.99	F(1,20)=.006, p=.9

Table 5 F values, degrees of freedom and main effects of genotype and hormone treatment on T-treated tg females. Groups were wt and tg females treated with and without testosterone.

	Undisturbed (No Flutamide) (n=925)	Prenatal Flutamide (n=236)
Wt male	311 (33.6%)	90 (38.1%)
Tg male	6 (0.6%)*	29 (12.2%) **
Wt female	340 (36.8%)	82 (34.7%)
Tg female	280 (30.3%)	51 (21.6%)

***Significantly fewer tg males than predicted (p<.0001)**

****Significantly fewer tg males than predicted (p<.0001), but significantly more males than undisturbed litters (p<.0001)**

Table 6 Number of L141 offspring alive at weaning based on 254 litters.

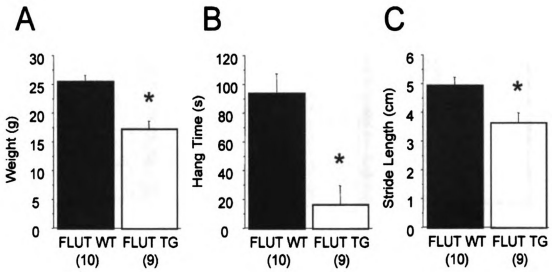

Figure 20 Tg males rescued by prenatal flutamide display symptoms of SBMA in adulthood. A) Tg males exposed to prenatal flutamide (FLUT TG) show a significant reduction in body weight compared to wildtype (FLUT WT) brothers ($p<.0004$) in adulthood. B) Rescued tg males also show a profound loss of motor function on the hang test ($p<.001$) and a shortened stride (C, $p<.007$) compared to wt brothers. Mean age of wt = 107 days, range 64-107 days. Mean age of tg = 111 days, range 65-197 days.

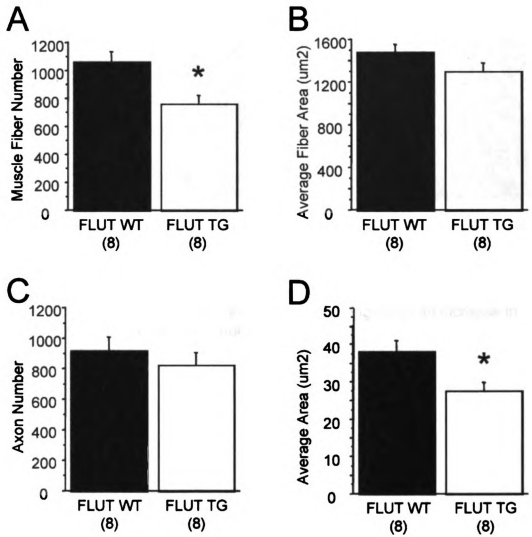

Figure 21 Prenatally flutamide rescued tg males show a reduction in the number of muscle fibers, but not motor axons. A) Tg male mice prenatally exposed to flutamide (FLUT TG) show a significant reduction in the number of muscle fibers in the extensor digitorum longus (EDL) muscle compared to wt (FLUT WT) control males ($p<.008$) in adulthood. B) No change in average fiber size was detected in tg males. C) There was no reduction in the number of L5 ventral root axons. D) L5 ventral root axons were significantly smaller in tg males compared to their wt brothers ($p< .0199$). Mean age of both wt and tg males = 111 days, range 94-197 days.

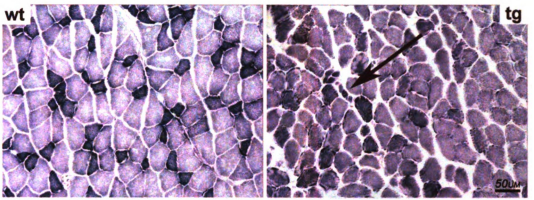

Figure 22 NADH staining reveals pathology in prenatally flutamide rescued tg males. Wt males show the typical checkerboard pattern of staining (left). Flutamide rescued tg males show occasional small atrophic fibers (arrow), and also appear darker, suggesting an increase in oxidative metabolism (right).

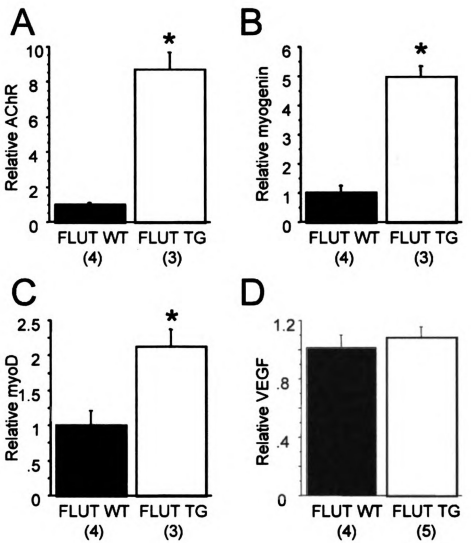

Figure 23 Prenatally flutamide rescued tg male mice (FLUT TG) display, in adulthood, similar changes in gene expression as untreated tg male mice in previous studies consistent with denervation. A) AChR mRNA is significantly upregulated in tg males compared to wt brothers ($p<.0002$). Myogenin mRNA levels are significantly upregulated (B; $p<.0002$), as is MyoD (C; $p<.019$). Upregulation of all three genes has been demonstrated in muscle following denervation. D) VEGF mRNA is not significantly different from wt brothers. Values are expressed relative to wt brothers. Age of both wt and tg males = 114 days.

Figure 24 Flutamide treatment of adult tg females prevented the androgen induced loss of motor function. A) A significant loss in body weight was seen in L141 tg females treated with testosterone (T) and propylene glycol vehicle. However this loss was completely prevented by daily flutamide administration (T + flutamide). By day 4, a significant effect of T treatment was evident in females not treated with flutamide, and continued throughout the experiment. B-F) Flutamide also ameliorated the behavioral effects of T, based on grip strength (B,C), hang test (D), rotarod (E), and stride length (F). * Significantly different from control (T + vehicle), $p < .05$. Mean age for both groups = 116 days, range 97-136 days.

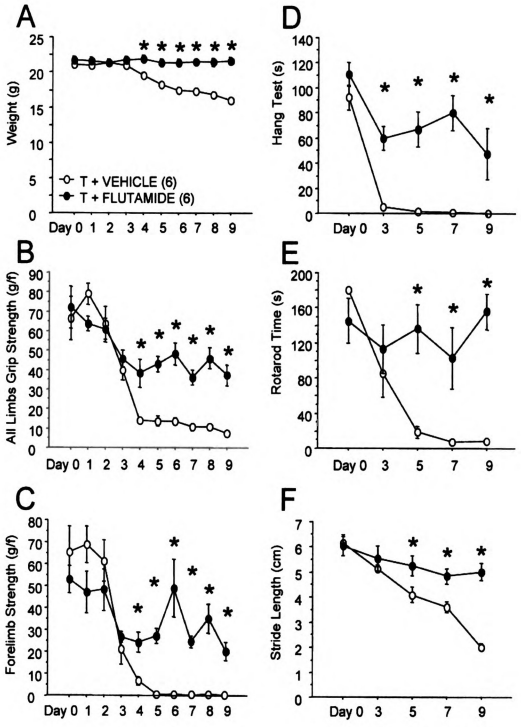
A
Weight (g)
T + VEHICLE (6)
T + FLUTAMIDE (6)
Day 0 1 2 3 4 5 6 7 8 9
B
All Limbs Grip Strength (g/f)
Day 0 1 2 3 4 5 6 7 8 9
C
Forelimb Strength (g/f)
Day 0 1 2 3 4 5 6 7 8 9
D
Hang Test (s)
Day 0 3 5 7 9
E
Rotarod Time (s)
Day 0 3 5 7 9
F
Stride Length (cm)
Day 0 3 5 7 9

	Treatment	Time	Time vs. Treatment
Body Weight	F(1,10)=23.718, p=.0007	F(9,90)=104.6, p<.0001	F(9,90)=93.4, p<.0001
Forelimb grip strength	F(1,10)=6.253, p=.031	F(9,90)=25.2, p<.0001	F(9,90)=8.1, p<.0001
Combined limb grip strength	F(1,10)=21.9, p=.0009	F(9,90)=28.2, p<.0001	F(9,90)=5.5, p<.0001
Hang test	F(1,10)=20.2, p=.001	F(4,40)=42.8, p<.0001	F(4,40)=5.8, p<.0009
Rotarod	F(1,10)=9.776, p=.011	F(4,40)=13.0, p<.0001	F(4,40)=10.6, p<.0001
Stride Length	F(1,10)=10.048, p=.01	F(4,40)=39.1, p<.0001	F(4,40)=13.4, p<.0001

Table 7 F values, degrees of freedom and main effect of treatment, time and interaction on tg females treated with T and Flutamide or T and Vehicle.

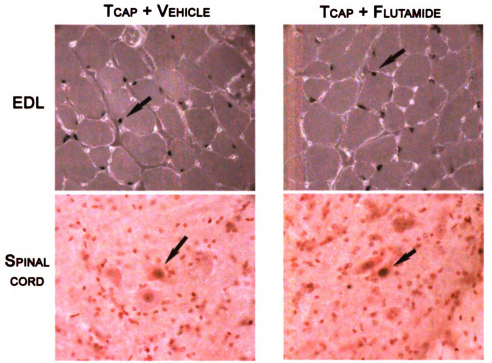

Figure 25 Flutamide induces nuclear translocation in tg female mice in the presence of testosterone. Top) EDL cross sections stained for AR immunohistochemistry show prominent nuclear AR (arrow), in both flutamide and vehicle treated tg females. Bottom) Motoneurons also show clear nuclear AR staining in both flutamide and vehicle treated tg female mice (arrow).

Figure 26 Tg males on a tfm background (tg/tfm), show a dramatic loss of motor function and body weight when treated with testosterone (T) compared to non-tg tfm males treated with T. Remarkably, tg/tfm males regained motor functions and body weight after the removal of T on day 9 (arrow). A) Tg/tfm males treated with T show a decline in body weight. Days 5 through 10 were significantly different from day 0 ($p<.05$), but by day 12 body weight had recovered to pretreatment levels ($p=.42$). B) Forelimb grip strength showed a similar decline, with days 3-10 significantly different from day 0 (B, $p<.05$), and had recovered by day 12 ($p=.48$). C) All limbs grip strength was significantly different on days 3-14 ($p<.05$), but recovered by day 16 ($p=.42$). D) Horizontal cage activity in an open field test was also significantly decreased with T treatment. Days 1-14 were significantly different from Day 0 ($p<.05$), and fully recovered by day 16 ($p=.18$). E) The number of rears in an open field test was significantly decreased on days 3-9 ($p<.05$), and returned to pretreatment levels by day 10, just one day after T treatment ended ($p=.24$). *Significantly decreased from Day 0. Age of tfm and tg/tfm males = 124 days.

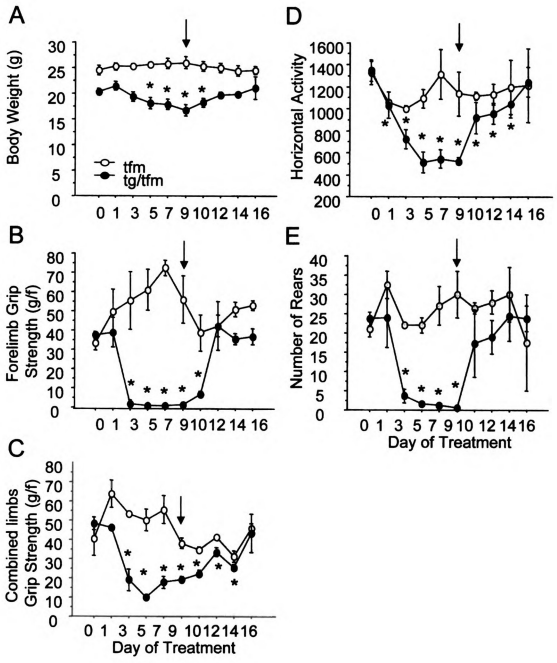
A
Body Weight (g)
30
25
20
15
10
5
0
tfm
tg/tfm
0 1 3 5 7 9 10 12 14 16
D
Horizontal Activity
1600
1400
1200
1000
800
600
400
200
0 1 3 5 7 9 10 12 14 16
B
Forelimb Grip Strength (g/f)
80
70
60
50
40
30
20
10
0
0 1 3 5 7 9 10 12 14 16
E
Number of Rears
40
35
30
25
20
15
10
5
0
0 1 3 5 7 9 10 12 14 16
Day of Treatment
C
Combined limbs Grip Strength (g/f)
80
70
60
50
40
30
20
10
0
0 1 3 5 7 9 10 12 14 16
Day of Treatment

	Genotype	Time	Time vs. Genotype
Body Weight	F(1,3)=19.4, p<.0217	F(9,27)=2.1, p<.05	F(9,27)=6.3, p<.0001
Forelimb grip strength	F(1,3)=120.2, p<.0016	F(9,27)=2.7, p<.01	F(9,27)=8.4, p<.0001
Combined limb grip strength	F(1,3)=431.6, p<.0002	F(9,27)=6.9, p<.0001	F(9,27)=5.8, p<.0002
Horizontal activity	F(1,3)=3.17, p<.17	F(9,27)=9.9, p<.0001	F(9,27)=6.6, p<.0001
Rears	F(1,3)=6.3, p<.08	F(9,27)=4.2, p<.0018	F(9,27)=4.0, p<.0023

Table 8 F values, degrees of freedom and main effect of genotype, time and interaction on tg/tfm and tfm males treated with T.

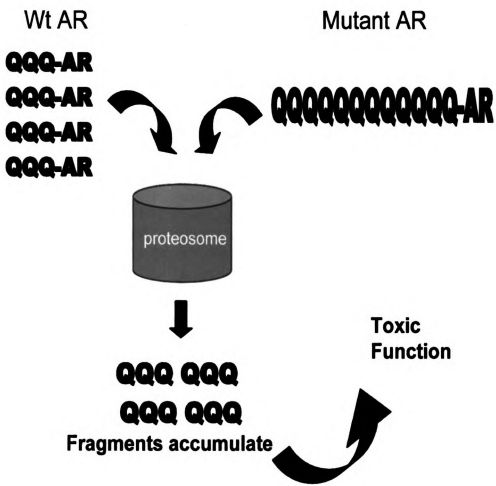

Figure 27 Proteosomal degradation of wt and mutant AR may result in similar toxic functions. Both wt and mutant AR proteins are degraded by the proteosome, however the proteosome may have difficulty degrading glutamines. This results in similar small fragments that accumulate inside the cell, and in both cases may contribute to a toxic gain of function.

REFERENCES

Abel A, Walcott J, Woods J, Duda J, Merry DE (2001) Expression of expanded repeat androgen receptor produces neurologic disease in transgenic mice. Hum Mol Genet 10:107-116.

Adachi H, Waza M, Tokui K, Katsuno M, Minamiyama M, Tanaka F, Doyu M, Sobue G (2007) CHIP Overexpression Reduces Mutant Androgen Receptor Protein and Ameliorates Phenotypes of the Spinal and Bulbar Muscular Atrophy Transgenic Mouse Model. J Neurosci 27:5115-5126.

Adachi H, Kume A, Li M, Nakagomi Y, Niwa H, Do J, Sang C, Kobayashi Y, Doyu M, Sobue G (2001) Transgenic mice with an expanded CAG repeat controlled by the human AR promoter show polyglutamine nuclear inclusions and neuronal dysfunction without neuronal cell death. Hum Mol Genet 10:1039-1048.

Adachi H, Katsuno M, Minamiyama M, Sang C, Pagoulatos G, Angelidis C, Kusakabe M, Yoshiki A, Kobayashi Y, Doyu M, Sobue G (2003) Heat shock protein 70 chaperone overexpression ameliorates phenotypes of the spinal and bulbar muscular atrophy transgenic mouse model by reducing nuclear-localized mutant androgen receptor protein. J Neurosci 23:2203-2211.

Antonarakis ES, Blackford AL, Garrett-Mayer E, Eisenberger MA (2007) Survival in Men With Nonmetastatic Prostate Cancer Treated With Hormone Therapy: A Quantitative Systematic Review. J Clin Oncol 25:4998-5008.

Antonio J, Wilson JD, George FW (1999) Effects of castration and androgen treatment on androgen-receptor levels in rat skeletal muscles. J Appl Physiol 87:2016-2019.

Arbizu T, Santamaria J, Gomez JM, Quilez A, Serra JP (1983) A family with adult spinal and bulbar muscular atrophy, X-linked inheritance and associated testicular failure. J Neurol Sci 59:371-382.

Arrasate M, Mitra S, Schweitzer ES, Segal MR, Finkbeiner S (2004) Inclusion body formation reduces levels of mutant huntingtin and the risk of neuronal death. Nature 431:805-810.

Azzouz M, Ralph GS, Storkebaum E, Walmsley LE, Mitrophanous KA, Kingsman SM, Carmeliet P, Mazarakis ND (2004) VEGF delivery with retrogradely transported lentivector prolongs survival in a mouse ALS model. Nature 429:413-417.

Bailey CK, Andriola IF, Kampinga HH, Merry DE (2002) Molecular chaperones enhance the degradation of expanded polyglutamine repeat androgen receptor in a cellular model of spinal and bulbar muscular atrophy. Hum Mol Genet 11:515-523.

Balice-Gordon RJ, Breedlove SM, Bernstein S, Lichtman JW (1990) Neuromuscular junctions shrink and expand as muscle fiber size is manipulated: in vivo observations in the androgen-sensitive bulbocavernosus muscle of mice. J Neurosci 10:2660-2671.

Banno H, Adachi H, Katsuno M, Suzuki K, Atsuta N, Watanabe H, Tanaka F, Doyu M, Sobue G (2006) Mutant androgen receptor accumulation in spinal and bulbar muscular atrophy scrotal skin: A pathogenic marker. Annals of Neurology 59:520-526.

Bernstein M, Lichtman JW (1999) Axonal atrophy: The retraction reaction. Current Opinion in Neurobiology 9:364-370.

Bhutani N, Venkatraman P, Goldberg AL (2007) Puromycin-sensitive aminopeptidase is the major peptidase responsible for digesting polyglutamine sequences released by proteasomes during protein degradation. Embo J 26:1385-1396.

Breedlove SM, Arnold AP (1980) Hormone accumulation in a sexually dimorphic motor nucleus of the rat spinal cord. Science 210:564-566.

Breedlove SM, Arnold AP (1981) Sexually dimorphic motor nucleus in the rat lumbar spinal cord: response to adult hormone manipulation, absence in androgen-insensitive rats. Brain Res 225:297-307.

Breedlove SM, Arnold AP (1983a) Hormonal control of a developing neuromuscular system: II. Sensitive periods for the androgen induced masculinization of the rat spinal nucleus of the bulbocavernosus. Journal of Neuroscience 3:424-432.

Breedlove SM, Arnold AP (1983b) Hormonal control of a developing neuromuscular system. II. Sensitive periods for the androgen-induced masculinization of the rat spinal nucleus of the bulbocavernosus. J Neurosci 3:424-432.

Breedlove SM, Arnold AP (1983c) Hormonal control of a developing neuromuscular system: I. Complete demasculinization of the spinal nucleus of the bulbocavernosus in male rats using the anti-androgen flutamide. Journal of Neuroscience 3:417-423.

Breedlove SM, Arnold AP (1983d) Hormonal control of a developing neuromuscular system. I. Complete Demasculinization of the male rat spinal nucleus of the bulbocavernosus using the anti-androgen flutamide. J Neurosci 3:417-423.

Brennan KJ, Hardeman EC (1993) Quantitative analysis of the human alpha-skeletal actin gene in transgenic mice. J Biol Chem 268:719-725.

Cardozo CP, Michaud C, Ost MC, Fliss AE, Yang E, Patterson C, Hall SJ, Caplan AJ (2003) C-terminal Hsp-interacting protein slows androgen receptor synthesis and reduces its rate of degradation. Arch Biochem Biophys 410:134-140.

Carmeliet P, Ferreira V, Breier G, Pollefeyt S, Kieckens L, Gertsenstein M, Fahrig M, Vandenhoeck A, Harpal K, Eberhardt C, Declercq C, Pawling J, Moons L, Collen D, Risau W, Nagy A (1996) Abnormal blood vessel development and lethality in embryos lacking a single VEGF allele. Nature 380:435-439.

Casto JM, Ward OB, Bartke A (2003) Play, copulation, anatomy, and testosterone in gonadally intact male rats prenatally exposed to flutamide. Physiology & Behavior 79:633-641.

Charest NJ, Zhou ZX, Lubahn DB, Olsen KL, Wilson EM, French FS (1991) A frameshift mutation destabilizes androgen receptor messenger RNA in the Tfm mouse. Mol Endocrinol 5:573-581.

Chen C, Fischbeck KH (2006) Clinical Features and Molecular Biology of Kennedy's disease. In: Genetic Instabilities and Neurological Diseases (Second Edition) (Robert DW, Tetsuo A, eds), pp 211-220. Burlington: Academic Press.

Chevalier-Larsen ES, O'Brien CJ, Wang H, Jenkins SC, Holder L, Lieberman AP, Merry DE (2004) Castration Restores Function and Neurofilament Alterations of Aged Symptomatic Males in a Transgenic Mouse Model of Spinal and Bulbar Muscular Atrophy. J Neurosci 24:4778-4786.

Chevrel G, Sendtner RHM (2006) The role of neurotrophins in muscle under physiological and pathological conditions. Muscle & Nerve 33:462-476.

Chung HW, Kim SC, Kim HL (1998) Frame-shift mutation in hormone binding domain of human androgen receptor gene causes complete androgen insensitivity. Mol Cells 8:741-745.

Cifuentes-Diaz C, Nicole S, Velasco ME, Borra-Cebrian C, Panozzo C, Frugier T, Millet G, Roblot N, Joshi V, Melki J (2002) Neurofilament accumulation at the motor endplate and lack of axonal sprouting in a spinal muscular atrophy mouse model. Hum Mol Genet 11:1439-1447.

Cihak R, Gutmann E, Hanzlikova V (1970) Involution and hormone-induced persistence of the M. sphincter (levator) ani in female rats. J Anat 106:93-110.

Clement AM, Nguyen MD, Roberts EA, Garcia ML, Boillee S, Rule M, McMahon AP, Doucette W, Siwek D, Ferrante RJ, Brown RH, Jr., Julien JP, Goldstein LS, Cleveland DW (2003) Wild-type nonneuronal cells extend survival of SOD1 mutant motor neurons in ALS mice. Science 302:113-117.

Clos V, Esteve A, Jane F, Salva P (1988) Microsomal effects of cyproterone acetate and flutamide in rat testis. Gen Pharmacol 19:393-397.

Cummings CJ, Sun Y, Opal P, Antalffy B, Mestril R, Orr HT, Dillmann WH, Zoghbi HY (2001) Over-expression of inducible HSP70 chaperone suppresses neuropathology and improves motor function in SCA1 mice. Hum Mol Genet 10:1511-1518.

de Ruijter AJM, van Gennip AH, Caron HN, Kemp S, van Kuilenburg ABP (2003) Histone deacetylases (HDACs): characterization of the classical HDAC family. Biochem J 370:737-749.

Dejager S, Bry-Gauillard H, Bruckert E, Eymard B, Salachas F, LeGuern E, Tardieu S, Chadarevian R, Giral P, Turpin G (2002) A Comprehensive Endocrine Description of Kennedy's Disease Revealing Androgen Insensitivity Linked to CAG Repeat Length. J Clin Endocrinol Metab 87:3893-3901.

Dobrowolny G, Giacinti C, Pelosi L, Nicoletti C, Winn N, Barberi L, Molinaro M, Rosenthal N, Musaro A (2005) Muscle expression of a local Igf-1 isoform protects motor neurons in an ALS mouse model. J Cell Biol 168:193-199.

Duclert A, Piette J, Changeux JP (1991) Influence of innervation of myogenic factors and acetylcholine receptor alpha-subunit mRNAs. Neuroreport 2:25-28.

Duennwald ML, Jagadish S, Muchowski PJ, Lindquist S (2006) Flanking sequences profoundly alter polyglutamine toxicity in yeast. Proc Natl Acad Sci U S A.

Eftimie R, Brenner HR, Buonanno A (1991) Myogenin and MyoD join a family of skeletal muscle genes regulated by electrical activity. Proc Natl Acad Sci U S A 88:1349-1353.

Fernandez-Funez P, Nino-Rosales ML, de Gouyon B, She WC, Luchak JM, Martinez P, Turiegano E, Benito J, Capovilla M, Skinner PJ, McCall A, Canal I, Orr HT, Zoghbi HY, Botas J (2000) Identification of genes that modify ataxin-1-induced neurodegeneration. Nature 408:101-106.

Ferrante RJ, Kubilus JK, Lee J, Ryu H, Beesen A, Zucker B, Smith K, Kowall NW, Ratan RR, Luthi-Carter R, Hersch SM (2003) Histone deacetylase inhibition by sodium butyrate chemotherapy ameliorates the neurodegenerative phenotype in Huntington's disease mice. J Neurosci 23:9418-9427.

Fischer LR, Culver DG, Tennant P, Davis AA, Wang M, Castellano-Sanchez A, Khan J, Polak MA, Glass JD (2004) Amyotrophic lateral sclerosis is a distal axonopathy: evidence in mice and man. Exp Neurol 185:232-240.

Fishman RB, Breedlove SM (1985) The androgenic induction of spinal sexual dimorphism is independent of supraspinal afferents. Brain Res 355:255-258.

Fishman RB, Breedlove SM (1992) Local perineal implants of anti-androgen block masculinization of the spinal nucleus of the bulbocavernosus. Brain Res Dev Brain Res 70:283-286.

Forger NG, Howell ML, Bengston L, MacKenzie L, DeChiara TM, Yancopoulos GD (1997) Sexual dimorphism in the spinal cord is absent in mice lacking the ciliary neurotrophic factor receptor. J Neurosci 17:9605-9612.

Freeman LM, Watson NV, Breedlove SM (1996) Androgen spares androgen-insensitive motoneurons from apoptosis in the spinal nucleus of the bulbocavernosus in rats. Horm Behav 30:424-433.

Frey D, Schneider C, Xu L, Borg J, Spooren W, Caroni P (2000) Early and selective loss of neuromuscular synapse subtypes with low sprouting competence in motoneuron diseases. J Neurosci 20:2534-2542.

Gatchel JR, Watase K, Thaller C, Carson JP, Jafar-Nejad P, Shaw C, Zu T, Orr HT, Zoghbi HY (2008) The insulin-like growth factor pathway is altered in spinocerebellar ataxia type 1 and type 7. Proceedings of the National Academy of Sciences 105:1291-1296.

Gladue BA, Clemens LG (1978) Androgenic influences on feminine sexual behavior in male and female rats: defeminization blocked by prenatal antiandrogen treatment. Endocrinology 103:1702-1709.

Goldstein LA, Kurz EM, Sengelaub DR (1990) Androgen regulation of dendritic growth and retraction in the development of a sexually dimorphic spinal nucleus. J Neurosci 10:935-946.

Harding AE, Thomas PK, Baraitser M, Bradbury PG, Morgan-Hughes JA, Ponsford JR (1982) X-linked recessive bulbospinal neuronopathy: a report of ten cases. J Neurol Neurosurg Psychiatry 45:1012-1019.

Hellwinkel OJ, Bull K, Holterhus PM, Homburg N, Struve D, Hiort O (1999) Complete androgen insensitivity caused by a splice donor site mutation in intron 2 of the human androgen receptor gene resulting in an exon 2-

lacking transcript with premature stop-codon and reduced expression. J Steroid Biochem Mol Biol 68:1-9.

Holmberg CI, Staniszewski KE, Mensah KN, Matouschek A, Morimoto RI (2004) Inefficient degradation of truncated poluglutamine proteins by the proteosome. EMBO 23:4307-4318.

Humbert S, Bryson EA, Cordelieres FP, Connors NC, Datta SR, Finkbeiner S, Greenberg ME, Saudou F (2002) The IGF-1/Akt Pathway Is Neuroprotective in Huntington's Disease and Involves Huntingtin Phosphorylation by Akt. Developmental Cell 2:831-837.

Jaarsma D, Teuling E, Haasdijk ED, De Zeeuw CI, Hoogenraad CC (2008) Neuron-Specific Expression of Mutant Superoxide Dismutase Is Sufficient to Induce Amyotrophic Lateral Sclerosis in Transgenic Mice. J Neurosci 28:2075-2088.

Jaarsma D, Haasdijk ED, Grashorn JAC, Hawkins R, van Duijn W, Verspaget HW, London J, Holstege JC (2000) Human Cu/Zn Superoxide Dismutase (SOD1) Overexpression in Mice Causes Mitochondrial Vacuolization, Axonal Degeneration, and Premature Motoneuron Death and Accelerates Motoneuron Disease in Mice Expressing a Familial Amyotrophic Lateral Sclerosis Mutant SOD1. Neurobiology of Disease 7:623-643.

Jordan CL, Padgett B, Hershey J, Prins G, Arnold A (1997) Ontogeny of androgen receptor immunoreactivity in lumbar motoneurons and in the sexually dimorphic levator ani muscle of male rats. J Comp Neurol 379:88-98.

Kaspar BK, Llado J, Sherkat N, Rothstein JD, Gage FH (2003) Retrograde Viral Delivery of IGF-1 Prolongs Survival in a Mouse ALS Model. Science 301:839-842.

Katsuno M, Adachi H, Inukai A, Sobue G (2003a) Transgenic mouse models of spinal and bulbar muscular atrophy (SBMA). Cytogenet Genome Res 100:243-251.

Katsuno M, Adachi H, Doyu M, Minamiyama M, Sang C, Kobayashi Y, Inukai A, Sobue G (2003b) Leuprorelin rescues polyglutamine-dependent phenotypes in a transgenic mouse model of spinal and bulbar muscular atrophy. Nat Med 9:768-773.

Katsuno M, Sang C, Adachi H, Minamiyama M, Waza M, Tanaka F, Doyu M, Sobue G (2005) Pharmacological induction of heat-shock proteins alleviates polyglutamine-mediated motor neuron disease.:-.

Katsuno M, Adachi H, Kume A, Li M, Nakagomi Y, Niwa H, Sang C, Kobayashi Y, Doyu M, Sobue G (2002) Testosterone reduction prevents phenotypic expression in a transgenic mouse model of spinal and bulbar muscular atrophy. Neuron 35:843-854.

Katsuno M, Adachi H, Minamiyama M, Waza M, Tokui K, Banno H, Suzuki K, Onoda Y, Tanaka F, Doyu M, Sobue G (2006a) Reversible Disruption of Dynactin 1-Mediated Retrograde Axonal Transport in Polyglutamine-Induced Motor Neuron Degeneration. J Neurosci 26:12106-12117.

Katsuno M, Adachi H, Minamiyama M, Waza M, Tokui K, Banno H, Suzuki K, Onoda Y, Tanaka F, Doyu M, Sobue G (2006b) Reversible disruption of dynactin 1-mediated retrograde axonal transport in polyglutamine-induced motor neuron degeneration. J Neurosci 26:12106-12117.

Kennedy WR, Alter M, Sung JH (1968) Progressive proximal spinal and bulbar muscular atrophy of late onset. A sex-linked recessive trait. Neurology 18:671-680.

Kinirons P, Rouleau GA (2006) Administration of testosterone results in reversible deterioration in Kennedy's disease. J Neurol Neurosurg Psychiatry:jnnp.2006.101899.

Klocke R, Steinmeyer K, Jentsch TJ, Jockusch H (1994) Role of innervation, excitability, and myogenic factors in the expression of the muscular chloride channel ClC-1. A study on normal and myotonic muscle. J Biol Chem 269:27635-27639.

Knobil E, Neill JD, eds (1998) Encyclopedia of reproduction. San Diego: Academic Press.

Kostrominova TY, Macpherson PC, Carlson BM, Goldman D (2000) Regulation of myogenin protein expression in denervated muscles from young and old rats. Am J Physiol Regul Integr Comp Physiol 279:R179-188.

Kostrominova TY, Dow DE, Dennis RG, Miller RA, Faulkner JA (2005) Comparison of gene expression of 2-mo denervated, 2-mo stimulated-denervated, and control rat skeletal muscles. Physiol Genomics 22:227-243.

Kurz EM, Sengelaub DR, Arnold AP (1986) Androgens regulate the dendritic length of mammalian motoneurons in adulthood. Science 232:395-398.

La Spada AR, Wilson EM, Lubahn DB, Harding AE, Fischbeck KH (1991) Androgen receptor gene mutations in X-linked spinal and bulbar muscular atrophy. Nature 352:77-79.

Lambrechts D et al. (2003) VEGF is a modifier of amyotrophic lateral sclerosis in mice and humans and protects motoneurons against ischemic death. Nat Genet 34:383-394.

Lecker SH, Goldberg AL, Mitch WE (2006) Protein Degradation by the Ubiquitin-Proteasome Pathway in Normal and Disease States. J Am Soc Nephrol 17:1807-1819.

Li M, Miwa S, Kobayashi Y, Merry DE, Yamamoto M, Tanaka F, Doyu M, Hashizume Y, Fischbeck KH, Sobue G (1998) Nuclear inclusions of the androgen receptor protein in spinal and bulbar muscular atrophy. Ann Neurol 44:249-254.

Li W, Brakefield D, Pan Y, Hunter D, Myckatyn TM, Parsadanian A (2007) Muscle-derived but not centrally derived transgene GDNF is neuroprotective in G93A-SOD1 mouse model of ALS. Experimental Neurology 203:457-471.

Lin HK, Wang L, Hu YC, Altuwaijri S, Chang C (2002) Phosphorylation-dependent ubiquitylation and degradation of androgen receptor by Akt require Mdm2 E3 ligase. Embo J 21:4037-4048.

Lino MM, Schneider C, Caroni P (2002) Accumulation of SOD1 mutants in postnatal motoneurons does not cause motoneuron pathology or motoneuron disease. J Neurosci 22:4825-4832.

Marchetti B, Labrie F (1988) Characteristics of flutamide action on prostatic and testicular functions in the rat. J Steroid Biochem 29:691-698.

McBride JL, During MJ, Wuu J, Chen EY, Leurgans SE, Kordower JH (2003) Structural and functional neuroprotection in a rat model of Huntington's disease by viral gene transfer of GDNF. Exp Neurol 181:213-223.

McCampbell A, Taye AA, Whitty L, Penney E, Steffan JS, Fischbeck KH (2001) Histone deacetylase inhibitors reduce polyglutamine toxicity. Proc Natl Acad Sci U S A 98:15179-15184.

McCampbell A, Taylor JP, Taye AA, Robitschek J, Li M, Walcott J, Merry D, Chai Y, Paulson H, Sobue G, Fischbeck KH (2000) CREB-binding protein sequestration by expanded polyglutamine. Hum Mol Genet 9:2197-2202.

McManamny P, Chy HS, Finkelstein DI, Craythorn RG, Crack PJ, Kola I, Cheema SS, Horne MK, Wreford NG, O'Bryan MK, De Kretser DM, Morrison JR (2002) A mouse model of spinal and bulbar muscular atrophy. Hum Mol Genet 11:2103-2111.

Mejat A, Ramond F, Bassel-Duby R, Khochbin S, Olson EN, Schaeffer L (2005) Histone deacetylase 9 couples neuronal activity to muscle chromatin acetylation and gene expression. Nat Neurosci 8:313-321.

Messi ML, Clark HM, Prevette DM, Oppenheim RW, Delbono O (2007) The lack of effect of specific overexpression of IGF-1 in the central nervous system or skeletal muscle on pathophysiology in the G93A SOD-1 mouse model of ALS. Experimental Neurology 207:52-63.

Miller TM, Kim SH, Yamanaka K, Hester M, Umapathi P, Arnson H, Rizo L, Mendell JR, Gage FH, Cleveland DW, Kaspar BK (2006) From the Cover: Gene transfer demonstrates that muscle is not a primary target for non-cell-autonomous toxicity in familial amyotrophic lateral sclerosis. PNAS 103:19546-19551.

Mills SE (2007) Histology for Pathologists, 3rd Edition. Philadelphia: Lippincott Williams & Wilkins.

Minamiyama M, Katsuno M, Adachi H, Waza M, Sang C, Kobayashi Y, Tanaka F, Doyu M, Inukai A, Sobue G (2004) Sodium butyrate ameliorates phenotypic expression in a transgenic mouse model of spinal and bulbar muscular atrophy. Hum Mol Genet 13:1183-1192.

Mochizuki H, Yasuda T, Mouradian MM (2008) Advances in gene therapy for movement disorders. Neurotherapeutics 5:260-269.

Monks DA, Vanston CM, Watson NV (1999) Direct androgenic regulation of calcitonin gene-related peptide expression in motoneurons of rats with mosaic androgen insensitivity. J Neurosci 19:5597-5601.

Monks DA, O'Bryant EL, Jordan CL (2004) Androgen receptor immunoreactivity in skeletal muscle: enrichment at the neuromuscular junction. J Comp Neurol 473:59-72.

Monks DA, Kopachik W, Breedlove SM, Jordan CL (2006a) Anabolic responsiveness of skeletal muscles correlates with androgen receptor protein but not mRNA. Can J Physiol Pharmacol 84:273-277.

Monks DA, Kopachik W, Breedlove SM, Jordan CL (2006b) Anabolic responsiveness of skeletal muscles correlates with androgen receptor protein but not mRNA. Can J Physiol Pharmacol 84:273-277.

Monks DA, Johansen JA, Mo K, Rao P, Eagleson B, Yu Z, Lieberman AP, Breedlove SM, Jordan CL (2007) Overexpression of wild-type androgen receptor in muscle recapitulates polyglutamine disease. Proceedings of the National Academy of Sciences 104:18259–18264.

Morris JA, Jordan CL, Breedlove SM (2004) Sexual differentiation of the vertebrate nervous system. Nat Neurosci 7:1034-1039.

Motelica-Heino I, Castanier M, Corbier P, Edwards DA, Roffi J (1988) Testosterone levels in plasma and testes of neonatal mice. J Steroid Biochem 31:283-286.

Nagashima T, Seko K, Hirose K, Mannen T, Yoshimura S, Arima R, Nagashima K, Morimatsu Y (1988) Familial bulbo-spinal muscular atrophy associated with testicular atrophy and sensory neuropathy (Kennedy-Alter-Sung syndrome). Autopsy case report of two brothers. J Neurol Sci 87:141-152.

Nordeen EJ, Nordeen KW, Sengelaub DR, Arnold AP (1985) Androgens prevent normally occurring cell death in a sexually dimorphic spinal nucleus. Science 229:671-673.

Nucifora FC, Jr., Sasaki M, Peters MF, Huang H, Cooper JK, Yamada M, Takahashi H, Tsuji S, Troncoso J, Dawson VL, Dawson TM, Ross CA (2001) Interference by Huntingtin and Atrophin-1 with CBP-Mediated Transcription Leading to Cellular Toxicity. Science 291:2423-2428.

Ohsako S, Kubota K, Kurosawa S, Takeda K, Qing W, Ishimura R, Tohyama C (2003) Alterations of gene expression in adult male rat testis and pituitary shortly after subacute administration of the antiandrogen flutamide. J Reprod Dev 49:275-290.

Ono S, Geller LN, Lai EV (1974) TfM mutation and masculinization versus feminization of the mouse central nervous system. Cell 3:235-242.

Orr HT, Zoghbi HY (2007) Trinucleotide repeat disorders. Annu Rev Neurosci 30:575-621.

Palazzolo I, Burnett BG, Young JE, Brenne PL, La Spada AR, Fischbeck KH, Howell BW, Pennuto M (2007) Akt blocks ligand binding and protects against expanded polyglutamine androgen receptor toxicity. Hum Mol Genet 16:1593–1603.

Pelosi L, Giacinti C, Nardis C, Borsellino G, Rizzuto E, Nicoletti C, Wannenes F, Battistini L, Rosenthal N, Molinaro M, Musaro A (2007) Local expression of IGF-1 accelerates muscle regeneration by rapidly modulating inflammatory cytokines and chemokines. FASEB J 21:1393-1402.

Pramatarova A, Laganiere J, Roussel J, Brisebois K, Rouleau GA (2001) Neuron-specific expression of mutant superoxide dismutase 1 in transgenic mice does not lead to motor impairment. J Neurosci 21:3369-3374.

Pun S, Santos AF, Saxena S, Xu L, Caroni P (2006) Selective vulnerability and pruning of phasic motoneuron axons in motoneuron disease alleviated by CNTF. Nat Neurosci 9:408-419.

Rabinovsky ED, Gelir E, Gelir S, Lui H, Kattash M, DeMayo FJ, Shenaq SM, Schwartz RJ (2003) Targeted expression of IGF-1 transgene to skeletal muscle accelerates muscle and motor neuron regeneration. Faseb J 17:53-55.

Rand MN, Breedlove SM (1987) Ontogeny of functional innervation of bulbocavernosus muscles in male and female rats. Brain Res 430:150-152.

Rouaux C, Loeffler JP, Boutillier AL (2004) Targeting CREB-binding protein (CBP) loss of function as a therapeutic strategy in neurological disorders. Biochem Pharmacol 68:1157-1164.

Rouaux C, Panteleeva I, Rene F, Gonzalez de Aguilar J-L, Echaniz-Laguna A, Dupuis L, Menger Y, Boutillier A-L, Loeffler J-P (2007) Sodium Valproate Exerts Neuroprotective Effects In Vivo through CREB-Binding Protein-Dependent Mechanisms But Does Not Improve Survival in an Amyotrophic Lateral Sclerosis Mouse Model. J Neurosci 27:5535-5545.

Sacheck JM, Ohtsuka A, McLary SC, Goldberg AL (2004) IGF-I stimulates muscle growth by suppressing protein breakdown and expression of atrophy-related ubiquitin ligases, atrogin-1 and MuRF1. Am J Physiol Endocrinol Metab 287:E591-601.

Sachs BD (1982) Role of striated penile muscles in penile reflexes, copulation, and induction of pregnancy in the rat. J Reprod Fertil 66:433-443.

Sanes JR, Lichtman JW (1999) Development of the vertebrate neuromuscular junction. Annu Rev Neurosci 22:389-442.

Sanes JR, Lichtman JW (2001) Induction, assembly, maturation and maintenance of a postsynaptic apparatus. Nat Rev Neurosci 2:791-805.

Saudou F, Finkbeiner S, Devys D, Greenberg ME (1998) Huntingtin acts in the nucleus to induce apoptosis but death does not correlate with the formation of intranuclear inclusions. Cell 95:55-66.

Schertzer JD, Ryall JG, Lynch GS (2006) Systemic administration of IGF-I enhances oxidative status and reduces contraction-induced injury in skeletal muscles of mdx dystrophic mice. Am J Physiol Endocrinol Metab 291:E499-505.

Sedehizade F, Klocke R, Jockusch H (1997) Expression of nerve-regulated genes in muscles of mouse mutants affected by spinal muscular atrophies and muscular dystrophies. Muscle Nerve 20:186-194.

Shang Y, Brown M (2002) Molecular Determinants for the Tissue Specificity of SERMs. Science 295:2465-2468.

Sherman MY, Goldberg AL (2001) Cellular defenses against unfolded proteins: a cell biologist thinks about neurodegenerative diseases. Neuron 29:15-32.

Shi X, Garry DJ (2006) Muscle stem cells in development, regeneration, and disease. Genes Dev 20:1692-1708.

Singleton AB et al. (2003) alpha-Synuclein locus triplication causes Parkinson's disease. Science 302:841.

Snider WD (1994) Functions of the neurotrophins during nervous system development: What the knockouts are teaching us. Cell 77:627-638.

Sobue G, Hashizume Y, Mukai E, Hirayama M, Mitsuma T, Takahashi A (1989) X-linked recessive bulbospinal neuronopathy. A clinicopathological study. Brain 112 (Pt 1):209-232.

Sopher BL, Thomas PS, Jr., LaFevre-Bernt MA, Holm IE, Wilke SA, Ware CB, Jin LW, Libby RT, Ellerby LM, La Spada AR (2004) Androgen receptor YAC transgenic mice recapitulate SBMA motor neuronopathy and implicate VEGF164 in the motor neuron degeneration. Neuron 41:687-699.

Steffan JS, Bodai L, Pallos J, Poelman M, McCampbell A, Apostol BL, Kazantsev A, Schmidt E, Zhu YZ, Greenwald M, Kurokawa R, Housman DE, Jackson GR, Marsh JL, Thompson LM (2001) Histone deacetylase inhibitors arrest polyglutamine-dependent neurodegeneration in Drosophila. Nature 413:739-743.

Stitt TN, Drujan D, Clarke BA, Panaro F, Timofeyva Y, Kline WO, Gonzalez M, Yancopoulos GD, Glass DJ (2004) The IGF-1/PI3K/Akt Pathway Prevents Expression of Muscle Atrophy-Induced Ubiquitin Ligases by Inhibiting FOXO Transcription Factors. Molecular Cell 14:395-403.

Strand AD, Aragaki AK, Shaw D, Bird T, Holton J, Turner C, Tapscott SJ, Tabrizi SJ, Schapira A, Kooperberg CL, Olson JM (2005) Gene expression in Huntington's disease skeletal muscle: a potential biomarker. Hum Mol Genet 14:1863-1876

Takeyama K, Ito S, Yamamoto A, Tanimoto H, Furutani T, Kanuka H, Miura M, Tabata T, Kato S (2002) Androgen-dependent neurodegeneration by polyglutamine-expanded human androgen receptor in Drosophila. Neuron 35:855-864.

Taylor MD, Vancura R, Patterson CL, Williams JM, Riekhof JT, Wright DE (2001) Postnatal regulation of limb proprioception by muscle-derived neurotrophin-3. J Comp Neurol 432:244-258.

Thiele B, Weidemann W, Schnabel D, Romalo G, Schweikert HU, Spindler KD (1999) Complete androgen insensitivity caused by a new frameshift deletion of two base pairs in exon 1 of the human androgen receptor gene. J Clin Endocrinol Metab 84:1751-1753.

Thomas M, Harrell JM, Morishima Y, Peng H-M, Pratt WB, Lieberman AP (2006) Pharmacologic and genetic inhibition of hsp90-dependent trafficking reduces aggregation and promotes degradation of the expanded glutamine androgen receptor without stress protein induction. Hum Mol Genet 15:1876-1883.

Tsuda H, Jafar-Nejad H, Patel AJ, Sun Y, Chen HK, Rose MF, Venken KJ, Botas J, Orr HT, Bellen HJ, Zoghbi HY (2005) The AXH domain of Ataxin-1 mediates neurodegeneration through its interaction with Gfi-1/Senseless proteins. Cell 122:633-644.

Venkatraman P, Wetzel R, Tanaka M, Nukina N, Goldberg AL (2004) Eukaryotic proteasomes cannot digest polyglutamine sequences and release them during degradation of polyglutamine-containing proteins. Mol Cell 14:95-104.

Wagatsuma A, Osawa T (2006) Time course of changes in angiogenesis-related factors in denervated muscle. Acta Physiologica 187:503-509.

Walcott JL, Merry DE (2002) Ligand Promotes Intranuclear Inclusions in a Novel Cell Model of Spinal and Bulbar Muscular Atrophy. J Biol Chem 277:50855-50859.

Wang Y, Ou Mao X, Xie L, Banwait S, Marti HH, Greenberg DA, Jin K (2007) Vascular Endothelial Growth Factor Overexpression Delays Neurodegeneration and Prolongs Survival in Amyotrophic Lateral Sclerosis Mice. J Neurosci 27:304-307.

Ward IL, Weisz J (1980) Maternal Stress Alters Plasma Testosterone in Fetal Males. Science 207:328-329.

Waza M, Adachi H, Katsuno M, Minamiyama M, Sang C, Tanaka F, Inukai A, Doyu M, Sobue G (2005) 17-AAG, an Hsp90 inhibitor, ameliorates polyglutamine-mediated motor neuron degeneration. Nat Med 11:1088-1095.

Weis J (1994) Jun, Fos, MyoD1, and myogenin proteins are increased in skeletal muscle fiber nuclei after denervation. Acta Neuropathol 87:63-70.

Weisz J, Ward IL (1980) Plasma testosterone and progesterone titers of pregnant rats, their male and female fetuses, and neonatal offspring. Endocrinology 106:306-316.

Wilson CA, Davies DC (2007) The control of sexual differentiation of the reproductive system and brain. Reproduction 133:331-359.

Wu Y, Zhao W, Zhao J, Pan J, Wu Q, Zhang Y, Bauman WA, Cardozo CP (2007) Identification of androgen response elements in the insulin-like growth factor I upstream promoter. Endocrinology 148:2984-2993.

Wyttenbach A (2004) Role of heat shock proteins during polyglutamine neurodegeneration: mechanisms and hypothesis. J Mol Neurosci 23:69-96.

Yang Z, Chang YJ, Yu IC, Yeh S, Wu CC, Miyamoto H, Merry DE, Sobue G, Chen LM, Chang SS, Chang C (2007) ASC-J9 ameliorates spinal and bulbar muscular atrophy phenotype via degradation of androgen receptor. Nat Med 13:348-353.

Yarbrough WG, Quarmby VE, Simental JA, Joseph DR, Sar M, Lubahn DB, Olsen KL, French FS, Wilson EM (1990) A single base mutation in the androgen receptor gene causes androgen insensitivity in the testicular feminized rat. J Biol Chem 265:8893-8900.

Ying M, Xu R, Wu X, Zhu H, Zhuang Y, Han M, Xu T (2006) Sodium Butyrate Ameliorates Histone Hypoacetylation and Neurodegenerative Phenotypes in a Mouse Model for DRPLA. J Biol Chem 281:12580-12586.

Yu Z, Dadgar N, Albertelli M, Gruis K, Jordan C, Robins DM, Lieberman AP (2006a) Androgen-dependent pathology demonstrates myopathic contribution to the Kennedy disease phenotype in a mouse knock-in model. J Clin Invest 116:2663-2672.

Yu Z, Dadgar N, Albertelli M, Gruis K, Jordan C, Robins DM, Lieberman AP (2006b) Androgen-dependent pathology demonstrates myopathic contribution to the Kennedy disease phenotype in a mouse knock-in model. J Clin Invest 116:2663-2672.

Yu Z, Dadgar N, Albertelli M, Scheller A, Albin RL, Robins DM, Lieberman AP (2006c) Abnormalities of Germ Cell Maturation and Sertoli Cell Cytoskeleton in Androgen Receptor 113 CAG Knock-In Mice Reveal Toxic Effects of the Mutant Protein. Am J Pathol 168:195-204.

Zheng C, Nennesmo I, Fadeel B, Henter JI (2004) Vascular endothelial growth factor prolongs survival in a transgenic mouse model of ALS. Ann Neurol 56:564-567.

Zheng C, Sköld MK, Li J, Nennesmo I, Fadeel B, Henter J-I (2007) VEGF reduces astrogliosis and preserves neuromuscular junctions in ALS transgenic mice. Biochemical and Biophysical Research Communications 363:989-993.

Zoghbi HY, Orr HT (2000) Glutamine repeats and neurodegeneration. Annu Rev Neurosci 23:217-247.

Zuloaga DG, Puts DA, Jordan CL, Breedlove SM (2008a) The role of androgen receptors in the masculinization of brain and behavior: what we've learned from the testicular feminization mutation. Horm Behav 53:613-626.

Zuloaga DG, Morris JA, M. BS, Jordan CL (2008b) Mice with the Testicular Feminization Mutation Demonstrate a Role for Androgen Receptors in the Regulation of Anxiety-Related Behaviors and the Hypothalamic-Pituitary-Adrenal Axis. Horm Behav accepted.

Zuloaga DG, Morris JA, Monks DA, Breedlove SM, Jordan CL (2006) Androgen-sensitivity of somata and dendrites of spinal nucleus of the bulbocavernosus (SNB) motoneurons in male C57BL6J mice. Horm Behav 51:207-212.